

RUSSIAN GEOGRAPHICAL SOCIETY

FACULTY OF GEOGRAPHY,  
LOMONOSOV MOSCOW STATE UNIVERSITY

INSTITUTE OF GEOGRAPHY,  
RUSSIAN ACADEMY OF SCIENCES

No. 03 (v. 09)  
2016

**GEOGRAPHY**  
**ENVIRONMENT**  
**SUSTAINABILITY**

# EDITORIAL BOARD

## EDITORS-IN-CHIEF:

### **Kasimov Nikolay S.**

Lomonosov Moscow State University, Faculty of Geography, Russia

### **Kotlyakov Vladimir M.**

Russian Academy of Sciences Institute of Geography, Russia

### **Vandermotten Christian**

Université Libre de Bruxelles, Belgium

## DEPUTY EDITORS-IN-CHIEF:

### **Solomina Olga N.**

Russian Academy of Sciences, Institute of Geography, Russia

### **Tikunov Vladimir S.**

Lomonosov Moscow State University, Faculty of Geography, Russia

### **Chalov Sergei R. (Secretary-General)**

Lomonosov Moscow State University, Faculty of Geography, Russia

### **Baklanov Alexander**

Danish Meteorological Institute, Denmark

### **Baklanov Petr Ya.**

Russian Academy of Sciences, Pacific Institute of Geography, Russia

### **Chubarova Natalya E.**

Lomonosov Moscow State University, Faculty of Geography, Russia

### **De Maeyer Philippe**

Ghent University, Department of Geography, Belgium

### **Dobrolubov Sergey A.**

Lomonosov Moscow State University, Faculty of Geography, Russia

### **Haigh Martin**

Oxford Brookes University, Department of Social Sciences, UK

### **Gulev Sergey K.**

Russian Academy of Sciences, Institute of Oceanology, Russia

### **Guo Huadong**

Chinese Academy of Sciences, Institute of Remote Sensing and Digital Earth, China

### **Jarsjö Jerker**

Stockholm University, Department of Physical Geography and Quaternary Geography, Sweden

### **Kolosoov Vladimir A.**

Russian Academy of Sciences, Institute of Geography, Russia

### **Konečný Milan**

Masaryk University, Faculty of Science, Czech Republic

### **Kroonenberg Salomon**

Delft University of Technology Department of Applied Earth Sciences, The Netherlands

### **Kulmala Markku**

University of Helsinki, Division of Atmospheric Sciences, Finland

### **Malkhazova Svetlana M.**

Lomonosov Moscow State University, Faculty of Geography, Russia

### **Meadows Michael E.**

University of Cape Town, Department of Environmental and Geographical Sciences South Africa

### **Nefedova Tatyana G.**

Russian Academy of Sciences, Institute of Geography, Russia

### **O'Loughlin John**

University of Colorado at Boulder, Institute of Behavioral Sciences, USA

### **Pedroli Bas**

Wageningen University, The Netherlands

### **Radovanovic Milan**

Serbian Academy of Sciences and Arts, Geographical Institute "Jovan Cvijić", Serbia

### **Sokratov Sergei A.**

Lomonosov Moscow State University, Faculty of Geography, Russia

### **Tishkov Arkady A.**

Russian Academy of Sciences, Institute of Geography, Russia

### **Wuyi Wang**

Chinese Academy of Sciences, Institute of Geographical Sciences and Natural Resources Research, China

### **Zilitinkevich Sergey S.**

Finnish Meteorological Institute, Finland

# CONTENTS

## GEOGRAPHY

**Yurij K. Vasil'chuk, Julian B. Murton**

STABLE ISOTOPE GEOCHEMISTRY OF MASSIVE ICE ..... 4

**Ekaterina V. Lebedeva, Dmitry V. Mikhalev, Sergey V. Shvarev,  
Veniamin I. Gotvansky**

TENSION OF GEOMORPHOLOGIC CONDITIONS IN THE MARGINAL MOUNTAIN  
BELTS OF THE PACIFIC RIM ..... 25

## ENVIRONMENT

**Anna N. Tkachenko, Maria I. Gerasimova, Michael Yu. Lychagin, Nikolay S. Kasimov,  
Salomon B. Kroonenberg**

BOTTOM SEDIMENTS IN DELTAIC SHALLOW-WATER AREAS – ARE THEY SOILS? ..... 39

**Stanislav A. Ogorodov, Alisa V. Baranskaya, Nataliya G. Belova,  
Anatoly M. Kamalov, Dmitry E. Kuznetsov, Paul P. Overduin,  
Natalya N. Shabanova, Aleksey P. Vergun**

COASTAL DYNAMICS OF THE PECHORA AND KARA SEAS UNDER CHANGING  
CLIMATIC CONDITIONS AND HUMAN DISTURBANCES ..... 53

**Roman G. Zdorovenov, Galina G. Gavrilenko, Galina E. Zdorovenova,  
Nikolay I. Palshin, Tatyana V. Efremova, Sergey D. Golosov,  
Arkady Yu. Terzhevik**

OPTICAL PROPERTIES OF LAKE VENDYURSKOE ..... 74

## SUSTAINABILITY

**Alexander F. Finaev, Liu Shiyin, Bao Weijia, Jing Li**

CLIMATE CHANGE AND WATER POTENTIAL OF THE PAMIR MOUNTAINS ..... 88

**Emmanuel Oriola, Cynthia Chibuike**

FLOOD RISK ANALYSIS OF EDU LOCAL GOVERNMENT AREA  
(KWARA STATE, NIGERIA) ..... 106

### **Disclaimer:**

All materials are published as original versions submitted by the authors. The GES Journal has used its best endeavors to ensure that the information is correct and current at the time of publication but takes no responsibility for any error, omission, or defect therein. The views and opinions expressed in the articles are those of the authors and do not necessarily reflect the official policy or position of the GES Journal Editorial Board, the journal co-founders and editors.

DOI: 10.15356/2071-9388\_03v09\_2016\_01

**Yurij K. Vasil'chuk<sup>1\*</sup>, Julian B. Murton<sup>2</sup>**

<sup>1</sup> Faculty of Geography and Faculty of Geology, Lomonosov Moscow State University, Russia 119991, Moscow, Leninskie Gory, 1

<sup>2</sup> Permafrost Laboratory, Department of Geography, University of Sussex, Brighton, UK

\* **Corresponding author**; e-mail: vasilch@geol.msu.ru & vasilch\_geo@mail.ru

## STABLE ISOTOPE GEOCHEMISTRY OF MASSIVE ICE

**ABSTRACT.** The paper summarises stable-isotope research on massive ice in the Russian and North American Arctic, and includes the latest understanding of massive-ice formation. A new classification of massive-ice complexes is proposed, encompassing the range and variability of massive ice. It distinguishes two new categories of massive-ice complexes: homogeneous massive-ice complexes have a similar structure, properties and genesis throughout, whereas heterogeneous massive-ice complexes vary spatially (in their structure and properties) and genetically within a locality and consist of two or more homogeneous massive-ice bodies. Analysis of pollen and spores in massive ice from Subarctic regions and from ice and snow cover of Arctic ice caps assists with interpretation of the origin of massive ice. Radiocarbon ages of massive ice and host sediments are considered together with isotope values of heavy oxygen and deuterium from massive ice plotted at a uniform scale in order to assist interpretation and correlation of the ice.

**KEY WORDS:** massive ice, stable isotopes, radiocarbon dating, homogeneous and heterogeneous

### INTRODUCTION

The research on massive ice began for one of the authors in July 1977 during the boating expedition of the Geological Faculty of Moscow State University in the Yuribey River valley (68°26'N, 72°08'E) on central Yamal Peninsula, west Siberia. Here, the senior author encountered a complex exposure of massive-ice bodies that probably represent an assemblage of buried river ice and injection (intrusive) ice. This exposure has contributed significantly to the development of a new massive-ice classification by Y.K. Vasil'chuk, the basic principles of which are set out in Fig. 1. A new classification of massive ice, as well as most of the currently available data on the stable isotope geochemistry of massive ice are summarized in the two-volume monograph Yu.K. Vasilchuk [2012, 2014], a critical analysis which is mainly devoted to this paper.

### STUDY AREA

The paper is based primarily on the senior author's experience, involvement and field studies over more than 35 years (from 1977 to 2014) in numerous expeditions concerning massive ice in Russian permafrost. It also summarizes the experience of many international researchers, and describes exposures with large bodies of massive ice in west and east Siberia, Chukotka, Alaska and Yukon, the Tuktoyaktuk Coastlands, the Canadian Arctic Archipelago and Russian Arctic islands, China and the Antarctic.

### MASSIVE-ICE CLASSIFICATION

Yu. Vasil'chuk [2012] presents a new classification of massive-ice bodies and includes two new categories: homogeneous and heterogeneous (Fig. 1). Homogeneous

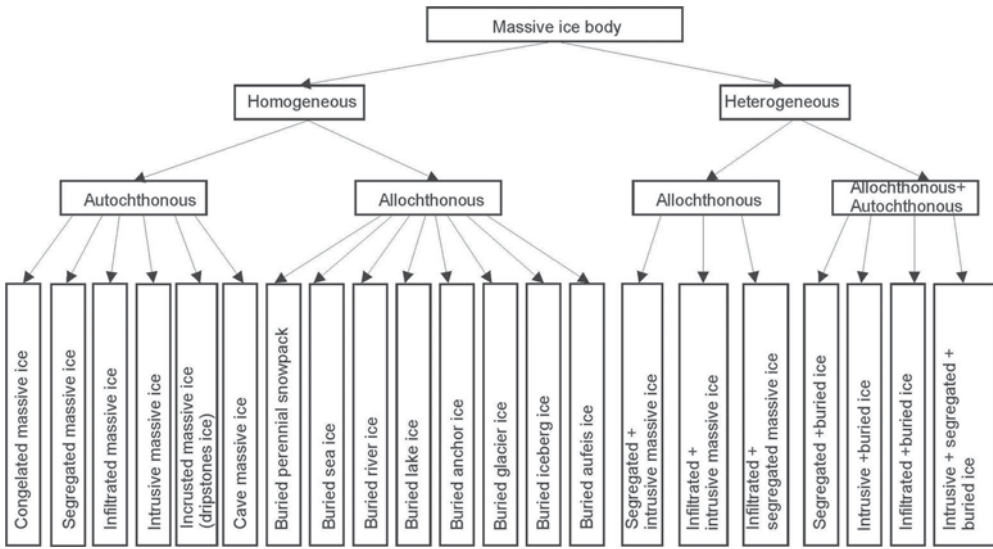


**Fig. 1. The classification of massive-ice bodies, involving a three-tier system: (tier 1) homogeneous and heterogeneous categories, (tier 2) autochthonous and allochthonous categories, and (tier 3) specific ice types.**

massive-ice bodies have a similar genesis, composition and properties in all parts of a massive-ice complex, whereas heterogeneous massive-ice bodies have a variable genesis, composition and properties across a massive-ice complex, and consist of two or more homogeneous ice bodies. The distinction between homogeneous and heterogeneous massive-ice bodies elucidates the wider complex structure of massive-ice bodies and encourages the search for different mechanisms of ice formation.

*Homogeneous massive-ice complexes*

Homogeneous massive-ice complexes are usually no more than a few meters high, ≤ 20–30 m wide and occur as single layers of ice or, less commonly, as multiple layers of the same genesis. Typical examples of segregated (or infiltrated and segregated) ice were studied by Y.K. Vasilchuk [1992] in the first terrace of the Gyda River estuary (70°53'N, 78°30'E). Four similar lens-shaped bodies of massive ice (up to 0.3–0.4 m thick and 6–8 m wide) were composed of clear ice and, as a rule, associated with peat. The structure of the ice bodies and their bedding parallel to the

sedimentary stratification suggest that they formed synchronously with the accumulation and freezing of the ground mass, consistent with the occurrence of a 4.5 m high syngenetic ice wedge in the sedimentary sequence. The ice is interpreted as infiltrated or segregated in origin. The wide range of δ<sup>18</sup>O values (–33.8 to –16.2‰) in these ice bodies indicates closed-system freezing with a small inflow of water from outside the system. Such a wide range of the heavy oxygen values indicates significant cryogenic fractionation during freezing of waters whose initial average composition was close to –20‰. This could occur only under conditions of closed-system freezing, when isotopically heavier ice was the first to form (δ<sup>18</sup>O values of about –16 and –18‰), while the δ<sup>18</sup>O values of the remaining water were about –22‰. The partial freezing of the water led to the formation of ice with δ<sup>18</sup>O values of about –20‰, while the rest of the water had δ<sup>18</sup>O values of about –24 to –25‰. Repeated freezing of this water provided extremely low δ<sup>18</sup>O values (about –34‰) in the last portions of the water to freeze. The low average δ<sup>18</sup>O values in this massive ice (about –20‰) indicate that the ice formed under conditions more severe than

those at present. In view of the radiocarbon age of the ground mass (more than 15  $^{14}\text{C}$  ages from 10,260 to 15,890 BP obtained on allochthonous peat), the accumulation of the ground mass and the formation of massive ice and the syngenetic ice wedge occurred no earlier than 14,000–11,000 years ago [Y.K. Vasilchuk, 1992].

### *Heterogeneous massive-ice complexes*

Heterogeneous massive-ice complexes comprise two or more ice layers (tiers) of different genesis. The layers may be in contact or adjacent to each other, influencing the shape of the ice complex and the conditions of its occurrence. Examples include massive

ice of the Yuribey River valley (Fig. 2a), massive ice in the Erkutayaha River valley [Y.K. Vasil'chuk et al., 2012] in the south of Yamal Peninsula (Fig. 2b, 3), and in many places in the Bovanenkovo gas condensate field [Y.K. Vasil'chuk et al., 2009, 2014; Kritsuk, 2012].

The second division of the classification distinguishes between autochthonous (i.e., intrasedimental in terms of Mackay and Dallimore [1992]) and allochthonous (i.e. buried) ice (see Fig. 1). Heterogeneous massive-ice complexes can include a combination of autochthonous and allochthonous deposits. The third division classifies the massive ice according to its specific genetic process (e.g., injection,

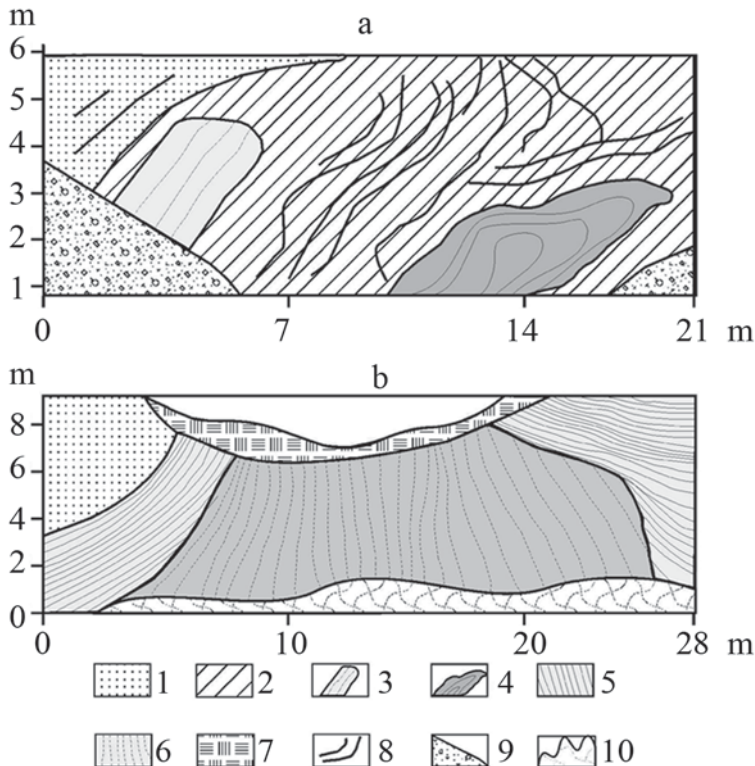


**Fig. 2. Vertical stratigraphic sections through heterogeneous massive-ice bodies in west Siberia: assemblage of buried and intrusive ice in the upper Yuribey River valley, central Yamal Peninsula (a) and assemblages of segregation and intrusive ice, Erkutayaha River valley, southern Yamal Peninsula (b).**

1 – sand; 2 – loam; 3 – layered pure ice; 4 – deformed intrusive ice rich in mineral inclusions; 5 – segregated layered massive ice; 6 – intrusive vertically layered massive ice; 7 – Holocene lacustrine–marsh loam and sandy loam and peat; 8 – laminated sediment; 9 – scree; 10 – slumped material (i.e. debris covering the section)



**Fig. 3. Assemblages of segregation and intrusive ice, Erkutayaha River valley, southern Yamal Peninsula. Photograph by Yu.Vasil'chuk.**

segregation, infiltration, burial) and shows the wide diversity of genetic ice types.

The proposed classification is illustrated through examples in Yu.Vasil'chuk's monograph [2012], which critically examines the main hypotheses of massive-ice formation.

#### MODERN AND HOLOCENE ANALOGUES OF PLEISTOCENE MASSIVE ICE, AND THE MAIN HYPOTHESES OF MASSIVE-ICE FORMATION

Vasil'chuk [2012] discusses modern and Holocene analogues of Pleistocene massive ice, beginning with massive ice in marine sediments. One of the most convincing analogues of Pleistocene massive ice is Holocene massive segregated ice 8–9 m thick on the Fosheim Peninsula, Ellesmere Island, in the Canadian Arctic (79°59'N, 85°56'W; Pollard and Bell, 1998). The  $\delta^{18}\text{O}$  values of the ice range between  $-28.9$  and  $-34.8\text{‰}$  for reticulate ice,  $-33.1$  and  $-36.8\text{‰}$  for massive ice, and  $-36.1\text{‰}$  for an ice vein in adjacent Tertiary sandstone. The massive ice is interpreted as intrasedimental ice because: a) it is conformably overlain by marine sediments and contains internal structures parallel the upper ice contact; the ice lacks evidence for primary thaw or erosional contacts, which would indicate buried ice; and b) sediment within inclusions in the massive ice is similar to the overlying marine sediments, indicating that the overlying sediment was deposited

before the ice formed. Radiocarbon ages of shells from raised marine deposits in the Slidre River valley suggest that the Holocene marine limit was likely established by 10.6 ka BP, with sea level remaining high (within 10 m of marine limit) until 8.7 ka BP or later. The massive-ice deposits formed time transgressively as permafrost aggraded into marine sediments during the Holocene [Pollard and Bell, 1998]. Ice segregation occurred as permafrost aggraded downward through a fine-grained layer of silt that overlay saturated sands with an ample water source. The injection of water under high pressure into the overlying frozen bedrock at Eureka Sound formed intrusive massive ice [Robinson and Pollard, 1998]. As a result, a heterogeneous massive-ice complex (according to Y.K. Vasil'chuk's classification) developed.

Massive-ice bodies are extraordinarily widespread in Holocene sediments of the first lagoon-marine terrace and the modern lagoon-marine floodplain of the Ob Bay, at the mouth of the Sabettayaha River, in west Siberia (71°15'N, 72°06'E). More than 1000 boreholes through Holocene marine lagoon and floodplain deposits have been analyzed [Y.K. Vasilchuk et al., 2016b] and show massive-ice bodies up to 5.7 m thick in the upper 5–10 m of Holocene silty sand. Their  $\delta\text{D}$  values vary from  $-107$  to  $-199.7\text{‰}$ , and their  $\delta^{18}\text{O}$  values vary from  $-15.7$  to  $-26.5\text{‰}$ . The massive ice is mostly autochthonous and of segregated origin [Y.K. Vasil'chuk et al., 2016b]. It formed

syngenetically during freezing of water-saturated soils under intensive cryogenic fractionation in the late Holocene. Thick massive-ice bodies also occur in saline sediments, for example a 14 m thick massive ice layer in beach sediments near the mouth of the Khatanga River [Ponomarev, 1960], fresh (salinity is 620 mg/l) massive ice at a depth of 19–29 m beneath the sea bottom [Melnikov and Spesivtsev, 2000], and a 1.5 m thick layer of salty ice at the depth about 10 m in sediments beneath the shallow waters of the Mechigmen Gulf (Chukotka). Y.K. Vasil'chuk proposed the original mechanism of the formation of icy bodies in saline lake (meromictic lakes) sediments.

Other possible modern and Holocene analogues of Pleistocene massive ice are freshwater ice deposits in shallow, saline (up to 103 g/l) lakes at 4117–4730 m above sea level (asl) in Bolivia. The ice deposits (consisting of several ice lenses, each up to 1 m thick) are up to several hundred meters wide and elevated up to 7 m above the lake or playa surface. They are located near the lake or salar (salt-crust desert) margins; some are completely surrounded by water, others by playa deposits or salt crusts [Hurlbert and Chang, 1984]. The  $\delta^{18}\text{O}$  values for the ice lenses (–10.6 to –11.5‰) are much lower than those of lakewater (+ 13.5‰) but similar to those of precipitation ( $\delta^{18}\text{O}$  value in fresh snow –13.2‰).

Ice in the cores of modern pingos provides another analogue of Pleistocene massive-ice deposits. The distribution of stable isotopes in pingo ice cores indicates that the ice formed under conditions of open and closed systems. Ice in the core of the Holocene pingo in the Pestsovoe gas field area (66°10' N 76°30'E) formed in closed-system conditions; its  $\delta\text{D}$  values vary from –93.2 to –123‰, and  $\delta^{18}\text{O}$  values vary from –11.6 to –15.8‰ [Y.K. Vasil'chuk et al., 2016a].

The main hypotheses of massive-ice formation identify the ice as segregated, intrusive, repeated intrusive and buried

glacier ice [Vtyurin, 1975; Mackay, 1973; Rampton, 1988; Zhestkova and Shur, 1978; Y.K. Vasil'chuk, 1992, 2012, 2014; Dubikov, 2002; Murton, 2005, 2009; French, 2007; Solomatin, 2013; Streletskaya et al., 2013; Belova, 2014]. Holmsen [1914] proposed the infiltrated and segregated hypothesis of massive-ice genesis. He hypothesized that the formation of thick (up to 15 m) massive ground-ice deposits is linked to the infiltration of surface water through seasonally thawed ground and the freezing of this water on the top [see also Zhestkova and Shur, 1978]. Vtyurin [1975] favoured ice segregation, with the most favorable conditions for the formation of massive segregated ice being near the contact between clayey sediments and water-bearing coarse-grained sediments. Gasanov [1969] hypothesized that the main factor of ice formation is water intrusion, and distinguished different types of intrusive ice: seasonal intrusive ice, multi-seasonal intrusive ice (short-term permafrost), intrusive ice, repeated intrusive ice and hydrolaccoliths. Mackay [1971, 1973] proposed that the mechanism of water injection and segregation in closed-system conditions that is widely applied to explain pingo growth can also apply to the mechanism of massive-ice formation.

#### COMPARISON OF POLLEN SPECTRA OF MASSIVE ICE AND GLACIERS FOR CRYOGENIC INDICATION

Palynological analysis of deposit-forming ground ice has identified several distinctive characteristics of the pollen spectra. First, pollen and spores are present in almost all types of deposit-forming ground ice, at concentrations from 50 to 1500 units per 1 kg ice or 1 litre of ice meltwater. Second, pollen spectra with characteristics similar to those of subfossil tundra, including the predominance of dwarf birch and ericaceous pollen and green moss spores, occur in most massive-ice deposits. Third, the massive-ice deposits frequently contain redeposited pre-Quaternary palynomorphs of Cenozoic, Mesozoic and Palaeozoic age. Fourth, pollen of

hydrophilous plants (e.g., pondweed, bur reed and reed mace), as well as horsetail spores, limnetic diatoms and green algae remains also occur in most of the studied massive-ice deposits, indicating a non-glacial genesis of the ice. Pollen spectra that are typical of non-glacial deposit-forming ice show: 1) a lack of exotic thermophilic species such as *Acer*, *Fraxinus*, *Quercus*, *Ulmus*, *Populus*, *Tilia* and *Abies* in the initial occurrence; 2) the presence of cloudberry, *aquiherbosa* species, as well as green moss and horsetail; and 3) the presence of redeposited pollen and spores. This palynological approach indicates that the massive ice on the Yamal Peninsula of west Siberia is mainly non-glacial in origin [A.C. Vasil'chuk and Y.K. Vasul'chuk, 2010, 2012].

#### ISOTOPIC COMPOSITION OF MASSIVE ICE IN RUSSIAN PERMAFROST

The senior author considers his own isotopic studies of massive ice in Siberia and interprets the isotope records obtained by others [Vasil'chuk, 2012]. He considers the vertical variations in more than 35 isotope plots published in the last 30 years [Vaikmäe and Karpov, 1986; Y.K. Vasil'chuk and Trofimov, 1988; Vaikmäe and Y.K. Vasil'chuk, 1991; Korolyov, 1993; Kotov, 1998; Dubikov, 2002; Leibman et al., 2003; Ingólfsson and Lokrantz, 2003; Y.K. Vasil'chuk et al., 2009, 2011, 2012, 2014; Kritsuk, 2010; Slagoda et al., 2012; Ivanova, 2012; Belova, 2014].

The isotope curves are plotted at a single vertical and horizontal scale to facilitate their comparison.

The isotope composition of the massive-ice deposits in northern European Russia is considered for a number of localities, including the More-Yu River valley, Cape Shpindler, and the Oyuyakha River valley (68°51'N, 66°44'E). For the massive-ice body at Cape Shpindler in the Yugorski Peninsula (69°43'N; 62°48'E), Ingólfsson and Lokrantz [2003] concluded that it is buried glacier ice and suggested that it is older than 190–200 kyr, whereas Leibman et al. [2003],

who also examined the internal structures, stratigraphy and isotopic composition of the massive ice, attributed it to syngenetic or epigenetic freezing after marine regression. The senior author assumes that this massive ice is intrasedimental, heterogeneous and autochthonous because the  $\delta^{18}\text{O}$  values in different types of massive ice at Cape Spindler vary from  $-13.1$  to  $-25.6\text{‰}$ . Such variability may be explained by fractionation during ice segregation in a closed system.

The isotope composition of massive-ice deposits is also considered for northwest Siberia. Localities there include: 1) the Erkutayaha River valley (68°11'N, 68°51'E), 2) the Bovanenkovo gas field area (70°21'N, 68°26'E), 3) the Morddyakha River valley (69°33'N, 68°59'E), 4) the Kharasavey settlement (71°10'N, 66°51'E), 5) near Marre-Sale meteorostation (69°45'N; 66°50'E), 6) at Tyurinto Lake (70°44'N, 67°57'E), 7) at Voivareto Lake (68°43'N; 72°25'E), 8) near Gyda settlement (70°53'N, 78°30'E), 9) the Yuribey River valley (68°26'N, 72°08'E), 10) near Tab-Salya settlement (71°45'N; 82°45'E), 11) near Dorofeevskaya settlement (71°23'N; 82°58'E), 12) at the Sopochnaya Karga Cape (71°50'N, 82°40'E) and 13) Ledyanaya Gora in the Yenisey River valley (66°35'N, 86°34'E).

On the southernmost Yamal Peninsula heterogeneous autochthonous massive ice is located on the left bank of the Erkutayaha River (68°11'N, 68°51'E). A massive-ice body approximately 100 m long is embedded predominantly in stratified sand. The ice layers sharply drop on both sides of the central part, and just 15 m from the centre the cover of the massive ice appears at a depth of 8 m. The central part of the massive-ice body takes a form similar to a stock (a type of igneous intrusion), with vertical and subvertical ice layers, whereas the peripheral parts comprise horizontally layered ice. The range of  $\delta^{18}\text{O}$  ( $\sim 4\text{‰}$ ) and  $\delta\text{D}$  ( $\sim 20\text{‰}$ ) values indicates comparatively small fluctuations of the isotopic composition for ice with different characteristics: pure white ice has  $\delta^{18}\text{O}$  values from  $-19.6$  to  $-20.5\text{‰}$ , and  $\delta\text{D}$  varies from

–152.4 to –156.9‰; clear transparent ice has  $\delta^{18}\text{O}$  values from –19.2 to –20.3‰, and  $\delta\text{D}$  varies from –149.6 to –160.7‰; transparent gray ice with a steely shimmer has  $\delta^{18}\text{O}$  values from –19.4 to –21.3‰, and  $\delta\text{D}$  varies from –150.3 to –163.8‰; and gray ice and in the dirty gray ice has  $\delta^{18}\text{O}$  values from –22.1 to –23.4‰, and  $\delta\text{D}$  varies from –165.5 to –172.7‰. Hence, the difference between the isotope signal of the initial water and ice is comparatively small. The isotopic differences almost did not exceed the usual isotopic difference that results from fractionation when free water freezes. Significantly, the pollen spectra in the vertically layered ice from the central stock (most likely of injection genesis) lack reworked pollen and spores, whereas those from the horizontally layered peripheral ice (most likely of segregation or infiltration-segregation genesis) contain a high concentration of reworked pollen and spores (35 %).

On the central part of the Yamal Peninsula (69°33'N, 68°59'E) beside the upper Mordyyakha River is a heterogeneous autochthonous massive-ice body at 66–70 m a.s.l. The ice body is more than 4 m thick and has horizontal bedding that passes laterally into vertical bedding and is crossed by syngenetic ice wedges 4–5 m in high. The isotopic composition of ice from obliquely oriented ice lenses (lenticular-layered cryostructure) in the north part of the outcrop shows insignificant isotopic variations (from –22.4 to –23.3‰  $\delta^{18}\text{O}$ ) and thus suggests that ice segregation occurred under open-system conditions. The pollen spectra are characterized by high contents of pollen and spores of hygrophilous plants, with sedge pollen and horsetail spores dominant. Such specific features were noted for sediments of small floodplain lakes. It can be assumed that the ice deposits formed during freezing of a talik after a former lake drained.

In the Bovanenkovo gas field area (70°21'N, 68°26'E) heterogeneous autochthonous and allochthonous massive-ice bodies occur as layers, laccoliths, rods and lenses.

The maximum thickness of the tabular ice is 28.5 m, and the mean thickness is about 8 m.  $\delta^{18}\text{O}$  values of massive ice range from –12.4 to –22.9‰ [Michel, 1998; Y.K. Vasil'chuk et al., 2009], and deuterium ( $\delta\text{D}$ ) values vary from –91.7 to –177.1‰. The contrasting distribution (like vertical bilateral rake with very long teeth of different lengths)  $\delta^{18}\text{O}$  and ( $\delta\text{D}$ ) vs. depth in massive ice bodies suggests a segregated and/or infiltrated-segregated origin of the ice. Pollen, spores and algal spectra from the massive ice are similar to pollen characteristics of modern lacustrine and coastal floodplain sediments in the area. The senior author inferred that the ingress of cold seawaters on a coastal flood plain caused freezing and ice segregation, with the formation of extensive ice layers under the large but shallow lakes.

The material presented shows that the methodological use of isotopic data from massive ice is still far from ideal. Even within the same article, the authors have expressed different hypotheses about the origin of massive ice in Ledyanaya Gora (Ice Mountain) on the Yenisei River valley (66°35'N, 86°34'E) because intrasedimental ice may be difficult to distinguish from basal glacier ice, as both ice types can form by the same freezing processes [Vtyurin and Glazovskiy, 1986]. Stratigraphic and isotopic study of this massive ice and its host sediments led Vaikmäe and Karpov [1986] and Astakhov and Isayeva [1988] to interpret the ice as relict glacier ice, probably emplaced during the Early Weichselian. However, interpretation of the Ledyanaya Gora massive ice is problematic. Most of the  $\delta^{18}\text{O}$  values from the ice range from –20 to –21.5‰ [Vaikmäe and Y.K. Vasil'chuk, 1990; Vaikmäe et al., 1993], pointing to uniformity of the oxygen isotope profile. The isotopic composition of the massive ice is similar to that of vertical ice schlieren in the overlying diamicton ( $\delta^{18}\text{O} = -20.7$  ‰). This similarity, coupled with a significant change from a salinity of 10–80 mg/l in the upper part of the massive ice to one of 200–340 mg/l in the middle and lower parts of it, according Y.K. Vasil'chuk, indicates an intrasedimental

origin. In conclusion, the massive ice at Ledyanaya Gora can be regarded as heterogeneous autochthonous massive ice.

Isotope data summarized from Chukotka include homogeneous autochthonous massive ice at the Koolen'Lake, near the town of Anadyr' and at Onemen Bay [Vasil'chuk, 1992], Tanyurer River valley [Kotov, 1998], and heterogeneous allochthonous and autochthonous massive ice in the Amguema River valley [Korolyov, 1993].

Finally, heterogeneous allochthonous and autochthonous massive-ice bodies are found on Novaya Siberia Island (75°05'N, 148°27'E). Ivanova [2012] showed that  $\delta^{18}\text{O}$  values of massive ice there vary from  $-8.9$  to  $-29\text{‰}$ , and  $\delta\text{D}$  values vary from  $-66.8$  to  $-228.4\text{‰}$ . The  $\delta^{18}\text{O}$  and  $\delta\text{D}$  values in the upper and lower horizons of massive ice are very different. These data can be interpreted to indicate an injected origin for the lower horizon of massive ice, and a segregation origin for the upper horizon [Ivanova, 2012].

#### ISOTOPIC COMPOSITION OF MASSIVE ICE IN PERMAFROST OF THE CANADIAN ARCTIC

Vasil'chuk [2014] examines the vertical variations in more than 30 isotope plots of massive ice from the Canadian Arctic [Mackay, 1983; Fujino et al., 1983; Lorrain and Demeur, 1985; Michel, 1983, 2011; Dallimore and Wolfe, 1988; French and Harry, 1990; Mackay and Dallimore, 1992; Moorman et al., 1996, 1998; Robinson and Pollard, 1998; Pollard and Bell, 1998; Hyatt, 1998; Murton et al., 2004, 2005; Lacelle et al., 2004, 2007, 2009, 2011; Murton, 2005, 2009; Cardyn et al., 2007; French, 2007; Lacelle, 2011; Fritz et al., 2011]. Here we consider a few of them.

Massive ice adjacent to Tuktoyaktuk (69°27'N, 133°02'W), near the mouth of the Mackenzie River, has been isotopically studied by Mackay [1983], Fujino et al. [1983, 1988], Mackay and Dallimore [1992] and others. Fujino et al. [1983] concluded that most of the massive-

ice body at Peninsula Point originated from superimposed ice formed by congelation of water in which it was submerged. Mackay and Dallimore [1992], however, rejected this interpretation. They reported that the geochemical and stable isotope values of the massive ice were similar to those of ice dikes that extended from the ice into the overlying diamicton, which indicates a common water source and suggests that the massive ice is intrasedimental in origin. Y.K. Vasil'chuk concluded that massive ice at this site is heterogeneous: autochthonous and allochthonous.

A massive-ice complex is often well exposed by coastal erosion at North Head, on Richards Island (69°20'N, 134°30'W), in the Tuktoyaktuk Coastlands. According to Murton [2005], some of the massive ice is buried and some is intrasedimental. Y.K. Vasil'chuk agreed and identified the ice as heterogeneous: autochthonous and allochthonous.

Massive ground-ice bodies in the Sandhills Moraine of southern Banks Island, and the southern Eskimo Lakes region of the Tuktoyaktuk Coastlands, according to French and Harry [1990], are interpreted as basal glacier ice. Other massive ground-ice bodies in the Western Canadian Arctic, however, are explained better in terms of segregation-injection [French and Harry, 1990]. Assessing the isotopic variations in ice around the Eskimo Lakes, Y.K. Vasil'chuk noted that the bottom of the massive ice described by French and Harry [1990] is characterized by a relatively stable distribution and a small range (about 1.5 ‰) of  $\delta^{18}\text{O}$  values (from  $-33.5$  to  $-35$  ‰) and by abrupt changes in the upper 2 m of ice: upward, the value increases to  $-31$  ‰, and then sharply decreases to  $-36$  ‰. Y.K. Vasil'chuk suggested that the isotopic changes in the upper 2 m of ice are consistent with ice segregation commencing in a semi-closed or open system, and ending in a closed system, leading to an appreciable isotope differentiation in the top of the ice deposits.

Massive ice also occurs within glacially deformed permafrost in the coastal lowlands near Tuktoyaktuk (e.g. at Liverpool Bay – 70°N, 129°W, southwest of Nicholson Island; and on northern ‘Crane Island’, in the central Eskimo Lakes; Murton et al., 2004). The massive ice is at least 2.5–8 m thick, and either white and bubble-rich, or grey, debris-rich and banded. Two types of ground ice are identified in the deformed permafrost: (1) massive ice and ice clasts, both of which have been glacially deformed, eroded or moved; and (2) segregated ice and ice-wedge ice that have not been glacially disturbed because their postdate deformation. Y.K. Vasilchuk agreed with these interpretations and determined the massive ice as heterogeneous: autochthonous and allochthonous.

Within the limits of the Willow River drainage basin, on the Aklavik Plateau (69°N, 124°W), Lacelle et al. [2004] examined four exposures of debris-rich massive ice. The  $\delta^{18}\text{O}$  values of the ice change abruptly from an average of about  $-30\text{‰}$  (for Late Pleistocene ice) to  $-22.6\text{‰}$  (for Holocene ice). Physical and isotopic properties of the former suggest that it is segregated-intrusive ice, because the  $\text{CO}_2$  content and  $\delta^{13}\text{C}$  value in the debris-rich ice was acquired during movement of  $\text{CO}_2$  through the sediments, giving  $\text{CO}_2$  concentrations that are 3–9 times higher than those for air trapped in glacier ice and  $\delta^{13}\text{C}$  values in the range of  $\text{CO}_2$  produced by the decay of  $\text{C}_3$  plant material [Lacelle et al., 2004]. Y.K. Vasilchuk agreed with these interpretations and determined the massive ice as heterogeneous: autochthonous and allochthonous.

Massive ice within but close to the glacial limit of the Laurentide Ice Sheet, on Herschel Island (69°N, 139°W), in the southern Beaufort Sea, is highly depleted in heavy isotopes (mean  $\delta^{18}\text{O}$  value:  $-33\text{‰}$ ;  $\delta\text{D}$ :  $-258\text{‰}$ ; [Fritz et al., 2011, 2012]). These authors noted that such stable isotope signatures indicate a full-glacial water source for the massive ice on Herschel Island. However, an

origin as glacially deformed segregated or segregated-intrusive ice cannot be excluded. Pollard [1990] concluded that segregated ice is the most common massive-ice type in this area and in places constitutes up to 70 % of the upper 10–15 m of permafrost. Y.K. Vasilchuk suggested that the origin of massive ice on Herschel Island varies, and the ice includes both heterogeneous and homogeneous types.

#### DATING OF MASSIVE ICE OF RUSSIA AND NORTH AMERICA, AND CORRELATION OF STABLE ISOTOPE CURVES

Radiocarbon dating of organic material in the sediments that surround massive ice in Russia and Canada, and direct accelerator mass spectrometry (AMS) radiocarbon dating of organic microinclusions and trapped gases within massive ice in Canada are analyzed by Vasilchuk [2014]. The radiocarbon ages suggest that most of the massive ice accumulated between the Holocene and 20–40 ka BP (Fig. 4).

Comparison of isotopic plots of massive ice in Russia and Canada (Fig. 5–7) shows that they have more similarities than differences in the regional isotopic record of ice formation. An initial isotopic signature indicates the nature of the water and the conditions of ice formation. Ice segregation in a closed system leads to a contrasting distribution of  $\delta^{18}\text{O}$  and  $\delta\text{D}$  values, both vertically and laterally (Fig. 5). The shape of isotopic plots of massive ice relates to the type of ice formation. Homogeneous, undifferentiated isotope plots with a narrow range of isotopic changes ( $\delta^{18}\text{O}$  range  $< 4\text{‰}$ ,  $\Delta\delta\text{D}$  range  $< 32\text{‰}$ ) characterize massive ice formed in an open system, with freezing of inflowing water under homogeneous conditions. By contrast, isotope plots with a wide range of isotopic changes ( $\Delta\delta^{18}\text{O}$  range  $> 8\text{‰}$ ,  $\Delta\delta\text{D}$  range  $> 64\text{‰}$ ) characterize massive ice formed in a closed system, where there is no inflowing water. Closed-system freezing is typical of segregation ice formation, or rarely for the final phase of injection ice formation when there is no inflow of water (Fig. 6 and 7).

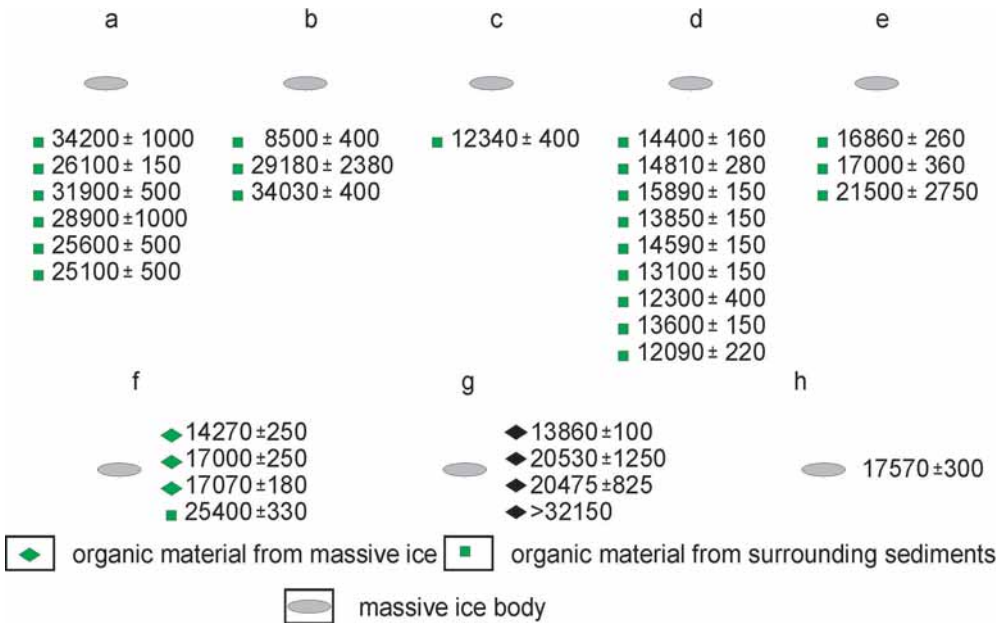


**Fig. 4. Comparison of the radiocarbon ages (years BP) of massive ice: a–e obtained by <sup>14</sup>C dating of organic material from host sediments surrounding massive ice in Russian permafrost, f–h obtained by direct AMS <sup>14</sup>C dating of organic material from ice in Canadian permafrost. Sites:**

a – Bovanenkovo [Y.K. Vasil'chuk, 2012], b – Tyurinto Lake, c – Tab-Salya town, d – Gyda town [Y.K. Vasil'chuk, 1992], e – Tanyurer River valley [Kotov, 1998], f – Peninsula Point (4.5 km southwest of Tuktoyaktuk) [Kato et al., 1988], g – Peninsula Point [Moorman et al., 1998]; h – Herschel Island [Moorman et al., 1996].

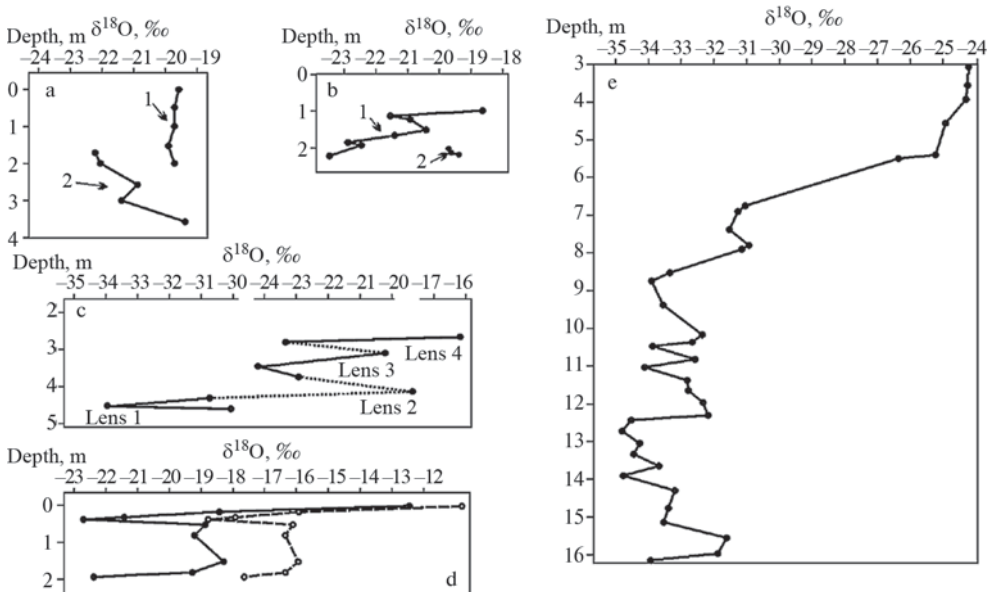


**Fig. 5. The comparison of oxygen isotope plots of massive ice of Russian (a–d) and Canadian (e) permafrost, formed under closed-system freezing.**

a–d Yamal Peninsula: a – Erkutayakha [Y.K. Vasil'chuk, 2012]; b – Kharasavey [Belova, 2012]; c – Gyda [Y.K. Vasil'chuk, 1992]; d – Bovanenkovo [Y.K. Vasil'chuk, 2012]; e – borehole 96BGS-06, Contwoyto Lake [Wolfe, 1998].

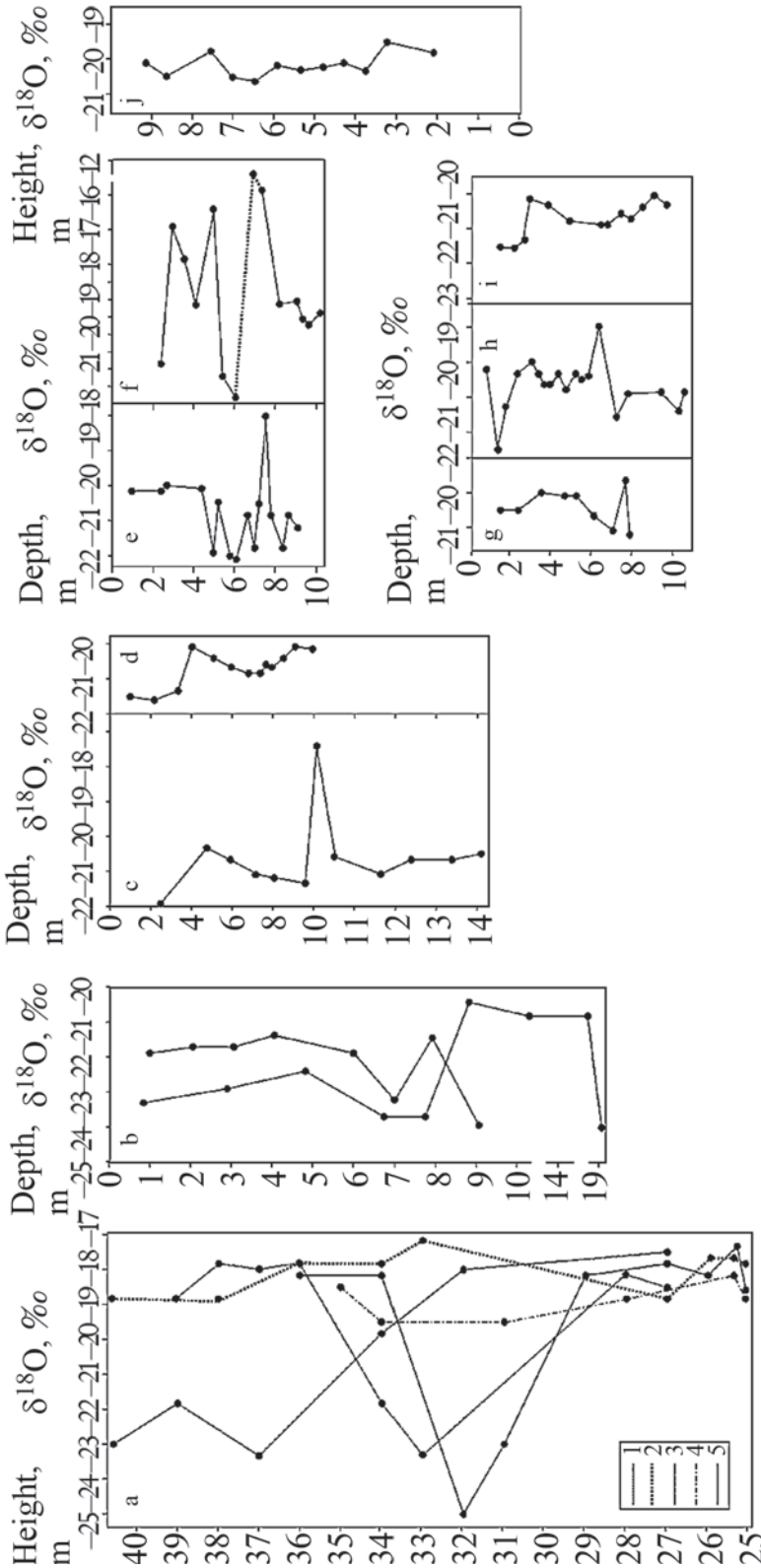


**Fig. 6. The comparison of oxygen isotope plots of massive ice from Russian permafrost, formed under open- and closed-system freezing.**

a – Cape Shpindler on Yugorski Peninsula: 1–5 – different parts of exposure [Ingólfsson and Lokrantz, 2003]; b – Yuribey, Gydan Peninsula [Kritsuk, 2010];  
 c–j – different parts of the Ledyanaya Gora (or Ice Mountain) exposure, on the right bank of the Yenisey River near the Arctic Circle [Vaikmäe and Karpov, 1986; Vaikmäe and Y.K. Vasil'chuk, 1991]; j – Onemen Bay, Chukotka [Kotov, 2001].

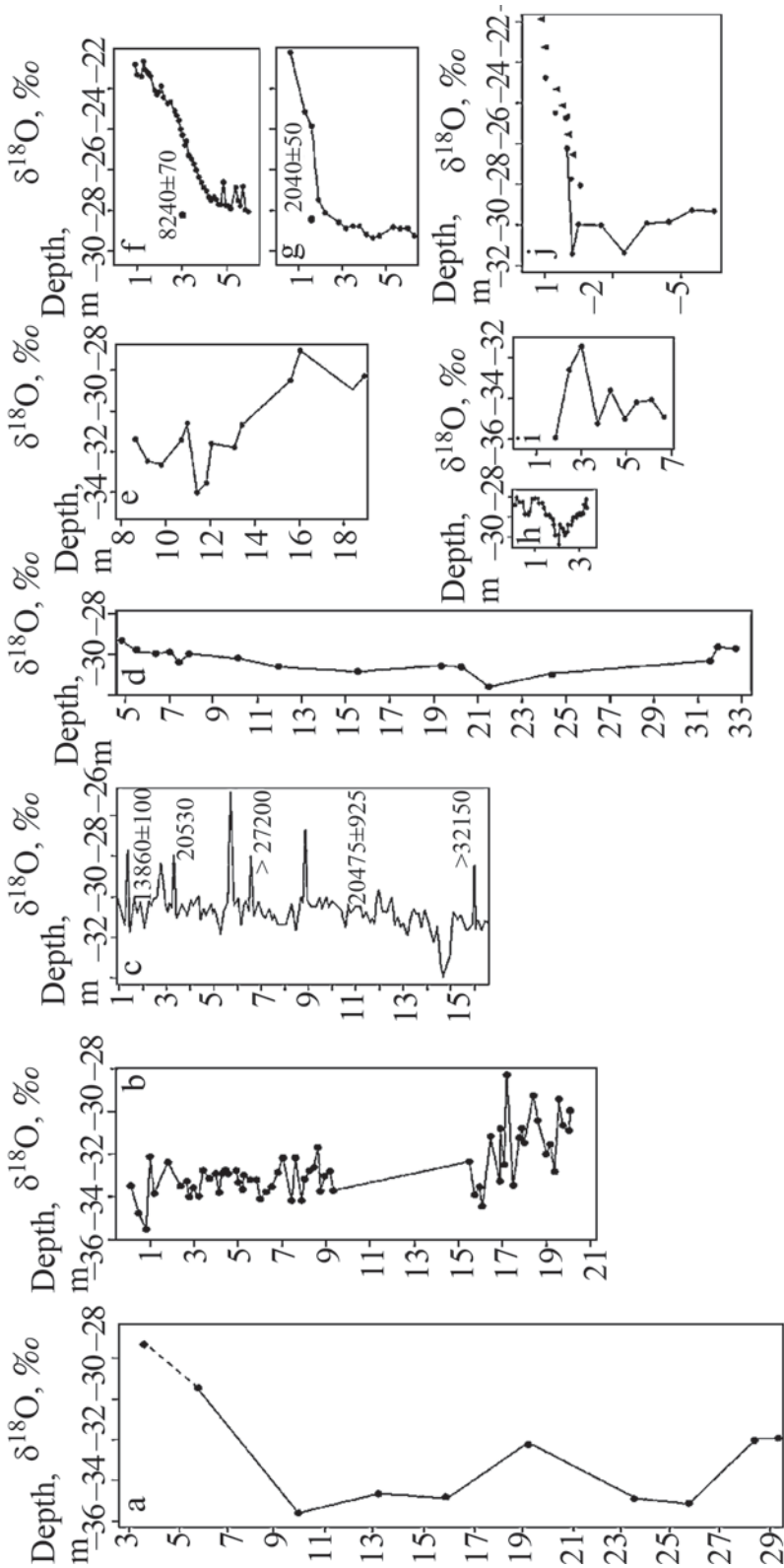


**Fig. 7. The comparison of oxygen isotope plots of massive ice of Canadian permafrost, formed under open- and closed-system freezing:**

- a – Involut Hill site, to the northeast of Tuktoyaktuk [Mackay, 1983]; b – Peninsula Point (4.5 km southwest of Tuktoyaktuk) [Fujino et al., 1988];
- c – Peninsula Point [Moorman et al., 1998]; d – 7 km to the east of Ya Ya Lake, on southern Richard Island [Dallimore and Wolfe, 1988];
- e – Lousy Point, near Ya Ya Lake, on southern Richard Island [Dallimore and Wolfe, 1988]; f – g Willow River region, Aklavik Plateau, Richardson Mountains;
- f – profile of site WR-00-5, g – profile of site WR-00-3 [Lacelle et al., 2004]; h – 5 km southwest of Tuktoyaktuk [Kato and Fujino, 1981];
- i – southern Eskimo Lakes region, Tuktoyaktuk Coastlands [French and Harry, 1990], j – Crumbling Point, Summer Island, Tuktoyaktuk Coastlands [Murton et al., 2005].

## CONCLUSIONS

- The study considers practically all the selected ages and mechanisms of massive-ice formation. The senior author proposed the original mechanism of the formation of massive ice in saline lake sediments. New mechanisms will undoubtedly be proposed in the future.
- A new genetic classification of massive-ice deposits introduces two new categories at its highest level: homogeneous and heterogeneous massive-ice deposits.
- Assemblages of different massive-ice types are common in permafrost exposures in the Yamal Peninsula of west Siberia and

the Tuktoyaktuk Coastlands and Yukon of northwest Canada.

- Plotting of isotopic data from massive ice on graphs with a single vertical and horizontal size facilitates objective assessment of the isotopic characteristics of massive ice.

## ACKNOWLEDGMENTS

Research by Yu.Vasil'chuk is financially supported by the Russian Scientific Foundation (grant RSF No. 14-27-00083, generalisation of stable isotope data) and by a grant from the Russian Foundation for Basic Research (grant RFBR No. 14-05-00795, stable isotope analyses). ■

## REFERENCES

1. Astakhov V.I., Isayeva L.L. (1988). The "Ice Hill": an example of 'redarded deglaciation" in Siberia. *Quaternary Science Reviews*, vol. 7, pp. 29–40. DOI: 10.1016/0277-3791(88)90091-1.
2. Belova N.G. 2014. *Plastovye ldy yugo-zapadnogo poberezhya Karskogo morya (Massive ice beds of south-western coast of the Kara Sea)*. Moscow: MAK Press, 180 pp. (in Russian).
3. Cardyn R., Clark I.D., Lacelle D., Lauriol B., Zdanowicz C., Calmels F. (2007). Molar gas ratios of air entrapped in ice: A new tool to determine the origin of relict massive ground ice bodies in permafrost. *Quaternary Research*, vol. 68, pp. 239–248. DOI: 10.1016/j.yqres.2007.05.003.
4. Dallimore S.R., Wolfe S.A. (1988). Massive ground ice associated with glacial sediments, Richards Island, N.W.T., Canada. In *Proceedings of the Fifth International Conference on Permafrost*, Senneset K. (ed.). Tapir Publishers: Trondheim, Norway, pp. 132–138.
5. Danilov I.D. 1989. *Plastovye ldy i subakvalnyj kriolitogenez (Massive ice and subaqueous cryolithogenesis)*. In *Geokriologicheskie Issledovaniya (Geocryological Study)*, Yershov ED (ed.). Moscow: Moscow University Press, pp. 16–29. (in Russian).
6. Dubikov G.I. (2002). *Sostav i kriogennoe stroenie merzlykh tolshch Zapadnoj Sibiri (Composition and Cryogenic Structure of the Permafrost Strata of Western Siberia)*. Moscow: Geos Publishing House, 246 pp. (in Russian).
7. French H.M. (2007). *The Periglacial Environment*. Third Edition. John Wiley and Sons Ltd: Chichester.
8. French H.M., Harry D.G. (1990). Observations on buried glacier ice and massive segregated ice, western arctic coast, Canada. *Permafrost and Periglacial Processes*, vol. 1, pp. 31–43. DOI: 10.1002/ppp.3430010105.

9. Fritz M., Wetterich S., Meyer H., Schirrmeister L., Lantuit H., Pollard W.H. (2011). Origin and characteristics of massive ground ice on Herschel Island (Western Canadian Arctic) as revealed by stable water Isotope and hydrochemical signatures. *Permafrost and Periglacial Processes*, vol. 22, pp. 26–38. DOI: 10.1002/ppp.714.
10. Fritz M., Wetterich S., Schirrmeister L., Meyer H., Lantuit H., Preusser F., Pollard W.H. (2012). Eastern Beringia and beyond: Late Wisconsinan and Holocene landscape dynamics along the Yukon Coastal Plain, Canada. *Palaeogeography, Palaeoclimatology, Palaeoecology*, vols. 319–320, pp. 28–45. doi: 10.1016/j.palaeo.2011.12.015.
11. Fujino K., Horiguchi K., Shinbori M., Kato K. (1983). Analysis and characteristics of cores from a massive ice body in Mackenzie delta, N.W.T., Canada. In *Proceedings of the Fourth International Conference on Permafrost*. National Academy Press: Washington, D.C., pp. 316–321.
12. Fujino K., Sato S., Matsuda K., Sasa G., Shimizu O., Kato K. (1988). Characteristics of the massive ground ice body in the western Canadian Arctic. In *Proceedings of the Fifth International Conference on Permafrost*, Senneset K. (ed.). Tapir Publishers: Trondheim, Norway, pp. 143–146.
13. Gasanov S.S. (1969). *Stroenie i istoriya formirovaniya myorzlykh porod Vostochnoj Chukotki* (The Structure and the Formation History of the Frozen Grounds in Eastern Chukotka): Moscow: Nauka, 168 pp. (in Russian).
14. Holmsen G. (1914). Spitsbergens jordbunds is og de bidrag dens undersøkelse har kunnet gi til forstaaelsen a de i arktiske land optrædende varige isleier i jorden. (Ground ice in Spitsbergen and contributions toward the understanding of perennial ground ice found in Arctic environments). *Det Norske Geografiske Selskabs Årbok*, B XXIV, 1912–1913, Kristiania: 1–150 pp.
15. Hurlbert S.H., Chang C.C.Y. (1984). Ancient Ice Islands in Salt Lakes of the Central Andes. *Science*, vol. 224, pp. 299–302. DOI: 10.1126/science.224.4646.299.
16. Hyatt J.A. (1998). The origin of lake-bed ground ice at Water Supply Lake, Pond Inlet, Nunavut, Canada. In *Proceedings of the 7th International Conference on Permafrost*, Yellowknife, Canada, Lewkowicz A.G., Allard M. (eds.). Universite Laval, Canada. *Collection Nordicana*, N 57, pp. 757–762.
17. Ingólfsson Ó., Lokrantz H. (2003). Massive ground ice body of glacial origin at Yugorski Peninsula, Arctic Russia. *Permafrost and Periglacial Processes*, vol. 14, pp. 199–215. DOI: 10.1002/ppp.455.
18. Ivanova V.V. (2012). *Geokhimiya plastovykh Idov ostrova Novaya Sibir, Novosibirskie ostrova, Rossijskaya Arktika kak otrazheniye uslovij ikh genezisa* (Geochemical features of formation of massive ground ice bodies (New Siberia Island, Siberian Arctic). *Kriosfera Zemli*, N 1, pp. 56–70 (in Russian).
19. Kato K., Fujino K. (1981). Oxygen isotopic composition of massive ice at Tuktoyaktuk, North Canada. In *Joint Studies on physical and biological environments in the permafrost, North Canada, July to August 1980, and February to March, 1981*, S. Kinoshita S. (ed.). Institute of Low Temperature Science: Hokkaido University, Sapporo, pp. 13–20.

20. Kato K., Sato S., Fujino K. (1988). Radiocarbon dating by accelerator mass spectrometry on sediment in a core from a massive ice body in Mackenzie Delta, N.W.T., Canada: preliminary report. In *Characteristics of the massive ground ice body in the western Canadian Arctic related to paleoclimatology 1986–1987*, Fujino K. (ed.). Institute of Low Temperature Science: Hokkaido University, Sapporo, pp. 58–69.
21. Korolev S.Y. (1993). Nakhodka v doline reki Amguehmy pozdneplejstocenovogo gletchernogo lda, Severnaya Chukotka (The discovery of the Late Pleistocene glacier ice in the valley of the Amguema River (Northern Chukotka). *Doklady Rossijskoj Akademii Nauk*, vol. 329, pp. 195–198 (in Russian).
22. Kotov A.N. (1998). Kriolitogennye gryady v doline reki Tanyurer, Chukotka (The cryolithogenic ridges in the valley of the Tanurer River (Chukotka). *Kriosfera Zemli*, vol. 4, pp. 62–71 (in Russian).
23. Kritsuk L.N. (2010). *Podzemnye ldy Zapadnoj Sibiri (Ground Ice of Western Siberia)*. Nauchny Mir Publishing House: Moscow, 351 pp. (in Russian).
24. Lacelle D. (2011). On the  $\delta^{18}\text{O}$ ,  $\delta\text{D}$  and d-excess relations in meteoric precipitation and during equilibrium freezing: theoretical approach and field examples. *Permafrost and Periglacial Processes*, vol. 22, pp. 13–25. DOI: 10.1002/ppp.712.
25. Lacelle D., Bjornson J., Lauriol B., Clark I.D., Troutet Y. (2004). Segregated-intrusive ice of subglacial meltwater origin in retrogressive thaw flow headwalls, Richardson Mountains, N.W.T., Canada. *Quaternary Science Reviews*, vol. 23, pp. 681–696. DOI: 10.1016/j.quascirev.2003.09.005.
26. Lacelle D., Lauriol B., Clark I.D., Cardyn R., Zdanowicz C.H. (2007). Nature and origin of a Pleistocene-age massive ground-ice body exposed in the Chapman Lake moraine complex, central Yukon Territory. *Quaternary Research*, vol. 68, pp. 249–260. DOI: 10.1016/j.yqres.2007.05.002.
27. Lacelle D., St-Jean M., Lauriol B., Clark I.D., Lewkowicz A., Froese D.G., Kuehn S.C., Zazula G. (2009). Burial and preservation of a 30,000 year old perennial snowbank in Red Creek valley, Ogilvie Mountains, central Yukon, Canada. *Quaternary Science Reviews*, vol. 28, pp. 3401–3413. DOI: 10.1016/j.quascirev.2009.09.013
28. Lacelle D., Davila A.F., Pollard W.H., Andersen D., Heldmann J., Marinova M., McKay C.P. (2011). Stability of massive ground ice bodies in University Valley, McMurdo Dry Valleys of Antarctica: Using stable O–H isotope as tracers of sublimation in hyper-arid regions. *Earth and Planetary Science Letters*, vol. 301, pp. 403–411.
29. Leibman M.O., Hubberten H.-W., Lein A.Y., Streletskaia I.D., Vanshtein B.G. (2003). Tabular ground ice origin: cryolithological and isotope-geochemical study. In *Proceedings of the 8th International Conference on Permafrost*, M. Phillips M., Springman S.M., Arenson L. (eds.). A.A. Balkema Publishers: Lisse, Netherlands, pp. 645–650.
30. Lorrain R.D., Demeur P. (1985). Isotopic evidence for relic Pleistocene glacier ice on Victoria Island, Canadian Arctic Archipelago. *Arctic and Alpine Research*, 17, pp. 89–98. DOI: 10.2307/1550964.
31. Mackay J.R. (1971). The Origin of Massive lcy Beds in Permafrost, Western Arctic Coast, Canada. *Canadian Journal of Earth Sciences*, vol. 8/4, pp. 397–422. DOI: 10.1139/e71-043.

32. Mackay J.R. (1973). Problems in the origin of massive ice beds, western Arctic Canada. In Proceedings of the 2nd International Conference on Permafrost, Yakutsk, USSR, 13–28 July 1973, Péwé TL, Mackay JR (eds). National Academy of Sciences: Washington D.C., North American Contributions, pp. 223–238.
33. Mackay J.R. (1983). Oxygen isotope variations in permafrost, Tuktoyaktuk Peninsula area, Northwest Territories. In Current Research, Part B. Geological Survey of Canada, Paper 83–1B, pp. 67–74.
34. Mackay J.R., Dallimore S.R. (1992). Massive ice of the Tuktoyaktuk area, western Arctic coast, Canada. *Canadian Journal of Earth Sciences*, vol. 29, pp. 1235–1249. DOI: 10.1139/e92-099.
35. Melnikov V.P., Spesivtsev V.I. (2000). Cryogenic formations in the earth's lithosphere (graphic version). Konishchev VN (ed.). Novosibirsk: Scientific Publishing Center of the UIGGM, Siberian Branch of the RAS, Publishing House, Siberian Branch of the RAS, 2000, 343 pp.
36. Michel F.A. (1983). Isotope variations in permafrost waters along the Dempster Highway pipeline "corridor" In Proceedings of the 4th International Conference on Permafrost. Fairbanks. Alaska. National Academy Press: Washington, pp. 843–848.
37. Michel F.A. (1998). The relationship of massive ground ice and the Late Pleistocene history of Northwest Siberia. *Quaternary International*, vol. 45/46, pp. 43–48. DOI: 10.1016/S1040-6182(97)00005-0.
38. Michel F.A. (2011). Isotope characterisation of ground ice in northern Canada. *Permafrost and Periglacial Processes*, vol. 22, pp. 3–12. DOI: 10.1002/ppp.721.
39. Moorman B.J., Michel F.A., Wilson A. (1996).  $^{14}\text{C}$  dating of trapped gases in massive ground ice, Western Canadian Arctic. *Permafrost and Periglacial Processes*, vol. 7, pp. 257–266. DOI: 10.1002/(SICI)1099-1530(199609)7:3<257::AID-PPP220>3.0.CO;2-P.
40. Moorman B.J., Michel F.A., Wilson A.T. (1998). The development of tabular massive ground ice at Peninsula Point, N.W.T., Canada. In Proceedings of the 7th International Conference on Permafrost, Lewkowicz AG, Allard M. (eds.). Université Laval, Canada. Collection Nordicana, N57, pp. 757–762.
41. Murton J.B. (2005). Ground-ice stratigraphy and formation at North Head, Tuktoyaktuk Coastlands, western Arctic Canada: a product of glacier–permafrost interactions. *Permafrost and Periglacial Processes*, vol. 16, pp. 31–50. DOI: 10.1002/ppp.513.
42. Murton J.B. (2009). Stratigraphy and palaeoenvironments of Richards Island and the eastern Beaufort Continental Shelf during the last glacial–interglacial cycle. *Permafrost and Periglacial Processes*, vol. 20, pp. 107–125. DOI: 10.1002/ppp.647.
43. Murton J.B., Waller R.I., Hart J.K., Whiteman C.A., Pollard W.H., Clark I.D. (2004). Stratigraphy and glaciotectonic structures of permafrost deformed beneath the northwest margin of the Laurentide Ice Sheet, Tuktoyaktuk Coastlands, Canada. *Journal of Glaciology*, vol. 49, pp. 399–412. DOI: 10.3189/172756504781829927.
44. Murton J.B., Whiteman C.A., Waller R.I., Pollard W.H., Clark I.D., Dallimore S.R. (2005). Basal ice facies and supraglacial melt–out till of the Laurentide Ice Sheet, Tuktoyaktuk

- Coastlands, western Arctic Canada. *Quaternary Science Reviews*, vol. 24: 681–708. DOI: 10.1016/j.quascirev.2004.06.008.
45. Pollard W. (1990). The nature and origin of ground ice in the Herschel Island area, Yukon Territory. In *Permafrost – Canada. Proceedings of the Fifth Canadian Permafrost Conference. Collection Nordicana, N 54. Centre d'études Nordiques, Université Laval. Québec: National Research Council of Canada*, pp. 23–30.
  46. Pollard W., Bell T. (1998). Massive ice formation in the Eureka Sound Lowlands: A landscape model. In *Proceedings of the 7th International Conference on Permafrost, Yellowknife. Canada, Lewkowicz A.G., Allard M. (eds.). Université Laval, Canada. Collection Nordicana, N 57*, pp. 903–908.
  47. Ponomarev V.M. (1960). Formirovanie podzemnykh vod po poberezh'yu severnykh morey v zone vechnoj merzloty (Underground waters formation in the permafrost along the coast of the northern seas). Moscow: Publishing House of the USSR Academy of Sciences. 1960. 95 pp. (in Russian).
  48. Rampton V.N. (1988). Origin of massive ground ice on Tuktoyaktuk Peninsula, Northwest Territories, Canada. In *Proceedings of the Fifth International Conference on Permafrost, Senneset K. (ed.). Tapir Publishers: Trondheim, Norway*, pp. 850–855.
  49. Robinson S., Pollard W. (1998). Massive ground ice within Eureka Sound bedrock, Fosheim Peninsula, Ellesmere Island, N.W.T. In *Proceedings of the 7th International Conference on Permafrost, Yellowknife. Canada, Lewkowicz A.G., Allard M. (eds.). Université Laval, Canada. Collection Nordicana, N 57*, pp. 949–954.
  50. Slagoda E.A., Opokina O.L., Kurchatova A.N., Rogov V.V. (2012). Structure and composition of complex massive ice bodies in Late Pleistocene-Holocene sediments of the Marre-Sale Cape, West Yamal. In *Proceedings of the Tenth International Conference on Permafrost, Melnikov V.P., Drozdov D.D., Romanovsky V.E. (eds.). Salekhard, 25–29 June 2012. Vol. 2. The Northern Publisher: Salekhard, Russia*, pp. 415–420.
  51. Shpolyanskaya N.A. (2014). Permafrost (Cryolithozone) of the Russian Arctic Shelf. *Universal Journal of Geoscience*, vol. 2, pp. 7–17. DOI: 10.13189/ujg.2014.020102.
  52. Solomatin V.I. (2013). *Fizika i geografiya podzemnogo oledeneniya (Physics and Geography of Ground Glaciation)*. Novosibirsk: Academic Publishing House "Geo", 246 pp. (in Russian).
  53. Streletskaya I.D., Gusev E.A., Vasiliev A.A., Oblogov G.E., Molodkov A.N. (2013). Pleistocene – Holocene paleoenvironmental records from permafrost sequences at the Kara Sea coasts (NW Siberia, Russia). *Geography, Environment, Sustainability*, N 3, pp. 60–76.
  54. Vaikmäe R.A., Karpov Y.G. (1986). Study of tabular ground ice bodies from the Ledyanaya Gora section in the Yenisey valley using the Oxygen isotope method. *Polar Geography and Geology*, vol. 10, pp. 32–38. DOI:10.1080/10889378609377270.
  55. Vaikmäe R.A., Vasil'chuk Y.K. (1991). Izotopno kislorodnyy analiz podzemnykh ldiv severa Zapadnoj Sibiri, Yakutii i Chukotki (Oxygen isotope analyses of ground ice north-west

- Siberia, Yakutia and Chukotka). Tallinn: Institut geologii Akademii Nauk Ehstonii (Geology Institute of the Estonia Academy of Science). 70 pp. (in Russian).
56. Vaikmäe R., Michel F.A., Solomatin V.I. (1993). Morphology, stratigraphy and oxygen isotope composition of fossil glacier ice at Ledyanaya Gora, Northwest Siberia, Russia. *Boreas*, vol. 22, pp. 205–213. DOI: 10.1111/j.1502-3885.1993.tb00180.x.
57. Vasil'chuk A.C., Vasil'chuk Y.K. 2010. Local pollen spectra as a new criterion for nonglacial origin of massive ice. *Transactions (Doclady) of Russian Academy of Sciences, Earth Sciences*, vol. 433, pp. 985–990. DOI: 10.1134/S1028334X10070305.
58. Vasil'chuk A.C., Vasil'chuk Y.K. (2012). Pollen and Spores as Massive Ice Origin Indicators. In *Proceedings of the Tenth International Conference on Permafrost*, Melnikov V.P., Drozdov D.D., Romanovsky V.E. (eds.). Salekhard, 25–29 June 2012. Vol. 2. The Northern Publisher: Salekhard, Russia, pp. 487–491.
59. Vasil'chuk Y.K. (1992). Izotopno kislorodnyj sostav podzemnykh ldiv (opyt paleogeokriologicheskikh rekonstrukcij (Oxygen Isotope composition of Ground Ice (Application to Paleogeocryological Reconstruction)). Izd. Otdel teoreticheskikh problem ran, MGU, PNIIS (Department of theoretical problems the Russian Academy of Sciences. Moscow State University, Industrialand Research Institute of Engineering Survey for Construction). In 2 volumes. Vol. 1, 420 pp., vol. 2, 264 pp. (in Russian).
60. Vasil'chuk Y.K. (2011). Gomogennye i geterogennye plastovye ledyanye zalezhi v mnogoletnyorzlykh porodakh (Homogeneous and Heterogeneous Massive Ice in Permafrost). *Kriosfera Zemli 1*, vol. 40–51 (in Russian).
61. Vasil'chuk Y.K. (2012). Classification of Massive Ice. In *Proceedings of the Tenth International Conference on Permafrost*, Melnikov V.P., Drozdov D.D., Romanovsky V.E. (eds.). Salekhard, 25–29 June 2012. Vol. 2. Salekhard: The Northern Publisher, Russia, pp. 493–497.
62. Vasil'chuk Y.K. (2012). Izotopnye metody v geografii. Chast 2. Geohimiya stabilnyh izotopov plastovyh ldiv. Tom 1. (Stable Isotope Geochemistry of Massive Ice. Vol. 1.). Moscow: Izdatelstvo Moskovskogo Uiversiteta, 472 pp. (in Russian).
63. Vasil'chuk Y.K. (2013). Syngenetic ice wedges: cyclical formation, radiocarbon age and stable-isotope records. *Permafrost and Periglacial Processes*, vol. 24, pp. 82–93. DOI: 10.1002/ppp.1764.
64. Vasil'chuk Y.K. (2014). Izotopnye metody v geografii. Chast 2. Geohimiya stabilnyh izotopov plastovyh ldiv. Tom 2. (Stable Isotope Geochemistry of Massive Ice. Vol. 2.). Moscow: Izdatelstvo Moskovskogo Uiversiteta, 244 pp. (in Russian).
65. Vasil'chuk Y.K., Trofimov V.T. (1988). Oxygen isotope variations in ice-wedge and massive ice. In *Proceedings of the Fifth International Conference on Permafrost*, Senneset K. (ed.). Trondheim. Norway. Tapir Publishers, pp. 489–492.
66. Vasil'chuk Y.K., Vasil'chuk A.C., Budantseva N.A., Chizhova J.N., Papesch W., Podborny Y.Y., Sulerzhitsky L.D. 2009. Oxygen Isotope and Deuterium Indication of the Origin and  $^{14}\text{C}$  Age of the Massive Ice, Bovanenkovo, Central Yamal Peninsula. *Doklady Earth Sciences* 429, pp. 1326–1332. DOI: 10.1134/S1028334X09080194.

67. Vasil'chuk Y.K., Budantseva N.A., Vasil'chuk A.C. (2011). Variations in  $\delta^{18}\text{O}$ ,  $\delta\text{D}$ , and the concentration of pollen and spores in autochthonic heterogeneous massive ice on the Erkutayaha River in the southern part of the Yamal Peninsula. *Doklady Earth Sciences*, vol. 438, pp. 721–726. DOI: 10.1134/S1028334X11050382.
68. Vasil'chuk Y.K., Vasil'chuk A.C., Budantseva N.A. (2012). Isotopic and palynological compositions of a massive ice in the Mordyyakha River, Central Yamal Peninsula. *Doklady Earth Sciences*, vol. 446, pp. 1105–1109. DOI: 10.1134/S1028334X12090164.
69. Vasil'chuk Y, Vasil'chuk A. (2014). Spatial distribution of mean winter air temperatures in Siberian permafrost at 20–18 ka BP using oxygen isotope data. *Boreas*, vol. 43, pp. 43–52. DOI: 10.1111/bor.12033.
70. Vasil'chuk Y.K., Vasil'chuk A.C., Budantseva N.A., Chizhova J.N., Papesch W., Podborny Y.Y. (2014).  $^{14}\text{C}$  age, stable isotope composition and pollen analysis of massive ice, Bovanenkov gas field, Central Yamal Peninsula. *Geography, Environment, Sustainability*, N 2, pp. 49–70.
71. Vasil'chuk Y.K., Lawson D.E., Yoshikawa K., Budantseva N.A., Chizhova J.N., Podborny Y.Y., Vasil'chuk A.C. (2016a). Stable Isotopes in the closed-system Weather Pingo, Alaska and Pestsovoye Pingo, northwestern Siberia. *Cold Regions Science and Technology*, vol. 128, pp. 13–21.
72. Vasil'chuk Y., Budantseva N., Vasil'chuk A., Chizhova J., Podborny Y., Vasil'chuk J. (2016b). Holocene multistage massive ice, Sabettayakha River mouth, Yamal Peninsula, northern-west Siberia. *GeoResJ*, 9, pp. 54–67. DOI: 10.1016/j.grj.2016.09.002.
73. Vtyurin B.I. (1975). *Podzemnye ldy SSSR (Ground Ice of the USSR)*. Moscow: Nauka, 214 pp. (in Russian).
74. Vtyurin B.I., Glazovskiy A.F. (1986). Composition and structure of the Ledyanaya Gora tabular ground ice body on the Yenisey. *Polar Geography and Geology*, vol. 10, pp. 273–285. DOI: 10.1080/10889378609377297.
75. Wolfe S.A. (1998). Massive ice associated with glaciolacustrine delta sediments Slave geological province, N.W.T., Canada. In *Permafrost. Seventh International Conference. Proceedings*. Yellowknife, Canada. Lewkowicz AG, Allard M (eds.). Universite Laval, Collection Nordicana, N 57. Canada, pp. 1133 – 1139.
76. Zhestkova T.N., Shur Y.L. (1978). O genezise plastovykh ldov (On the genesis of tabular massive ice). *Vestnik Moskovskogo universiteta. Seria geologiya*, N 3, pp. 35–42 (in Russian).

**Received 24.04.2016****Accepted 29.08.2016**



**Yurij Vasil'chuk** is Professor of Permafrost Science at the Lomonosov Moscow State University, the Department of Landscape Geochemistry and Soil Geography. He is a geographer and geologist who specializes in the permafrost environments. His research focuses on isotope geochemistry, ground ice and glaciers. He obtained his PhD from the Moscow State University in 1982, and his D. Sc. degree from the Permafrost Institute of RAS in 1991. He has held professorial positions at the Cryolithology and Glaciology Department of Moscow State University in 1996, and was appointed to the position of full professor at the Department Landscape Geochemistry and Soil Geography in 2009. He was elected as a member of the Russian Academy of Natural Sciences in 2004. His research interests have been concerned with the use of stable and radioactive isotopes in massive ice and ice wedges, palsas and pingos, as well as in soils and landscapes. His ice-wedge isotope work is based on a field study in 1976–2016 of the Russian stratotypes of the 'Yedoma Suite', at Seyaha and Mongatalyangyakha, northwestern Siberia, at Zelyony Mys, Plakhinsii Yar, Bison, Duvanny Yar, in the lower Kolyma River, northern Yakutia, Phoenix and Utinaya mountain polygonal ice-wedge complexes at upper Kolyma River, Mamontova Gora polygonal ice-wedge complexes of Aldan River, Ayon Island, Mayn River etc. He has studied the isotope composition of massive ice at Bovanenkovo, on the Erkutayaha River, in the Mordyyakha River and unique Holocene multistage massive ice, Sabettayakha River mouth, Yamal Peninsula, of eastern Chukotka, etc. His publications include as lead-author about 250 papers on stable and radioactive isotopes in the ice wedges, massive ice, palsas, lithalsas, pingos and glaciers, as well as in soils and landscapes (including more than 60 papers into English). He has written four university textbooks and 15 geocryological monographs, more of them are devoted to isotope composition and radiocarbon age of Siberian yedoma and massive ice.



**Julian Murton** is Professor of Permafrost Science at the University of Sussex. He obtained his PhD in geology from the University of Ottawa in 1993. He is a geologist who specialises in the geomorphology, sedimentology and stratigraphy of permafrost environments. His research focuses on permafrost as a driver and archive of environmental change, with the aims to elucidate: ground-ice and permafrost thaw processes (e.g. rock fracture, thermokarst, solifluction); permafrost-glacier interactions (e.g. Laurentide Ice Sheet, Canada; Anglian Ice Sheet, UK), and reconstruction of cold Quaternary environments (glacial, periglacial). To achieve these aims, he performs physical modelling experiments in the Sussex Permafrost Laboratory to test hypotheses and develop new technologies on cryogenic processes in rock and soil. This experimental work is complemented by geological research in present-day permafrost regions (Canada, Alaska and Siberia) and in past permafrost regions (NW Europe) to examine the geological effects of glacier-permafrost interactions and to reconstruct cold Quaternary environments. A current focus is on yedoma sedimentology and stratigraphy during Marine Isotope Stages 2 and 3. This research is based on a field study in 2009–2016 of the Russian stratotypes of the 'Yedoma Suite', at Duvanny Yar, in the lower Kolyma River, northern Yakutia and a megaslump at Batagaika, in the Yana Uplands of northern Yakutia. His publications include two papers on ground ice and involutions reproduced in a benchmark volume on Periglacial Geomorphology, and lead-author papers on rock fracture and Lake Agassiz outburst flooding published in *Science* and *Nature*. He has written a geological monograph on Siberian yedoma.

**Ekaterina V. Lebedeva<sup>1\*</sup>, Dmitry V. Mikhalev<sup>2</sup>, Sergey V. Shvarev<sup>3</sup>,  
Veniamin I. Gotvansky<sup>4</sup>**

<sup>1</sup> Institute of Geography, Russian Academy of Sciences, Moscow, Russia;  
Staromonetny per., 29, 119017; Tel: + 7-499-238-03-60, Fax: + 7-495-959-00-33,  
e-mail: Ekaterina.lebedeva@gmail.com,

**\* Corresponding author**

<sup>2</sup> Faculty of Geography, Lomonosov Moscow State University, Moscow, Russia;  
Leninskie Gory, 1, 119991; Tel: + 7-495-939-25-26, e-mail: mikhalev.dmitry@gmail.com

<sup>3</sup> Institute of Geography, Russian Academy of Sciences, Moscow, Russia;  
Staromonetny per., 29, 119017; Tel: + 7-499-238-03-60, Fax: + 7-495-959-00-33,  
e-mail: s.v.shvarev@gmail.com

<sup>4</sup> Member of Russian Geographical Society, Moscow, Russia; 3th Vladimirskaya str., 4,  
fl. 37; Tel: + 7-926-137-29-96, e-mail: gotvanski@yandex.ru

## TENSION OF GEOMORPHOLOGIC CONDITIONS IN THE MARGINAL MOUNTAIN BELTS OF THE PACIFIC RIM

**ABSTRACT.** The maps of naturally determined geomorphologic tension, scale 1:8 million, for the territory of the Russian Far East and the central fragment of the mountain system of the Andes (between 5°S – 19°S) were compiled. We are using the term “tension” to define predisposition of the territory for the development of catastrophic processes. Tension was evaluated in nominal scores accordingly to the regional level of generalization. Assessment was based on the analysis of seismicity, amount of precipitation, the depth of the relief dissection and the spectrum of the dominant geomorphologic processes. The value of geomorphologic tension in the Russian Far East region ranges from 3 to 16 conventional points: in the Western Okhotsk Sea coast area it was estimated at 7–10 points, in the Sakhalin – 10–12, in the Eastern Kamchatka – 13–15 and in separate Kuril Islands – 16 points. Thus, the study results confirmed the formerly stated supposition about the increase of nature-defined geomorphologic tension of the NW Pacific Ocean sector from the west to the east.

The zone of maximum potential development of catastrophic processes in the SE sector of the Pacific Rim is situated at the western mega slope of the Peruvian Andes between 9°S and 13°30'S and in the band width of 100 km along the Pacific coast. The geomorphologic tension of this area reaches 15–16 points due to natural causes. The tension on the eastern mega slope of the Andes ranges from 9 to 12 points, except for some areas where it increases to 13–14; on the Altiplano it decreases to 6–10 points. An important feature of the study area is the asymmetric distribution of geomorphologic processes, so the geomorphologic tension, which significantly different at the oceanic and the inland (continental) slopes of the mountain chain. Comparison of data obtained for the two segments (NW and SE) of the Pacific Rim allows reaching a conclusion about the general regularities of the distribution of geomorphologic tension in the territory of marginal mountain belts around the Pacific Ocean with more confidence. The areas of potential catastrophic processes are located near the edge of the continent in either case.

**KEY WORDS:** geomorphologic tension, catastrophic processes, mapping, marginal mountain belts, the Far East, Andes

## INTRODUCTION

Research of dangerous and catastrophic relief forming processes has been underway for a long time, and the terms "hazard" and "risk" are widely applied in the geomorphology studies. However, in recent years the new terms have appeared: such as "susceptibility" to certain hazardous processes [Corominas, 2008] and geomorphic "tension" (or intensity) [Lebedeva, 2013a; Lebedeva, 2013b; Lebedeva et al., 2014b; Alizade, Tarikhazer, 2015; Lebedeva et al., 2015]. This allows for more precise determination of the areas which are potential subjects to various geomorphologic catastrophes.

Analysis of the distribution of natural disasters allows concluding that there are areas with more intensive development of catastrophic processes than others. The Russian Far East is one of them: here, according to statistics, the number of emergencies is approximately 2 times greater than the national average. We suggest to name the territories susceptible to catastrophic relief processes *the zones of increased tension (or intensity) of geomorphologic processes or situation of increased geomorphologic tension* [Gotvansky, Lebedeva, 2010; Lebedeva, 2013a, b; Lebedeva et al., 2014b]. The second definition seems to be more correct, since catastrophic processes in these areas are not constant, but the potential of its development, provided by certain forces-conditions, is real, and it materializes with certain probability of additional (in relation to average data) impact of these forces (seismic movements, anomalous hydrometeorological events and others).

Domination of relief features with high background velocities of morphogenesis is a typical situation for these territories, as long as processes which can sharply increase their spatial (volume, coverage, extension) and temporal (transmission rate, frequency and others) properties, in other words, which can develop catastrophically. In addition to the internal features (conditions) of catastrophic appearance (relief with potentially unstable

properties, prone to different influences) acting in these regions it is necessary to have external forces, which cause the extreme character of the area's geomorphologic processes. Seismicity plays the key role among endogenous factors of intensity of contemporary geomorphologic processes in these regions. Among exogenous factors, the most important is the heavy rainfall which provokes a wide range of catastrophic processes. The cumulative effect of these factors greatly increases the probability of natural disasters.

G. Ananyev [Ananyev, 1998] linked the concept of intensity of geomorphologic processes with the balance of lithodynamic flows of the areas. He offered to calculate the value of the tension as the ratio of the maximum and the average volumes of transported material. Without denying the relevance of such calculations for sites where there are data of long-term stationary observations, we propose to analyze the parameters of relief and processes of morphogenesis in complex with endogenous and exogenous factors causing catastrophic development of geomorphic processes for areas where such data are not available.

The geomorphologic tension is defined by the authors as the readiness of geomorphologic system to pull out of the balanced condition and the danger of catastrophic processes developing under the action of external and/or internal forces, both natural and anthropogenic [Lebedeva, 2013, a, b].

Such zones of high geomorphologic tension are situated at the marginal continental mountainous systems of the Pacific Ocean with high parameters of tectonic, seismic and volcanic activity. Unstable state of geomorphologic systems and active relief-forming processes here are enhanced by deep and intensely dissected relief. Climatic factors (precipitation amount and character) also play a vital role. The anthropogenic activities occasionally promote natural processes and enforce the danger of local catastrophes.

Our work is devoted to the north-western and south-eastern segments of the Pacific Ocean coast – the Russian Far East and the central part of the Andes mountain system. We set a goal to analyze specific features and regularities of distribution of the main factors that provoke catastrophic activation of geomorphologic processes and to find out zones of highest geomorphologic tension in these parts of the Pacific Rim as well. In this regard we mapped the geomorphologic tension of key segments.

The Russian Far East is the territory which exhibits extreme diversity of natural processes and phenomena including catastrophic. It can be clearly noted on the maps of current relief dynamics of North Eurasia [2003], of zoning of the territory of Russia to the degree of extreme ecologic-geomorphologic situation [Kozlova et al., 2005] and the map "The ecologic-geomorphologic hazard level of contemporary relief-forming processes" [2006]. The authors refer the major part of the Far East to the territories with the high rate of general ecologic-geomorphologic hazard, where several danger relief-forming processes with high index of intensity act simultaneously, and catastrophic occurrence of the certain processes are possible.

However, it is clear that there are very different areas – with more and less rate of catastrophic processes development. But these maps were compiled based on analysis of geomorphologic processes distribution, which (processes) contribute to formation or escalation of dangerous ecologic-geomorphologic situations, forced by anthropogenic impact, but without consideration of existing endogenous and exogenous forces that can provoke activation of these processes and considerably leverage the risk of natural disasters. Later, the author of one of these maps S.K. Gorelov wrote about necessity of working out the questions of endogenous factors of relief forming for the natural risk estimation [Gorelov, 2008]. Thus, for allocating the certain regions of increased geomorphologic processes

intensity and forecasting possibility of its catastrophic development, additional data of seismic activity of the territory, precipitation distribution character, relief morphology and others were analyzed.

As far as SE sector of the Pacific Rim is concerned, the Andes are the world's most extended mountain system and one of the least explored. In 2007 under the international project, a group of experts from 7 countries, situated within the territory of Andes mountains, have compiled an integral map (scale 1:7500000) of the most disastrous consequences of natural processes and events [Conozcamos los peligros..., 2007]. The nineteen of such events during last 200 years were noted in territory of the Peruvian Andes. A more detailed research of the region has not been conducted yet despite its high relevance.

## RESEARCH METHODS

A mapping method for geomorphologic tension for a small-scale level (1:2.5–1:8 mln) was described in detail by the authors early [Lebedeva, 2013b; Lebedeva et al., 2014b; Lebedeva et al., 2015]. It is based on analysis of the following characteristics: 1) *complex of relief-forming processes* of the territory and their ability to gain catastrophic character, 2) *distinctions of relief morphology*, which contribute to catastrophic development of relief-forming processes, 3) *presence and zonation of demonstration of factors*, which makes background processes extreme.

The authors tested 2 methods of assessing geomorphologic settings tension for 2 Pacific coast segments. These methods are based on the same principles, but differ in the scheme of retrieval of factual material. However, the results were quite comparable. The methods require further improvement, but generally this approach to reconnaissance evaluation of territories is attractive. Moreover, it allows allocating the increased tension zones even within such poorly studied, in geomorphologic respect, mountainous systems as the Andes.

Geomorphologic tension was assessed at the regional level of generalization and scale of the map: we used relative points based on the analysis of seismicity, precipitation quantity, features of relief and a spectrum of relief forming processes.

The leading complex of relief forming processes for the Russian Far East territory, their activity and areas of distribution are shown on the map "The ecologic-geomorphologic hazard level of contemporary relief-forming processes" [2006], which we had taken as the basis. There are 3 levels of hazard evaluation on this map: 1) high – several dangerous relief-forming forces with generally high intensity occur, 2) middle – variety of dangerous processes also occur, but with lower intensity, 3) low – narrow range of processes with low intensity.

Among relief *morphology characteristics*, which promote the development of catastrophic relief-forming processes, we placed special emphasis on the depth of erosion dissection and used the data of the map of "Erosion hazard of relief" [Timofeev, Bylinskaya, 1987]. Considerable depth of dissection is indicative of the higher intensity – e.g. potential possibility – of the vast variety of hazardous slope processes development – landslides, subsidences and others.

*Seismic activity of territory* plays the key role among factors, provoking the intensification of geomorphologic processes and increasing the dangerous situations risk. Even a small earthquake may cause many catastrophic processes: subsidences, landfalls, landslides, avalanches, mudslides, tsunami and others. We used the data from the seismic zoning map OSR-97 [Ulomov, 2013].

The overall quantity, type and intensity of precipitation influence the character and development of relief-forming processes of many regions. Coastal and intercontinental slopes often crucially differ in the marginal continental mountainous systems. Moreover, this difference may reach 500,

1000 and more mm of precipitation, which doubtlessly influence the trend and intensity of geomorphologic processes on slopes of different aspect. Numerical score may estimate the influence of this index.

In carrying out these small-scale cartographic works, evaluation of other factors proved to be problematic. We considered the presence of loose permafrost sediments mass only if the area of its spreading was really extensive and we can show places of influence of contemporary volcanic processes only by marking these active volcanoes with additional symbols.

The technique of geomorphic intensity mapping which was used for the Russian Far East has been adapted by us with the utilization of materials that existed for the territory of the central sector of the Andes. In this case, compilation process for the mapping was more complex than the same process for the Far East due to the absence of some basic maps that were available for the Russian territory. First of all, these include the map of "The ecologic-geomorphologic hazard level of contemporary relief-forming processes" [2006]. That is why the series of additional associated maps was compiled for the Central Andes segment: these are the maps of contemporary relief dynamics and dangerous and catastrophic processes; 16 types of regions with different ranges of prevailing catastrophic processes were determined [Lebedeva et al., 2014a]. This was the base for the final map of ecologic-geomorphologic hazard according to the methods developed by S.K. Gorelov [2008]. Three types of territories were isolated on the map: with high, middle and low rate of ecologic-geomorphologic danger.

Data of relief dissection deepness, available for the Russian part of the Pacific Rim according to the map of "Erosion hazard of relief" (1:2 500 000, IG RAN, [Timofeev, Bylinskaya, 1987]), were also absent for the Andes territory. Profiles of relief (cross-sections) were made to close this gap, using data of the global digital

terrain model GTOPO 30 and digital data SRTM. The GTOPO 30 data, produced based on topographic maps distributed by the Earth Resources Observation and Science (EROS) Center [<http://eros.usgs.gov>], have spatial resolution of around 1 km and guarantee effective 3D-modeling for identification of regional relief characteristics in the study scales up to 1:1000000. A more detailed relief structure research, particularly evaluation of its characteristics, such as dissection depth, is based on the satellite radar data SRTM with spatial resolution of around 90 m and absolute altitude evaluation precision of around 20 m, and allows differentiating relief elements with amplitude of up to the first meters. The depth of dissection was evaluated for squares with the sides of 20 km and profiles 200–300 km long. Thus we found the dissection depth for every surface segment, approximately 400 km<sup>2</sup> in size, which is comparable to the data of “Erosion hazard of relief” map that we have used for the Far East.

For seismic zoning we used the Global Seismic Hazard Assessment Program (GSHAP) data. A probabilistic map of seismic hazard, obtained from the GFZ German Research Centre for Geosciences [<http://gmo.gfz-potsdam.de>], is represented with the data on ground acceleration, which can be exceeded during 50 years with 10 % probability, which corresponds with the following frequency period of such a seismic impact – 1 time in 500 (475 is more correct) years (the Russian analogue is the map “A» OSR-97). Revaluation of the GSHAP data on a 12-point intensity scale, which is used in Russian seismic zoning, is made using normative correlations.

Evaluation of the annual precipitation of this territory is based on the South American map of precipitation, compiled from climatic and weather data, handled, archived and distributed by the Earth System Research Laboratory of the National Oceanic and Atmospheric Administration, USA [<http://www.esrl.noaa.gov>]. The map represents the averaged data of annual precipitation for the

period 1976–2009 years in a spatial grid with 2.50 mesh.

It should be pointed out that the most large scale geomorphologic disasters of the region are distinguished by overlapping and interconnecting the number of extreme processes. Thus, in that case we consider acceptable to add data on the magnitude of the studied characteristics, relevant increasing action of external agents, provoking catastrophic processes, or showing the morphosystem inner characteristics specificity (geomorphologic circumstances), also leading to increasing exogenous processes intensification. However, because of the different dimension and magnitude of the studied characteristics, the straight addition is not correct; thus, we, according to [Simonov, 1997; Liang at al., 2012], conducted “normalization” of the values by formula  $X' = (X - X_{\min}) / (X_{\max} - X_{\min})$ , where  $X$  is the real value of the characteristic,  $X_{\max} - X_{\min}$  is the range of its possible values, and  $X'$  – the normalized characteristic’s value within the interval from 0 to 1. Also, for calculation convenience [Liang at al., 2012] we converted the fraction values into the whole values, and considered them as the relative tension points. Moreover, due to the regional nature of our research, we analyzed not the characteristics’ particular values, but their specific intervals.

Thus, for the estimation of more important, in our opinion, factors – seismicity and precipitation – we used a 10-point scale. However, this approach is not flexible to accommodate every characteristic. Thus, the scale of conducted mapping does not allow us to show in details the true relief dissection depth and requires specific generalization. Moreover, although tension increase (susceptibility to catastrophic processes) does not depend on dissection depth, but beginning from certain values it does not grow at the same rate, as, for example, after quakes intensity increases. In turn, the ecologic-geomorphologic hazard level of the territory (the range of dominating relief forming processes) is the qualitative characteristic and

Table 1. Interrelation of points and ranges of values of the main factors of geomorphologic tension

Factors	Ranges of values	Points
Seismicity (intensity of shocks), points	VI–VII	1
	VII–VIII	2
	VIII–IX	4
	IX–X	6
	X–XI	8
	> XI	10
Precipitation quantity, mm per year	500–1000	1
	1000–1500	2
	...	...
	> 5000	10
Erosion dissection depth, m	400–800	1
	800–1600	2
	> 1600	3
Ecological-geomorphologic hazard	Low	1
	Middle	2
	High	3

is noted for some subjectivity. As the result, in both cases, when grading this index, we had to prefer the expert evaluation and use the less fractionary scale with the maximum value of 3 points. Interrelations of the relative points and input value intervals of tension forces are shown in Table 1.

We understand that such an approach is quite conventional, and relies on expert assessment, but in case of this small-scale mapping it is the most correct method. This has been supported by our attempts of using a single (10 or 3) scale for all indicators. Actually, in the case of a single scale for all indicators, correction factors introduced usually are also based on expert assessment, as we see, for example, in [Bolysov et al., 2015].

All of these allowed us to obtain the so-called semi-quantitative reconnaissance evaluation, which, in its turn, allows comparing certain regions and isolating the zones of increased geomorphologic tension, i.e., sites with the maximum rates of characteristics, promoting intensification of morpholithogenesis processes.

## DISCUSSION

Preliminary analysis of the natural preconditions of the geomorphologic tension in the Russian Far East [Gotvansky, Lebedeva, 2010] suggests increase of the tension towards the Pacific Ocean due to increase of impact of endogenous and exogenous factors, the features of contemporary tectonics and volcanism, of moisture of air masses and of the proximity of the main basis of denudation – the ocean level. Maps of naturally determined geomorphologic tension of processes (scale 1:2500000 and 1:8000000) were compiled firstly for the key parts of the Russian Far East – Kamchatka, Sakhalin and the Western Okhotsk region. These territories vary on geodynamic processes, landscape-climatic conditions and character of modern geomorphologic processes, and are indicative of differentiated estimation of geomorphologic tension. This allowed us to clarify and correct the method. For the key areas we also defined the territories under intense anthropogenic impact (the result of construction and mining). However, on the integral map of the Russian Far East (scale 1:8 000 000) (Fig. 1) we had to limit our efforts

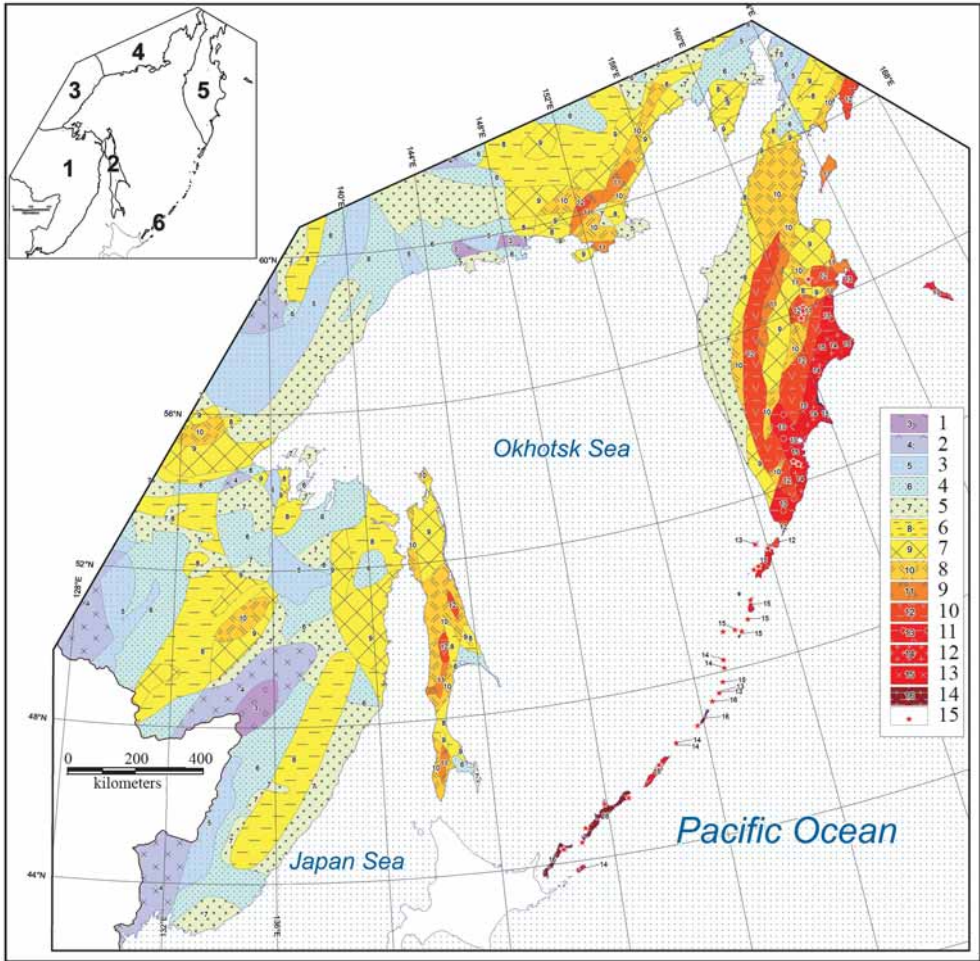


**Fig. 1. Map of geomorphologic tension of the Russian Far East, scale 1:8000000. Legend:**

1–14 – naturally determined geomorphologic tension (in points), 15 – active volcanoes.

On inset: regions: 1 – Primorye and Amur River Region; 2 – Sakhalin; 3 – Western Okhotsk Sea coast region, 4 – Northern Okhotsk Sea coast region; 5 – Kamchatka, 6 – Kuril Islands

to only naturally determined tension of the processes.

In the mainland of the Russian Far East, the naturally determined tension of geomorphologic conditions generally ranges from 3 to 10 points. For the Stanovoy ranges' roof-block uplift (the activated margin of the Aldanian shield with traces of late Pliocene volcanic activity) the deep dissection (up to 1000 m), seismic activity of up to 8 points and a wide range of dangerous geomorphologic processes are characteristic. Near interstream areas, seismogenic splits exist and there

are many traces of seismic landslides. The total tension of Tokinsky Stanovik is 10 points. The Badzhalsky range, located at the junction of the Bureinsky platform massive and the Sikhote-Alin folded region, also belongs to a 8-point earthquakes zone. Seismic landslides occurred here in historical time, forming barrier lakes in the Gerby river confluents valleys. The erosion dissection depth here is close to 1000 m. Badzhalsky lies on the monsoon route, which results in a high level of precipitation here of more than 1000 mm annually, causing summer river flooding and winter snow avalanches in the mountains. The

total tension in the central part of the range reaches 10 points also.

Geomorphologic tension, determined by natural forces, on the continental part is the highest in the Taigonos Peninsula and adjacent mountainous ranges (Tumansky, Nenkat), where it reaches 10–12 points. This is a zone of VIII–IX points earthquakes with numerous traces of paleo seismic dislocations. The peninsula itself is limited by faults stretching north-east, located as fault scarps in the relief. Its absolute heights reach 1600 m and dissection depths reaches 600–800 m. There is up to 1000 mm precipitation annually on the north-eastern mountainous slopes.

Geomorphologic tension, determined by natural forces, for the Sakhalin Island, which was divided onto 21 regions, fluctuates from 6 to 12 points. Eleven regions are the areas of extremely high tension (10–12 points): the Shmidt Peninsula, the north-western lowland, the West-Sakhalin mountains (excluding the Poyasok land bridge) and the northern and central parts of the East-Sakhalin mountains. The main features are high seismic activity (VIII–IX points), a wide range of dangerous geomorphologic processes, abundance of precipitation (over 1000 mm/year), and, in the certain parts, dissection deepness (400–800 m) and perennially icy frozen rocks (North-Western lowland).

Within Kamchatka we isolated 48 regions with tension from 7 (Western coast) to 15 (Eastern coast) points. The maximum tension (15 points) is on the Kronotsky and Shipunsky Peninsulas, on the Gamchen and Balaganchik ranges and some parts of the Koryaksky and Kronotsky volcano massifs. These areas have high seismic activity (X points), abundance of dangerous geomorphologic processes, deep territory dissection (over 800 m) and abundance of precipitation (over 1000 mm/year). Tension is lower (14 points) on the Kronotsky and Avachinsky bay shores and on the Mutnovsky volcano due to decrease of the dissection deepness. This, along with decrease of annual precipitation, reduces the index of

geomorphologic tension to 13 points in the Kamchatsky Mys Peninsula, Kamchatsky bay coast, Ilyinskaya and Zheltovskaya volcano massifs and in the Ganalsky range southern part. For the Sredinny range on Kamchatka and the Kumroch, Tumrok, Valaginskii and other ranges, tension is 12 points, which is determined by decrease of seismic activity to IX points in the territory towards the west.

The maximum of naturally determined tension of 16 points (which we determined as potentially catastrophic) is typical of the Kuril Islands – Paramushir, Kotoj, Simushir, Iturup, and Kunashir. A high degree of ecologic-geomorphologic hazard (vast extent of dangerous geomorphologic processes) is combined with high seismic activity (X points), abundance of precipitation (over 1000 mm/year) and considerably deep relief dissection (altitude difference of up to 1000–1500 m and more). Active volcano presence increases the risk of potential catastrophic processes.

Geomorphologic tension, determined by natural forces, generally varies from 3 to 16 points in the Russian Far East region. The distribution regularities of the zones of naturally determined tension of geomorphologic processes in the Far East region were considered earlier [Gotvansky, Lebedeva, 2010; Lebedeva and others, 2014b]. The results of the study have supported the suggested hypothesis that naturally determined geomorphologic tension (i.e., susceptibility to catastrophic morphogenesis processes) is generally increasing here from the west to the east towards the Pacific ocean: it was estimated at 7–10 points for the Western Okhotsk Sea coast, at 10–12 points for the Sakhalin, at 13–15 points for the Eastern Kamchatka and at 16 points for the Kurils.

Mapping of the Peruvian segment of the Andes (between 5–19°S) that we have conducted (Fig. 2) showed that geomorphologic tension of the region varies from 6 to 16 points. Therefore, the maximum tension of 15–16 points, which we consider as potentially

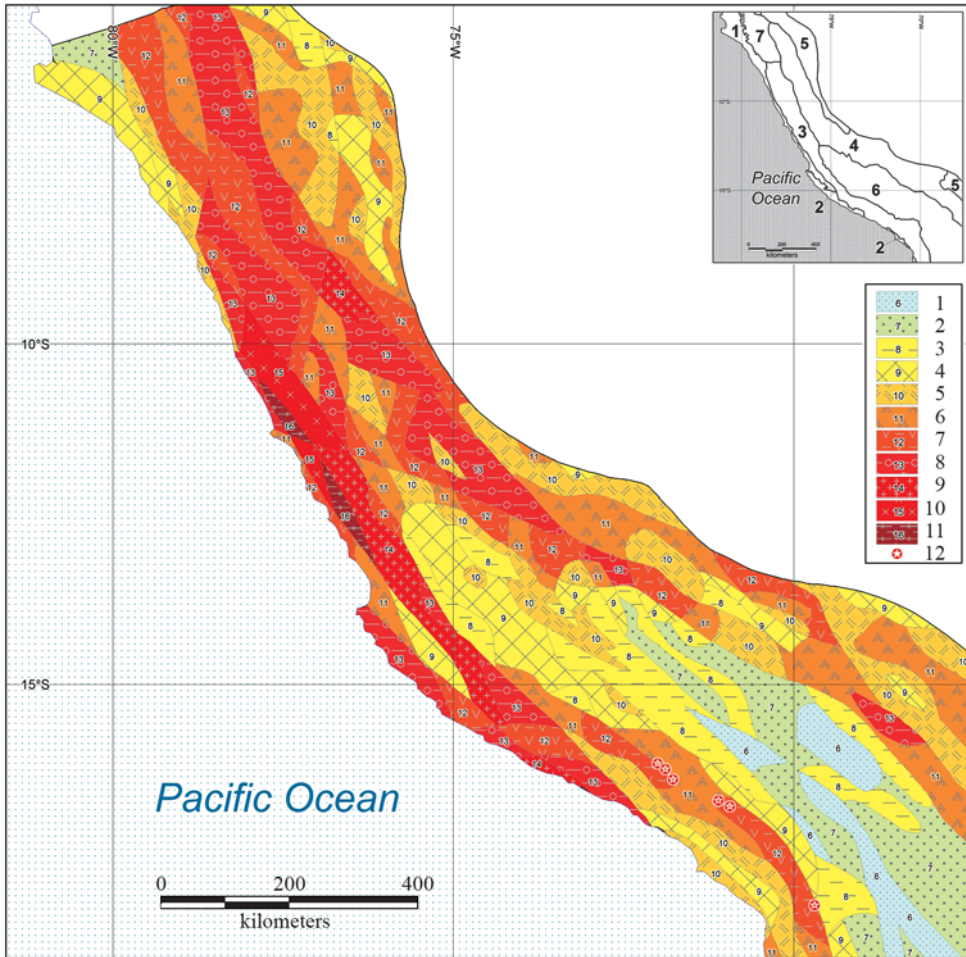


**Fig. 2. Map of geomorphologic tension of the Peruvian Andes, scale 1:8 000 000. Legend:**

1–11 – natural-determined geomorphologic tension (in points), 12 – active volcanoes.

On inset: orographic zoning elements: 1 – coastal plains, 2 – coast ranges, 3 – Western Cordillera, 4 – Eastern Cordillera, 5 – the Andes eastern branches, 6 – Altiplano, 7 – Amotape-Chanchan zone.

catastrophic, is typical of the western mega slope of the marginal-continental mountainous system in the interval from 9° to 13°30'S in a strip of up to 100 km from the coast. This territory is occupied by high (4000 m and higher) and very deeply dissected ridges and massifs of the Western Cordillera with a wide complex of large scale gravitative and seismic-gravitative processes (rockfalls, talus, landslides, avalanches and others), as well as it is subjected to active erosion and mudflows. This territory includes the river Santa basin, which associates with large catastrophes of the XX century in Uaras town

(1940) and near the foot of the Uascan massive (1962 and 1970), caused by mass movement of weathering waste under the influence of seismic events.

Southwards from this the most dangerous zone, tension of the western Andes mega slope (Western Cordillera) is estimated at 12–14 points due to a somewhat lesser seismic activity of the territory with the same high and deeply dissected ridges. Tension of geomorphologic settings of the extinct and active volcanoes chain, rimming Altiplano from the south-west, is estimated at 11–12 points.

Lahars, erosion and badlands forming on fragile volcanites are possible here along with gravitative processes (including debris avalanches).

The northern part of the western Andes mega slope within the studied area is represented by short differently oriented ridges of the Amotape-Chanchan zone with the absolute altitude, dividing ranges, of 600–3000 m with prevailing gravitative and seismic-gravitative processes, erosion and mudflows. Geomorphologic settings tension is estimated at 11–12 points.

Tension of 12–14 points were found for coastal densely and deeply dissected ranges with absolute elevations of up to 2500–3000 m. Within low coastal ranges (absolute altitude 200–300 m), tension reaches 12–13 points, and in coastal lowland plains it ranges from 7–9 points in the north to 11–12 in the central part. This variation is due to different seismic activity of the territory.

The Andean Eastern Cordillera in the north of studied territory is represented by block middle and high ridges and massifs, 1000–3000 m high. Gravitative and seismic-gravitative processes are dominating among dangerous and catastrophic processes and tension varies from 12 to 14 points. Southwards, deeply dissected block high mountainous ridges and massifs prevail (absolute altitude of 2000–4000 m), tension is 11–12 points and more rarely is 13 points. The eastern Andes mega slope also includes adjacent ridgy low-hills (absolute altitude of 500–1500 m) in the northern and the southern parts of the territory with dominance of gravitative and seismic-gravitative processes, fissuring and erosion. Geomorphologic tension of these areas is estimated at 9–11 points.

The central and the southern parts of the Andes axial region is occupied by Altiplano with absolute heights of 3000–4000 m, rimmed by the Western and Eastern Cordillera. In its northern, more dissected part (12°–17°S), erosion with gravitative processes is active

and geomorphologic tension is estimated at 8–10 points. In the southern Altiplano, dissection is ten times smaller, plain lands with separate farewell rock massifs prevail and tension is 6–8 points.

According to the conducted mapping, it has been concluded that potential naturally determined geomorphologic tension of the Peruvian Andes western mega slope, which is the zone of the maximum risk of catastrophic processes, reaches 16 points. For the eastern Andes mega slope, this index is 9–12 points, rarely reaching 13, and for Altiplano, it ranges within 6–10 points. The important feature of the studied territory is the asymmetric distribution of both geomorphologic processes and geomorphologic settings tension on the Pacific coastal and near-continental slopes of the mountainous system.

## CONCLUSION

The compiled maps allowed us to evaluate naturally determined intensity of the extent of geomorphologic processes of the studied regions, associated with geologic-tectonic and physiographic features of the territory, to isolate the potential risk zones and to analyze their location.

Thus, the map of geomorphologic tension can be considered as a stage of study and zoning, which allows selecting areas that are most at risk of unfavorable geomorphologic processes. It is very important for such dynamic, but actively explored regions of continental-margin mountain systems of the Pacific Ocean coast. The proposed method makes it possible, with a sufficient degree of objectivity, to identify territories of potential activation of geomorphologic processes in areas with high depth of erosional dissection, seismic hazard and a wide range of active geomorphic processes.

Comparison of material about two segments of the transitional zones of the Pacific Rim – the north-western and the south-eastern – allows

**Table 2. Geomorphologic parameters and nature factors for geomorphologic tension evaluation: capabilities of small scale and middle scale mapping**

Parameters /Factors	Scale of the map	
	1:2 500 000– 1:8 000 000	1:500 000–1:1 000 000
Relief forming processes	Ecological-geomorphologic hazard, points	Dominant geomorphic processes spectrum Catastrophic processes spectrum
Features of relief morphology	Depth of the relief dissection, m	Depth of the relief dissection Density of erosion dissection
Seismicity hazard	Intensity of shocks, points	Focuses of earthquakes with a magnitude > 7 Highly seismic zones of linear structures intersection Active contemporary vertical and horizontal movements
Precipitation	Precipitation quantity, mm per year	Irregularity rainfall during the year Intensity of precipitation
Volcanism	–	Active volcanoes
Composition of bedrock	–	Stability of rocks (solid, loose, karst rocks) Permafrost

confidently identifying common regularities of developing tension of geomorphologic settings of the marginal-continental Pacific Coastal region mountainous systems and isolating the zones of high risk of catastrophic processes: the areas of potential catastrophic processes are located near the edge of the continent in either case.

However, it became obvious that the used mapping scale can hardly consider all factors, which we initially were going to take into account, notably, the density of erosional dissection, types of precipitation, presence of highly seismic zones of linear structures intersection, active contemporary vertical and horizontal movements and others. All these are possible in case of a medium-scale mapping. The next step of further research on geomorphologic tension and forecast estimates of the risk of catastrophic processes is analysis of selected zones

of maximum tension at larger scales. We propose [Lebedeva, 2015] to map these potentially the most dangerous sections at a scale of 1:500 000–1:1 000 000 considering additional factors listed above (Table 2). As a result, for the key areas identified earlier, regional zones of high geomorphologic tension and potential crises will be delineated on medium-scale maps. The next step is the identification of the most dangerous sections and within these new zones at a large scale (1:100 000).

Such an approach is justified for the selected region because of a considerable length of marginal mountain belts of the Pacific Rim. In the future, it will solve not only applied, but also the fundamental problems – evaluation of geomorphologic tension and distribution of areas of the maximum tension (where the risk of catastrophic processes is the highest) in the mountain systems the Pacific Ocean coast on the whole. ■

## REFERENCES

1. Alizade E.K. and Tarikhazer S.A. (2015) Ekogeomorfologicheskii risk i opasnosti territorii Bol'shogo Kavkaza (v predelakh Azerbaidzhana) (Ecogeomorphologic danger and hazards at Major Caucasus (in the limits of Azerbaijan)). Moscow: MAK Press, 208 p. (in Russian).

2. Ananyev G.S. (1998) Katastroficheskie protsessy reliefoobrazovaniya (Catastrophic relief forming processes). Moscow: MGU. 100 p. (in Russian).
3. Bolysov S.I., Bredikhin A.V., Eremenko E.A. (2015) Geomorfologicheskaya bezopasnost' Rossii (Geomorphologic safety of Russia). Geomorfologicheskije resursy i geomorfologicheskaya bezopasnost': ot teorii k praktike / Materialy Vserossi'skoi konferentsii "VII Schukinskie chtenija" (Geomorphologic resources and geomorphologic safety: from theory to practice. VII Schukin Conference: Extended abstracts) M.: MAKS Press. 11–16 pp. (in Russian)
4. Conozcamos los peligros geologicos en la region Andina/ Servicio Nacional de Geologia y Minería. (2007) Publication Geologica Multinacional. N 5. 78 p.
5. Corominas J. (2008) Guidelines for landslide susceptibility hazard and use planning / Engineering Geology. DOI: 10.1016/j.enggeo.2008.03.022
6. Gorelov S.K. (2008) O probleme ekologo-geomorfologicheskogo kartirovaniya (na primere territorii Severnoi Evrazii) (On the problem of ecologic-geomorphologic mapping (the Northern Eurasia as an example)) // Geomorfologiya, N 2: 61–66. (in Russian with English summary).
7. Gotvansky V.I. and Lebedeva E.V. (2010) Vlijanie prirodnyh i antropogennyh faktorov na napriazhionnost' geomorfologicheskikh protsessov na Dal'nem Vostoke (Natural and anthropogenic factors influence on geomorphologic processes intensity in the Far East) // Geomorfologiya, N 2: 26–36. (in Russian with English summary)
8. Kozlova A.E., Lokshin G.P., and Chesnokova I.V. (2005) Karta rajonirovaniya territorii Rossii po stepeni ekstremal'nosti razvitija ekologo-geomorfologicheskikh protsessov (Map of zoning of the territory of Russia on the degree of extreme ecologic-geomorphologic situation). Scale 1:9 000 000. M.: IG RAN.
9. Lebedeva E.V. (2013a) Prirodnye i tehnogennye predposylki napriazhionnosti geomorfologicheskikh protsessov And (Natural and anthropogenic basis of geomorphologic processes intensity in the Andes) // Geomorfologiya, N 4: 48–61 (in Russian with English summary)
10. Lebedeva E.V. (2013b) Printsipy sostavleniya karty napriazhionnosti geomorfologicheskikh protsessov okrainno-kontinental'nyh gornyh system Dal'nego Vostoka (The foundation of the map on intensity of geomorphologic processes of the Far East continental margin mountain belts). // Geomorfologiya i kartografiya. Materialy XXXIII plenuma Geomorfologicheskoi Komissii RAN (Geomorphology and Cartography: Proceed. of XXXIII plenum of Geomorphological Commission RAS). Saratov: SGU. 507–511 pp. (in Russian)
11. Lebedeva E.V. (2015) Napriazhionnost' geomorfologicheskikh obstanovok okrainno-kontinental'nyh gornyh system Pritihookeanija (Tension of geomorphologic conditions of the marginal -continental mountain belts of the Pacific Ocean coast). Geomorfologicheskije resursy i geomorfologicheskaya bezopasnost': ot teorii k praktike / Materialy Vserossi'skoi konferentsii "VII Schukinskie chtenija" (Geomorphologic resources and geomorphologic safety: from theory to practice. VII Schukin Conference: Extended abstracts) M.: MAKS Press. 129–132 pp. (in Russian)

12. Lebedeva E.V., Mikhalev D.V., Novoa J.E., and Kladovschikova M.E. (2014a) Geomorphological hazard and disasters in the South American Andes // *Geography. Environment. Sustainability*, N 1: 80–98.
13. Lebedeva E.V., Mikhalev D.V., and Shvarev S.V. (2015) Geomorfologicheskaya napriazhionnost' tsentral'nogo sektora gornoj sistemy And (Geomorphologic tension of the Central Andes) // *Geomorfologiya*, N 2:77–88. (in Russian with English summary)
14. Lebedeva E.V., Shvarev S.V., and Gotvansky V.I. (2014b) Prirodno-obuslovlennaja napriazhionnost' geomorfologicheskikh protsessov territorii Dal'nego Vostoka Rossii (Naturally determined geomorphologic processes tension of the Russian Far East territory) / *Geomorfologiya*, N 4: 48–59 (in Russian with English summary)
15. Liang W.J., Zhuang D.F., Jiang D., Pan J.J., and Ren H.Y. (2012) Assessment of debris flow hazard using a Bayesian Network. *Geomorphology*, v. 171–172: 94–100.
16. Simonov Y.G. (1997) Ball'nye otsenki v prikladnyh geograficheskikh issledovaniyah I puti ih sovershenstvovaniya (Scoring in applied geographical studies and its development). *Vestnik MGU, ser. 5. geogr.*, N 4: 7–10 (in Russian with English summary).
17. Karta sovremennoi dinamiki reliefa Severnoi Evrazii (The map of current relief dynamics of North Eurasia). (2003) Scale 1:5 000 000. M.: IG RAN.
18. Karta "Stepen' ekologo-geomorfologicheskoi opasnosti sovremennyh reliefoobrazujushchih protsessov" (The map "The ecologic-geomorphologic hazard level of contemporary relief-forming processes") (2006) Scale 1:8 000 000. M.: IG RAN.
19. Timofeev D.A. and Bylinskaya L.N. (1987) Karta otsenki erosiionnoi opasnosti territorii SSSR (USSR map of erosion hazard evaluation)/ *Erosionnye I ruslovye protsessy v razlichnyh prirodnyh uslovijah* (Erosion and river bed processes in different natural conditions). Moscow: MGU. 24–25 pp. (in Russian).
20. Ulomov V.I. (2013) Obschee seismicheskoe zonirovanie territorii Rossijskoi Federatsii (The General Seismic Zoning of the territory of Russian Federation) // *Problemy ingenernoi seismologii*, v. 4, N 4: 5–20 (in Russian)
21. <http://eros.usgs.gov>
22. <http://gmo.gfz-potsdam.de>
23. <http://www.esrl.noaa.gov>



**Ekaterina V. Lebedeva** is Senior Researcher of the Laboratory of Geomorphology, the Institute of Geography, RAS, and Executive Secretary of the editorial board of the journal "Geomorphology". She graduated from the Lomonosov Moscow State University and received her Ph. D. degree in 1992. The area of her scientific interest: relief evolution in the changing natural conditions and under the influence of anthropogenic factors, intensity of geomorphologic processes, relief of volcanic regions, ecologic-geomorphologic problems. Regions of Research: Russian Far East, South and East Africa, South and Central America, Australia. She is the author of about 100 scientific papers.



**Dmitry V. Mikhalev** is Senior Researcher of the Laboratory of Geoecology of the North, Lomonosov Moscow State University. He received his Ph. D. degree in 1990. The area of his scientific interest: isotope geocryology, paleogeography, paleoclimatology, cryogenic processes, geoecology. Regions of Research: Russian Arctic, South and East Africa, South and Central America, Australia. He is the author of about 70 scientific papers.



**Sergey V. Shvarev** graduated from the Geomorphology Department of the Faculty of Geography, Lomonosov Moscow State University in 1986. He received his Ph. D. degree in geoecology from the Moscow University of Geodesy and Cartography in 2006. He is Lead Researcher at the Laboratory of Geomorphology of the Institute of Geography, RAS, and Research Fellow (part time) at the Schmidt Institute of Earth Physics, RAS. The areas of his scientific interests include exogenic processes, geotechnical systems, natural-techogenic disasters, morphotectonics, paleoseismology and neotectonics. He has participated in scientific field expeditions in different regions of Eurasia. He is the author (co-author) of five monographs, and about 100 papers in journals and conference proceedings.



**Veniamin I. Gotvansky** is Senior Researcher; he received his Ph.D. degree in geography. He has been a member of the Russian Geographical Society since 1957. He worked for many years in the Far East of Russia. Not only problems of geomorphology but also ecology are in the focus of his research; for example, preservation of watercourses of the Amur River basin is under his special attention

**Anna N. Tkachenko<sup>1\*</sup>, Maria I. Gerasimova<sup>1</sup>, Michael Yu. Lychagin<sup>1</sup>,  
Nikolay S. Kasimov<sup>1</sup>, Salomon B. Kroonenberg<sup>2</sup>**

<sup>1</sup> Department of Landscape Geochemistry and Soil Geography, Faculty of Geography, Lomonosov Moscow State University; Leninskiye Gory, Moscow, 119899, Russia

\* **Corresponding author**; e-mail: ekaterina.lebedeva@gmail.com

<sup>2</sup> Afdeling Geotechnologie, Stevinweg 1, 2628CN Delft; Tel: 00 31 (0)15 278 1328, Fax: 00 31 (0)15 278 1189, e-mail: salomonkroonenberg@gmail.com

## BOTTOM SEDIMENTS IN DELTAIC SHALLOW-WATER AREAS – ARE THEY SOILS?

**ABSTRACT.** This article is based on long-term research of aquatic landscapes in the Volga River delta which was held in 2010–2012 and included investigation and sampling of bottom sediments in deltaic lagoons, fresh-water bays, small channels, oxbow lakes, and part of the deltaic near-shore zone. Contrasting hydrological regime and suspended matter deposition together with huge amount of water plants in the river delta provide for the formation of different types of subaquatic soils. The purpose of this research is to reveal the properties of the subaquatic soils in the Volga River deltaic area and to propose pedogenetic approaches to the diagnostic of aquazems as soil types. It is suggested to name the horizons in aquazems in the same way as in terrestrial soils in the recent Russian soil classification system, and apply symbols starting with the combination of caps – AQ (for “aquatic”). The aquazems’ horizons are identified and their general properties are described. Most typical of aquazems is the aquagley (AQG) horizon; it is dove grey, homogeneous in color and permeated by clay. The upper part is usually enriched in organic matter and may be qualified for aquahumus (AQA) or aquapeat (AQT) horizons. In case of active hydrodynamic regime and/or strong mixing phenomena, the oxidized (AQOX or aqox) horizon, or property could be formed. It is yellowish-grey, thin, and depleted of organic matter. The main types of aquazems specified by forming agents and combinations of horizons are described.

**KEY WORDS:** subaquatic soils, soil classification, river deltas, aquatic landscapes, Volga River delta.

### INTRODUCTION

The upper layers of sediments in shallow lakes, ponds, coves, marine shelves and deltaic zones are referred to as soils by some scientists starting with the famous soil scientist and micromorphologist W. Kubiena, who separated the trunk of Subaqueous soils from the trunk of Semi-terrestrial and Terrestrial ones as early as in 1953 [Soils of Europe, 1953]. In the last decades, the traditional perception of soil as of a natural-historical

body on the earth surface with its genetic horizons and diverse ecological services (soil functions of [Dobrovolskiy and Nikitin, 1986]) has been expanded over technogenic and some other objects. The first “technozems” for rehabilitated coal mining wastes appeared in 1989 [Yeterevskaya, 1989], the next were the oil-modified soils [Solntseva, 1998, 2009] and sealed soils in towns [Prokofieva, 1998], then soils of other industrial and mining areas [Burghardt, 1996; Rossiter, 2007]; finally such soils found their place in the World References

Base for soil resources – WRB [2006, 2014] as Technosols. Among natural objects, the organomineral bloom on the walls of caves was argued to be soil as well [Semikolennykh, 2012]. Most striking was the inclusion of extremely thin algal films on the surfaces and in the fissures of hard rocks investigated in Antarctic [Goriachkin, et al., 2014]. In this array of objects pretending to be soils, those in shallow water with a differentiation into discernible strata with diffuse boundaries and affected by biota are not the last candidates.

This approach to some subaqueous bodies as to soils is proven by their inclusion into recent classification systems: the International system – WRB [2014], German system of 1975, and American Soil Taxonomy [1999]. They are absent in Chinese, Canadian, French, and Russian systems.

The history of subaqueous soil investigations is poor. Few publications are known in Russia [Batoyan 1983; Batoyan, Moiseenkov, 1988], simulation experiments with artificial gleying had some analogy with phenomena occurring in the underwater soils [Bloomfield, 1951; Zaidel'man, Narokova, 1978]. In landscape geochemistry, subaquatic landscapes are usually mentioned as final members of catenas [Perel'man, Kasimov, 1999], without specifying their soils. The tidal belts were studied not once by soil scientists, who identified special soils there, namely, acid sulfate soils [Krasil'nikov, Shoba, 1997] or Thionic Fluvisols of WRB, and there are no doubts on their pedogenic essence. At the same time, they seem to be intermediate members in the coastal soil-geochemical continuum: terrestrial alluvial soils – semiterrestrial acid sulphate soils – post-subaqueous soils [Kasatenkova, 2011].

A serious contribution to the subaqueous soils research was made by American scientists [Demas, Rabenhorst, 2001; Bradley, Stolt, 2003; Stolt, et al., 2011]. An important impetus for this research was an applied one: development of aquaculture of hard clams and oysters that require knowledge about the shallow-water environments [[http://nesoil.com/sas/Ditzler\\_SubaqueousPaper\\_Draft.pdf](http://nesoil.com/sas/Ditzler_SubaqueousPaper_Draft.pdf)].

com/sas/Ditzler\_SubaqueousPaper\_Draft.pdf].

Moreover, the subaqueous soils can be considered as a depot for pollutants. According to the isotope data analysis and, for example, heavy metals content, it is possible to follow the story of river landscapes pollution, and to assess the dynamics of pollution by comparing several water bodies in different places [Winkels et al., 1998; Chalov et al., 2016].

The thickness of subaqueous (or underwater) soil-like formations ranges from the first centimeters to a meter or even more. The reason to consider them soils is their vertical pattern resembling terrestrial (“normal”) soils with strata created by sedimentation of solids. In such underwater soils, the types of stratification patterns are repeated in similar environments, like types of soil profiles on the land; the transitions between strata are mostly gradual as between horizons in the majority of soils, and even some processes are common in terrestrial and underwater soils. In the latter, processes may operate in rather stable sites, where the currents are weak, and accumulation of bottom solid-phase substrates by sedimentation proceeds parallel to their pedogenic-like modification. Another important prerequisite is the growth of plants giving organic residues for humus-like layers to be formed in the upper parts of the underwater soils; fishes, mollusks and other animals surely contribute to accumulative and mixing phenomena.

Thus, among the numerous underwater objects only those may be identified as soils that meet the following requirements: (i) have a vertical differentiation; (ii) occur in shallow water bodies (< 2 m); (iii) are related to plants, either rooted, or floating. This means that they are in acceptable agreement with the classic Dokuchaev's formula  $s = f(c, o, r, p, t)$ ; the 'weaker links' of this chain are climate and relief ( $c$  and  $r$ , respectively): their effects are mitigated by the water layer and partly replaced by currents and casual sedimentation controlled by the underwater topography.

The purpose of this research is to reveal the properties of solid-phase bodies in the Volga River deltaic areas that allow qualifying these bodies as soils, and to propose pedogenetic approaches to them. Tackling them as soils, allows applying the appropriate methods for their investigation, namely, pedogenetic and landscape geochemical, enabling more adequate sampling, in particularly for isotope identification. Moreover, for their sustainable management, their functioning as soils should be taken into account.

**OBJECTS AND METHODS OF STUDY**

The advantage of deltaic areas for identification of subaqueous soils is the contrasting regime (hydrological and geochemical) of the ‘river – sea’ system [Kasimov et al., 1999]. The present research is based on the data obtained from the field studies of the Volga River estuarine zones in 2005–2012 [Lychagin et al., 2011]. The objects of the investigation were deltaic lagoons, fresh-water small bays, big and small channels, and also the part of deltaic near-shore zone (Fig. 1).

The methods to study the underwater soils are specific for morphological research,

and sampling, though they do not practically differ from the traditional methods used for analytical studies. Augering is the only means to obtain the profile and to identify horizons in it, which is rather a limitation versus the usual ‘field’ morphology: such common morphological properties as structure and consistence cannot be recorded; another limitation is the small horizontal size of the object determined by the diameter of the auger: 5–7 cm. However, there is also an advantage: all underwater soils are observed in similar conditions, and the inaccuracy caused by the differences in moisture content in terrestrial soils is avoided.

The following procedures were applied in the subaqueous soils investigation:

- morphological description of the whole thickness (profile) and of the individual layers (horizons), namely, thickness, color and its heterogeneity, texture, kind of transition, plant residues, and shell debris;
- pH, redox potential, and TDS express-test by HANNA-Instruments portable devices;

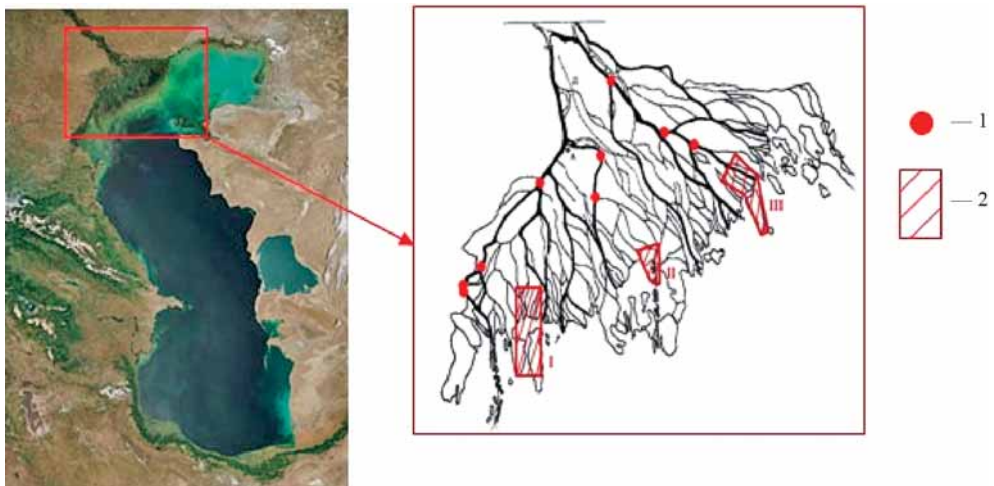


**Fig. 1. The study area:**

1 – The stations for studying water chemistry, suspended matter, and subaqueous soils in the Volga Delta;  
 2 – The key areas of the Astrakhan Biosphere Reserve, with a detailed study of subaqueous soils:  
 I – Damchiksky, II – Trehizbinsky, III – Obzhorovsky.

- granulometric analysis by Laser Particle Sizer “Analissette 22” (Fritsch GmbH, Germany);
- organic carbon content (by the method of Tiurin).

Unlike the methodology for terrestrial soils developed by several research groups and individuals [Soil Survey Manuals in the USA and USSR; FAO Guidelines for Soil Description. 4th edition. Rome; Rozanov, 1983], only first steps are made in respect of underwater soils, and the morphological methods of their studies should be improved and developed.

Nevertheless, investigations in the Volga delta key sites were performed during several years, in different seasons, and the variants of subaquatic soils were the same irrespective of the season, as well as the trends of processes recorded.

## RESULTS AND DISCUSSION

The studies performed and analysis of rather scarce publications enable us to propose some operational terms for subaquatic soils and their horizons following the terminology and conceptual background of the ‘Classification and Diagnostic of Soils of Russia’ [2004]. The first and the main one is *aquazem* as a general term for solid-phase formations in shallow-water bodies. Although the name itself is linguistically an oxymoron as it combines two mutually excluding elements (water and earth), it was used for paddy soils in the early version of the Russian soil classification system [1997], but it was excluded from the later versions. Well-known Japanese pedologists – “fathers of paddy soils” Kawaguchi and Kiuma named them “aquorizems” in 1974. Hence, the term *aquazem* is “free” to be used for subaqueous soils.

Assuming the study objects – aquazems – to be soils, they are discussed in terms and aspects applied to soils: profile and horizons, properties, environments or soil-forming agents, geography, ecological services.

### *Horizons and profiles of aquazems, and processes responsible for their formation.*

The profile of aquazems is weakly differentiated compared to terrestrial soils, and is dominated by ‘cold’ grey or dusky color. Its thickness ranges from 5 cm to 50-60 cm and even more, and two or three distinctly discernible horizons are common. It is suggested to name the horizons in aquazems in the same way as it is done for terrestrial soils in the recent Russian soil classification system, and apply symbols to them starting with the combination of caps – AQ (*aqua*).

The upper layer is usually represented by organic (humus?) horizons. Their thickness and organic carbon content vary from 3 to 10 cm and 1.5 to 6 % of humus; these parameters depend on soil formation conditions, the most significant among them being the kinds of water plants and current speed. The significant thickness of the horizon was recorded only in case of rooted plants providing the stability of substrate on one hand and regular input of organic residues on the other hand. Additional sources of organic material are not excluded; these may be fish and animal excrements, terrestrial sediments removed by erosion into shallow-water areas. According to our data, the rate of sedimentation in the lower part of the Volga delta is about 2–5 cm per year [Winkels et al., 1999]. The uppermost horizon is about 10 cm (up to 30 cm) thick, dove-grey, and humus content reaches 6 %. More favorable for humus formation is the lotus (*Nelumbo spp.*) community, less favorable – the reed (*Phragmites australis*) one (Fig. 2); reed is hard to decompose and its residues preserve recognizable plant tissues. (Future research is needed to reveal the dependence of the topsoils on plant communities). Hence, two variants of upper horizons may be identified: aquahumus horizon – AQA and aquapeat horizon – AQT.

Floating plants: chilim (*Trapanatans spp.*), water lily (*Nymphaea spp.*), floating moss (*Salvinia spp.*) etc. (Fig. 2) do not create any

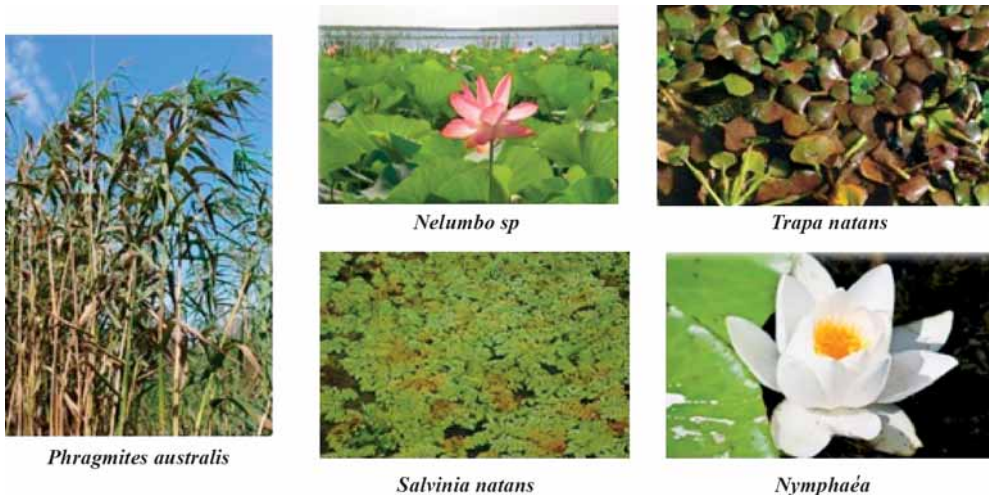


**Fig. 2. Water plants**

stable horizon if the hydrodynamic processes are active, whereas if they are weak, the suspended material enriched in organic matter (erosion loss from terrestrial soils) is accumulated contributing to formation of a discontinuous greyish-bluish horizon. Its thickness does not exceed 2–3 cm, and humus content is not more than 1–2 %.

In active channels, mixing of the upper part of aquazem profiles by currents results in the formation of a thin yellowish-grey oxidized layer tentatively named (AQOX) with a very low content of humus: less than 1 %. (Fig. 3).

**Soil-forming agents**

Most typical of aquazems is their aquagley AQG horizon – homogeneous in color and consistence, clay-permeated, completely dominated by dove-grey color; these features are the same as in terrestrial gleys. The AQG horizon gradually merges into the parent material – stratified bottom sediments. They are frequently enriched in shell fragments.

The physicochemical properties are rather homogeneous both throughout the profiles and among the soils. The pH values are close to neutral (see Fig. 3) in the upper horizons, and become weakly alkaline downward, which may be attributed to the stronger

influence of marine water. Presumably, this trend may be also explained by the acidifying effect of decaying organic residues in the upper part of the profile. The humus profile pattern is similar to that in terrestrial soils, although sometimes it is irregular due to buried humus-enriched layers. Unlike terrestrial soils, this pattern is typical and is in no way related to translocation events. Redox potential values are always low, and vary in accordance with the hydrological regime and plant communities. The average value is about –80 to –100 mV, in all soils they decrease downwards to –120 to –150 mV; in oxidized horizons they may reach +80 mV.

The main prerequisite for aquazem formation is the shallow depth of the water body and weak currents. Depth limitation – less than 2 m of water above the soil, was introduced in WRB [2006], and it agrees well with the data obtained. In our case, it may be explained by the requirements of rooted plants to their environment, namely, illumination, alteration of seasons, and access of oxygen. Moreover, at shallow depth, the oxidation phenomena occur owing to wind paddling, as well as accumulation of fine particles from the suspended loads of river and/or sheet erosion on the shore. Seasons of the year are pronounced, although mitigated by the water layer. The latter is also responsible for

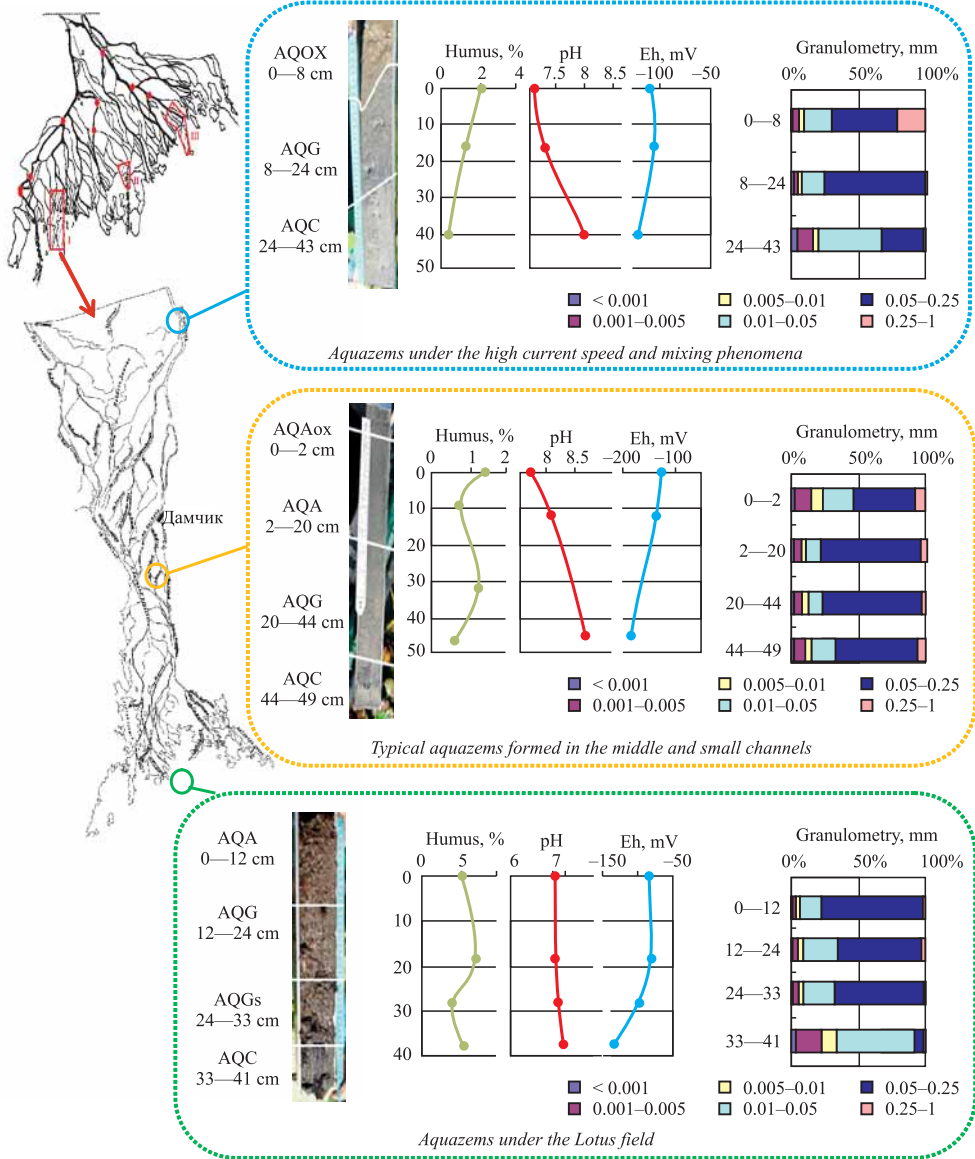


**Fig. 3. Properties of subaqueous soil in the different parts of the Volga delta**

the permanently reductive environment. The location of aquazems in the deltaic area and the history of the latter also affect the aquazem properties. Thus, aquazems in the marine edge of the deltas (Fig. 4) exist in an alternating subaqueous deep- and shallow-water regimes; they have stratified profiles: clay strata alternate with the sandy ones containing shell frag-

ments. Buried horizons may occur; they are dark, greyish and enriched in organic carbon.

In aquazems, like in terrestrial soils, the effect of parent material is distinct. Most soils of the Volga delta are formed on homogeneous silty loams, whereas specific soils are confined to the outcrops of contrasting rocks. For

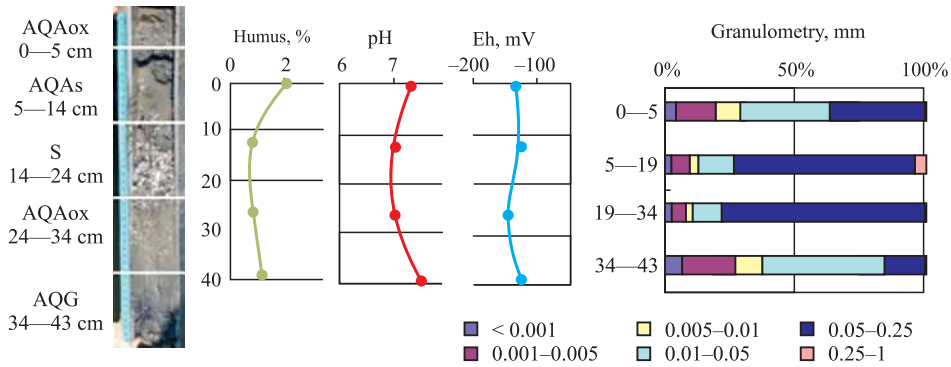


Fig. 4. Properties of subaqueous soil of the Volga marine delta edge

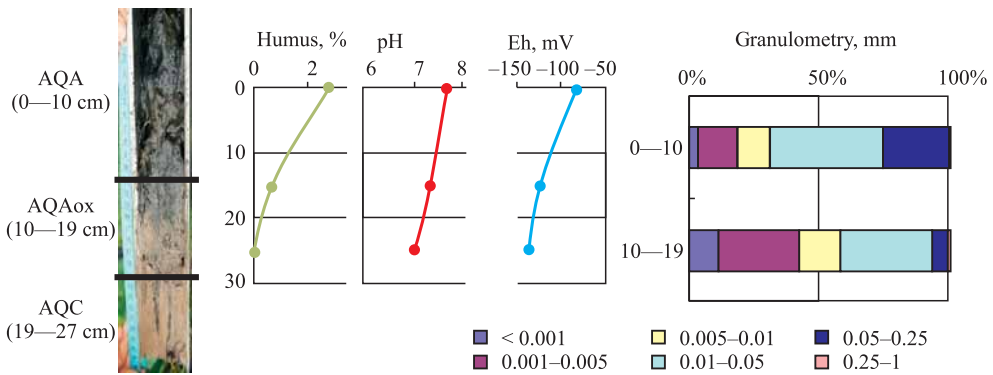


Fig. 5. Properties of subaqueous soils on "chocolate" clays

example, aquazems on the outcrops of Khvalyn "chocolate" clays [Svitoch, Makshaev, 2015] have a shallow profile and a specific color of the lower horizon (Fig. 5).

The particle-size composition primarily depends on the flowage degree and current rate (Fig. 6). In large channels with high current rate, the coarsest fractions are

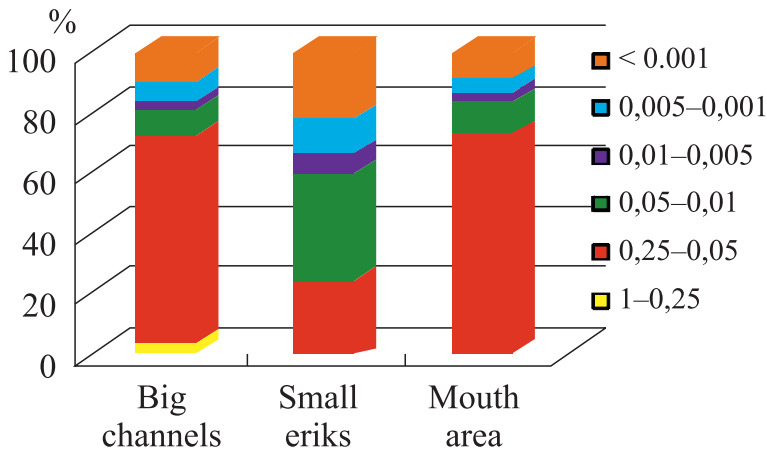


Fig. 6. Particle-size distribution in aquazems in different parts of the Volga delta.

deposited; fine fractions are predominant in weakly flowing watercourses. On the marine edge with its contrasting hydrodynamic conditions, effects of wind and waves, and intense water mixing characterized by texture heterogeneity, which rather depends on vegetation contributing to sediment stability, fine-textured substrates are formed.

### *Approaches to classification*

If accepting aquazems as soils, it seems reasonable to classify them within the framework of the new system of soil classification of Russia [2004], where the priority of soil properties is a basic principle. The data accumulated permit referring the aquazems to the *trunk of synlithogenic soils*, and provide a *special aquazems order* for them [Lychagin, Tkachenko, 2012]. For terrestrial soils, orders are specified by common trends of pedogenesis or by a common horizon; in our case both requirements are met. There is no need to argue the specific character of aquapedogenesis; as for a common horizon, the aquagley (AQG) horizon occurs in all aquazems. Following the rules of the classification system, types of aquazems may be specified by the combinations of horizons, hence, the following *types* may be recognized: typical (AQA-AQG-AQC-C), organogenic (AQT-AQG-AQC-C), oxidized (AQA-AQOX-AQG-AQC-C). The extension of studies is sure to find new types.

In American Soil Taxonomy [1999] the subaqueous soils refer to two suborders in two Orders: Wassents – subaqueous Entisols and Wassists – subaqueous Histosols. For the name of such soils the formative element *Wass* is used, which is derived from the German word “Wasser” for water. [[http://nesoil.com/sas/Freshwater\\_Subaqueous\\_Soils\\_RIWPC.pdf](http://nesoil.com/sas/Freshwater_Subaqueous_Soils_RIWPC.pdf)]

There is also a special place for subaqueous soils in WRB [2014]. The Subaquatic is a Principal qualifier in the Reference Soil Groups of Histosols, Fluvisols, and Gleysols. In Chinese,

Canadian, and French classification systems, subaqueous soils are absent.

### *Geography of aquazems*

It seems clear that if all necessary conditions are met, aquazems are formed in any water body, such as river, lake, pond, water storage reservoir, etc. Thus, the same aquazems types were found in the Don and Kuban Rivers deltas. The main differences between deltas are lower variability of aquazems types because of more homogeneous conditions in the Don deltaic landscapes, and higher pH and TDS values in the Don and Kuban aquazems because of the stronger sea influence there compared to the Volga delta aquazems.

Presumably, there is a zonal differentiation of the subaqueous soils like of the terrestrial soils. Aquazems may be subdivided in accordance with the organic/mineral material ratio. Aquazems dominated by organic material are mostly confined to the northern areas – tundra, northern and partially middle taiga, as well as to wetlands in other zones; aquazems on predominantly mineral parent material are more common in southern taiga, broadleaved forests, forest-steppe, and steppe. The first group may be correlated with Kubiena's organic subaqueous soils – Sapropel, Reed-Fen or Carex-Fen. The second group may resemble Gittja and Dy. It is not clear, whether the climatic (zonal) conditions affect the spatial differentiation of aquazems at a lower level.

Aquazems on the mineral substrates may be further differentiated in accordance with the chemical properties of the substrates. A special case is the artificial reservoirs since their bottom sediments are frequently composed of former terrestrial soils; moreover, some of these aquazems are enriched in organic material (remnants of former terrestrial plants) and artifacts. Aquazems compose their own ‘soil cover’ in a certain water body. It is regulated by ‘local’ topolithogenic factors that are more or less modified by the effects of currents.

The spatial diversity of aquazems seems to be lower than that of terrestrial soils, and there are at least three reasons for that.

1. More homogeneous and simple are the aquazems profiles, hence, lower is the 'aquapedodiversity'.
2. Whereas terrestrial soils have been studied during more than a century, the time dedicated to the aquatic soils reconnaissance hardly exceeds several years, and this relative homogeneity may decrease with the new knowledge acquired.
3. The aquatic environment is more homogeneous in comparison with the terrestrial soil cover owing to the mitigating effect of the water layer and particularities of the sedimentation process.

#### *Ecological services of the subaqueous soils*

Like the terrestrial soils, the aquazems perform several functions in the ecosystems. They serve as habitat for organisms and plants. Like the terrestrial soils, they could be changed and used for subaqueous agriculture, for example for algae cultivation, or shrimps and oysters production.

Furthermore, subaqueous soils, as the storage system, can accumulate pollutants, for example, heavy metals. Thus, in the Volga delta, the concentrations of the majority of heavy metals well correlate with the clay content in the subaqueous soils [Kasimov et al., 1999; Kasimov, Lychagin, 2002]. That is why, geochemical anomalies of heavy metals may be confined to the parts of watercourses with low current rates or with changes in redox conditions (mouths of channels on the marine edge, thickets of aquatic plants of the delta front); geochemical barriers are formed there, and fine particles are accumulated. The Volga delta is retaining a considerable portion of heavy metals [Kuryakova, 2011]. If the environment changes, for example, owing to the fluctuations of the sea level or river

discharge, heavy metals may be re-mobilized from bottom sediments (or subaqueous soils) in suspensions and contaminate the river water. Understanding their functioning as soils will help predicting the risks of environmental pollution.

#### CONCLUSIONS

The review of publications and the experimental data obtained in the deltaic areas of the Volga River delta permitted applying a 'pedological' approach to the unconsolidated sediments under shallow water. They have much in common with terrestrial soils, and may be named *aquazems*.

In aquazems, like in terrestrial soils, *diagnostic horizons* may be identified: subaqueous analogues of the humus-accumulative and peat horizons, gley and redoximorphic horizons, parent material that may be calcareous due to shells. The thickness of horizons is less compared to that in terrestrial soils. Combinations of these (and probably some other) horizons correspond to several *types of aquazems*.

*Methods* to study aquazems' properties are basically the same as for terrestrial soils, although the number of morphological characteristics is less; among the analytical procedures, measurement of redox potential is expedient.

The *subaqueous soil-forming agents* perform their functions less obviously compared to terrestrial soils; most important is vegetation, primarily, the rooted plants, the effect of climate is mitigated by the water layer, as well as that of relief owing to currents, which partially perform the function of matter redistribution; parent material is mostly homogenous, since its particle-size composition is determined by the sedimentation regime within the narrow range of depths: 0.5 to 2 m. Time is rather short for aquazem profiles to be formed, as the deltaic areas have a pronounced seasonal and annual dynamics.

The *ecological services* of aquazems comprise: substrate for aquatic plants, habitat for bottom living organisms, accumulation and immobilization of pollutants. In the same time, "secondary" release of some

pollutants caused by changes in the aquatic environment is not improbable, and once the changing currents may enhance the aggravation of pollution. ■

## REFERENCES

1. Batoyan, V.V. (1983) Osobennosti geokhimicheskogo profilya podvodnyh pochv v vo-domakh s neutralnoi reakciei (Some features of the geochemical profile of subaqueous soils in water bodies with neutral reaction), Vestnik MGU, ser. 5, geogr., N 3: 79–86 (in Russian).
2. Batoyan, V.V., Moiseenkov, O.V. (1988). Ocenka tekhnogennogo vozdeistviya na vodokhranilishche po donnym osadkam (Assessment of technogenic impact on a water reservoir by the properties of bottom sediments), Vestnik MGU, ser. 5, geogr., N 3: 65–71 (in Russian).
3. Bloomfield, C. (1951). Experiments on the mechanism of gley formation // J. Soil Sc., volume 2, N 2: 196–211.
4. Burghardt, W. (1996). "Boden und Böden in der Stadt," in: Urbaner Bodenschultz Arbeitskreis Stadtböden der DBG. Springer Verlag, Berlin, Heidelberg, New York: 7–24 (in German).
5. Chalov, S.; Thorslund, J.; Kasimov, N.S.; Nittrouer, J.; Iliycheva, E.; Pietron, J.; Shinkareva, G.; Lychagin, M.; Aybullatov D.; Kositky A.; Tarasov, M.; Akhtman, Y.; Garmaev, E.; Karthe D. & Jarsjö, J. (2016): The Selenga River delta: a geochemical barrier protecting Lake Baikal waters. Regional Environmental Change. doi: 10.1007/s10113-016-0996-1
6. Demas, G.P., Rabenhorst, M.C. (2001). Factors of Subaqueous Soil Formation: a System of Quantitative Pedology for Submersed Environments. // Geoderma, N 102: 189–204.
7. Dobrovolsky G.V., Nikitin E.D. (1986). Ekologicheskie funkcii pochvy (Ecological functions of soils), Moscow University Press, 136 pp. (in Russian).
8. Goriachkin, S.V., Gilichinsky D.A., Mergelov, N.S. et al. (2012) Pochvy Antarktity: pervie itogi, problemy i perspektivy issledovaniy (Soils of Antarctic: first results, problems and challenges) In: Landscape geochemistry and soil geography (100th birthday of Maria A. Glazovskaya). Ed. N.S. Kasimov and M.I. Gerasimova. Moscow Lomonosov Univ.: 365–392 (in Russian).
9. [http://nesoil.com/sas/Ditzler\\_SubaqueousPaper\\_Draft.pdf](http://nesoil.com/sas/Ditzler_SubaqueousPaper_Draft.pdf)
10. [http://nesoil.com/sas/Freshwater\\_Subaqueous\\_Soils\\_RIWPC.pdf](http://nesoil.com/sas/Freshwater_Subaqueous_Soils_RIWPC.pdf)
11. IUSS Working Group WRB (2014). World reference base for soil resources 2014. International soil classification system for naming soils and creating legends for soil maps. World Soil Resources Reports, 106. FAO, Rome.

12. Kasatenkova, M.S. (2011). Geokhimicheskaya struktura i evolyuciya lagunno-marshevykh landshaftov Zapadnogo Prikaspiya (Geochemical structure and evolution of the landscapes of lagoons and marshes in Western Caspian Lowland). Extended Abstract of the candidate thesis in geography. 25 pp. (in Russian)
13. Kasimov, N.S., Kasatenkova, M.S., Gennadiev, A.N., Lychagin M.Y. (2012). Modern geochemical evolution of lagoon-marshy landscapes in the Western Caspian Sea region // Eurasian Soil Science, volume 45, # 1, pp. 1–12.
14. Kasimov, N.S., Kroonenberg S.B., Lychagin, M.Yu., Oliferenko N.L., Tarusova O.V. (1999) Geokhimiya donnykh otlogenyi i pochv Astrakhanskogo zapovednika (Geochemistry of bottom sediments and soils in the Astrakhan Reserve) // GIS of the Astrakhan Reserve. Geochemistry of the Volga delta landscapes. Moscow: Mosk.Univ. Publ: 96–106 (in Russian).
15. Kasimov, N.S., Lychagin, M.Yu. (2002) Geokhimiya tyazhelykh metallov v donnykh otlozheniyah delty Volgi (Geochemistry of heavy metals in bottom sediments of the Volga delta) // Geochemistry of landscapes and geography of soils. Smolensk, Oecumena Publ: 137–169 (in Russian).
16. Kawaguchi, K., Kiama, K. (1974). Paddy soils in tropical Asia Description of material characteristics // Southeast Asian Stud., N 12 (2): 177–192.
17. Klassifikatsiya i diagnostika pochv Rossii (Classification and Diagnostic of Soils of Russia) / Shishov L.L., Tonkonogov V.D., Lebedeva I.I., Gerasimova M.I., Smolensk, 2004. 343 pp. (in Russian).
18. Krasilnikov, P.V., Shoba S.A. (1997) Sulfatnokislye pochvy Vostochnoi Fennoskandii (Acid sulphate soils of Eastern Fennoscandia), Petrozavodsk: Karelian Sc. Centre, 160 pp. (in Russian).
19. Kubiena, W.-L. (1953) Bestimmungsbuch und Systematik der Böden Europas. Illustriertes Hilfsbuch zur leichten Diagnose und Einordnung der wichtigsten europäischen Bodenbildungen unter Berücksichtigung ihrer gebräuchlichsten Synonyme. F. Enke-Verlag Stuttgart (in German).
20. Kuryakova (Tkachenko), A.N. (2011) Balans tyazhelykh metallov v delte Volgi (Budget of heavy metals in the Volga River delta), Reports of Academy of Sciences, volume 439, N 6: 818–821 (in Russian).
21. Lychagin, M.Yu., Tkachenko (Kuryakova), A.N. (2012) Donnye otlozheniya ust'evoy oblasti Volgi – pochvy li? (Bottom sediments in the Volga River delta – soils or sediments?) In: Proc. VI Congress Dokuchaev Soc. Soil Scientists, Petrozavodsk, Book 3: 77–78 (in Russian).
22. Lychagin, M.Yu., Kasimov, N.S., Kuryakova (Tkachenko), A.N., Kroonenberg, S.B. (2011) Geokhimicheskie osobennosti akvalnykh landshaftov delty Volgi (Geochemical features of aquatic landscapes of the Volga River delta), Izvestia RAN, ser. geogr. N 1: 100–113 (in Russian).

23. Michael P. Bradley and Mark H. Stolt. (2003). Subaqueous Soil-Landscape Relationships in a Rhode Island Estuary. *Soil Sc. Soc. Am. J.*, volume 67, Sept.–October: 1487–1495.
24. Mückenhausen, E. (1975). *Die Bodenkunde und ihre geologischen, geomorphologischen, mineralogischen und petrologischen Grundlagen*. DLG-Verlag, Frankfurtam Main, 579 pp. (in German).
25. Perel'man, A.I., Kasimov, N.S. (1999) *Geokhimiya landshafta (Geochemistry of landscape)*, Moscow, Astreya-2000, 768 pp. (in Russian).
26. Prokofieva, T.V. (1998) *Gorodskie pochvy zapechatannye dorozhnymi pokrytiyami (Urban soils sealed by road screens)*. Extended Abstract of the candidate thesis in biology, 2011, 25 pp. (in Russian).
27. Rossiter, D.G. (2007). Classification of urban and industrial soils in the World Reference Base for soil resources // *J. Soils and Sediments* volume 7, N 2: 96–100.
28. Rozanov B.G. (1983) *Morfologiya pochv (Soil Morphology)*, Moscow: Moscow University Press, 320 pp. (in Russian).
29. Semikolennykh, A.A. (2012) *Pochvoobrazovanie v usloviyah peshcher i podzemnykh gornyykh vyrabotok (Pedogenesis in caves and quarries)*. In: *Proc. VI Congress Dokuchaev Soc. Soil Scientists*, Book 1: 219–220 (in Russian).
30. Soil Survey Staff. (1999). *Soil Taxonomy. A Basic System of Soil Classification for Making and Interpreting Soil Surveys*. 2nd Ed. U.S. Dept. of Agric. Natural Resources Conservation Service. Agriculture Handbook No. 436 pp.
31. Solntseva, N.P. (1998) *Dobycha nefi i geokhimiya prirodnykh landshaftov (Oil mining and geochemistry of natural landscapes)*, Moscow Univ. Publ., 370 pp. (in Russian).
32. Solntseva, N.P. (2009). *Environmental effects of oil production*. Moscow, RPA "ARP", 224 pp.
33. Stolt, M., Bradley, M., Icchetti, G., Shumchenia, E., Guarinello, M., King, G., Boothroyd, J., Oakley, B., Thornber, C., and August, P. (2011). Mapping shallow coastal ecosystems: a case study of a Rhode Island lagoon. *Journal of Coastal Research*, 27 (6A), 1–15.
34. Svitoch, A.A., Makshaev, R.R. (2015) *Shokoladnye gliny Severnogo Prikaspiya (rasprostranenie, usloviya zaleganiya i stroenie) (Chocolate clays of the Northern Caspian Lowland (distribution, bedding and fabric))* // *Geomorphology*, N 1: 101–112 (in Russian).
35. Winkels H.J., Kasimov N.S., Lychagin M.Y., Marin G., Kroonenberg S.B., Rusakov G.V. (1999) *Geokhimiya polliutantov v akvosistemakh delty Volgi v sravnenii s deltami Reina i Dunaya (Geochronology of priority pollutants in aquasystems of the Volga delta in comparison with the Rhine and Danube deltas)*, GIS of the Astrakhan Reserve. *Landscape Geochemistry of the Volga delta*. Moscow: 132–141 (in Russian).
36. Winkels H.J., Kroonenberg S.B., Lychagin M.Y., Marin G., Rusakov G.V., Kasimov N.S. *Geochronology of priority pollutants in sedimentation zones of the Volga and Danube deltas*

in comparison with the Rhine delta. Applied Geochemistry, Pergamon Press Ltd. (United Kingdom), 1998, V. 13, N 5: 581–591.

37. Yeterevskaya, L.V. (1989) Pochvoobrazovanie i rekultivaciya zemel v tehnogennykh landshaftah Ukrainy (Soil formation and rehabilitation of lands in technogenic landscapes of Ukraine), Extended Abstract of the Dr. Sc. thesis in agriculture, 40 pp. (in Russian).
38. Zaidel'man, F.R, Narokova, R.P. (1978) Gleeobrazovanie pri zastoinom i promyvnom rezhimakh v usloviyakh laboratornogo modelirovaniya (Gley formation under stagnant and percolative water regimes in a laboratory simulation experiment), Pochvovedenie, 1978, N 3: 42–53 (in Russian).

Received 10.11.2015

Accepted 29.08.2016



**Anna N. Tkachenko** studied geography at the Lomonosov Moscow State University, Faculty of Geography, and received her Ph. D. degree in 2011 (Aquatic landscapes geochemistry of the Volga delta). She is Researcher in the Department of Landscape Geochemistry and Soil Geography. Her scientific interests focus on geochemistry of aquatic landscapes, particularly on heavy metals geochemistry in river mouths. Her main publications are "Heavy metals mass-balance in the Volga river delta" (2011), "Heavy metals in the water, plants, and bottom sediments of the Volga River mouth area" (2015, with co-authors).



Professor **Maria I. Gerasimova** works at the Department of Landscape Geochemistry and Soil Geography, Faculty of Geography, Lomonosov Moscow State University and also at the Dokuchaev Soil Science Institute, where she is involved in developing soil classification of Russia; she is also a member of WRB (the International Soil Classification) Board. Other spheres of her research interests are soil geography and soil micromorphology. She is the author of about 230 scientific works including: Micromorphology and Diagnostics of Soil Formation, 1982 (co-author A.Romashkevich); Soil Geography of USSR (1987), Soil Geography of Russia (2007); Classification and Diagnostics of Soils of Russia, 2004 & 2008 (co-authors V. Tonkonogov, I. Lebedeva, L. Shishov).



**Mikhail Lychagin** is Associate Professor of the Department of Landscape Geochemistry and Soil Geography, Faculty of Geography, Lomonosov Moscow State University. His research interests focus on environmental geochemistry, aquatic systems, environmental monitoring, and GIS. For 20 years he has been involved in the comprehensive research within the Caspian Sea basin: environmental consequences of the Caspian Sea-level fluctuations, environmental geochemical state of aquatic systems in the Volga delta and the Northern Caspian.



Academician **Nikolay S. Kasimov**, is Head of the Department of Landscape Geochemistry and Soil Geography since 1987; since 2015 he is the President of the Faculty of Geography, Lomonosov Moscow State University. His current research interests are: geochemistry of landscapes, paleo-geochemistry, and geochemistry of urban and aquatic landscapes. He is the author of about 300 scientific works, including: Landscape Geochemistry of Steppe and Desert Landscapes, 1988; Ecogeochemistry of Urban Landscapes, 1995 (author and editor); Landscape Geochemistry, 1999 (co-author A.I. Perel'man); Oil and Environment of Kaliningrad Region, 2008 (author and editor); Landscape Ecogeochemistry, 2013.



**Salomon Kroonenberg** is Emeritus Professor of Geology at Delft University of Technology, the Netherlands. He studied Physical Geography at the University of Amsterdam, and received his PhD degree from the same university in 1976 (the Precambrian of the Guiana Shield in Suriname). From 1972–1978, he worked as a geologist at the Geological and Mining Service of Suriname, from 1978–1979 as a lecturer of physical geography at the University College of Swaziland, Africa, and from 1979 to 1982 as a remote sensing geologist at the Centro Interamericano de Fotointerpretación in Bogotá, Colombia. In 1982, he was appointed Professor of Geology at the Department of Soil Science and Geology at Wageningen Agricultural University, and in 1996 he moved to Delft University of Technology where he worked until his retirement in 2009. He had extensive research programs on sedimentary geology and sea level change. He is the author of over 130 scientific articles.

**Stanislav A. Ogorodov<sup>1\*</sup>, Alisa V. Baranskaya<sup>2</sup>, Nataliya G. Belova<sup>3</sup>, Anatoly M. Kamalov<sup>4</sup>, Dmitry E. Kuznetsov<sup>5</sup>, Paul P. Overduin<sup>6</sup>, Nataliya N. Shabanova<sup>7</sup>, Aleksey P. Vergun<sup>8</sup>**

<sup>1</sup> Faculty of Geography, Lomonosov Moscow State University, Leninskie Gory 1, 119991 Moscow, Russia, Tel: + 7-495-939 25 26 Fax: + 7-495-932 88 36; e-mail: ogorodov@aha.ru

**\* Corresponding author**

<sup>2</sup> Faculty of Geography, Lomonosov Moscow State University, Leninskie Gory 1, 119991 Moscow, Russia, Tel: + 7-495-939 25 26 Fax: + 7-495-932 88 36; e-mail: alisa.baranskaya@yandex.ru

<sup>3</sup> Faculty of Geography, Lomonosov Moscow State University, Leninskie Gory 1, 119991 Moscow, Russia, Tel: + 7-495-939 25 26 Fax: + 7-495-932 88 36; e-mail: nataliya-belova@yandex.ru

<sup>4</sup> Faculty of Geography, Lomonosov Moscow State University, Leninskie Gory 1, 119991 Moscow, Russia, Tel: + 7-495-939 25 26 Fax: + 7-495-932 88 36; e-mail: kamalov-msu@mail.ru

<sup>5</sup> Faculty of Geography, Lomonosov Moscow State University, Leninskie Gory 1, 119991 Moscow, Russia, Tel: + 7-495-939 25 26 Fax: + 7-495-932 88 36; e-mail: dkzn.at@gmail.com

<sup>6</sup> Department of Geosciences, division of periglacial research, Alfred Wegener Institute Telegrafenberg A43, D-14473 Potsdam, Germany; e-mail: paul.overduin@awi.de

<sup>7</sup> Faculty of Geography, Lomonosov Moscow State University, Leninskie Gory 1, 119991 Moscow, Russia, Tel: + 7-495-939 25 26 Fax: + 7-495-932 88 36; e-mail: nat.volobuyeva@gmail.com

<sup>8</sup> Faculty of Geography, Lomonosov Moscow State University, Leninskie Gory 1, 119991 Moscow, Russia, Tel: + 7-495-939 25 26 Fax: + 7-495-932 88 36; Zubov State Oceanographic Institute, Kropotkinskiy pereulok, 6, 119034, Moscow, Russia, e-mail: alvergun@mail.ru

# COASTAL DYNAMICS OF THE PECHORA AND KARA SEAS UNDER CHANGING CLIMATIC CONDITIONS AND HUMAN DISTURBANCES

**ABSTRACT.** Coastal dynamics monitoring on the key areas of oil and gas development at the Barents and Kara Seas has been carried out by Laboratory of Geoecology of the North at the Faculty of Geography (Lomonosov Moscow State University) together with Zubov State Oceanographic Institute (Russian Federal Service for Hydrometeorology and Environmental Monitoring) for more than 30 years. During this period, an up-to-date monitoring technology, which includes direct field observations, remote sensing and numerical methods, has been developed. The results of such investigations are analyzed on the example of the Ural coast of Baydaratskaya Bay, Kara Sea. The dynamics of thermal-abrasion coasts are directly linked with climate and sea ice extent change. A description of how the wind-wave energy flux and the duration of the ice-free period affect the coastal line retreat is provided, along with a method of the wind-wave energy assessment and its results for the Kara Sea region. We have also

evaluated the influence of local anthropogenic impacts on the dynamics of the Arctic coasts. As a result, methods of investigations necessary for obtaining the parameters required for the forecast of the retreat of thermoabrasional coasts have been developed.

**KEY WORDS:** coastal dynamics, cryolithozone, thermoabrasion, monitoring, multitemporal imagery, climate change, ice extent, wave energy, human impact, Pechora and Kara Seas.

## INTRODUCTION

The development of natural gas extraction and transportation facilities on the coasts and shelf of the Russian Arctic seas requires construction of sea ports, approach channels, artificial islands, drilling platforms, terminals, ground-surface and underwater pipelines. The knowledge of natural processes, particularly coastal dynamics, is necessary for the geotechnical and geoecological safety during their construction and operation. The coastal zone in the polar regions is extremely sensitive due to the contact with the cryolithozone. The coasts of Barents and Kara Seas composed of frozen deposits have poor resistance to erosion. Considering eventual human impact and the ongoing and forecasted climatic change, coastal retreat rates may significantly increase in the coming years. Technogenic disturbances activate trigger mechanisms of wave-induced coastal erosion. Under the conditions of global warming and sea ice cover reduction; this effect is enhanced by the increase of the wave

fetch, together with the duration of the ice-free period, when waves act directly on the shores. As a result, local human impact and climate change form a synergetic effect, due to which coastal retreat rates can double and even triple.

In the present study, we describe the methods of the coastal retreat rates' determination, together with the assessment of the hydrometeorologic factors, mainly wind-wave energy, acting on the coasts. The key sites of investigations are the Varandey (Barents Sea) and Kharasavey (Kara Sea) industrial key areas, as well as the gas pipeline underwater crossing of the Baydaratskaya Bay, Kara Sea, where human impact has already brought in negative effects. To determine the speed of coastal retreat and shore zone profile deformations, approximately 120 permanent profiles for coastal dynamics monitoring have been established there in the 80–90s of the XX century (Fig. 1). Coastal dynamics monitoring from constant benchmarks is executed by direct measurements and by trigonometric

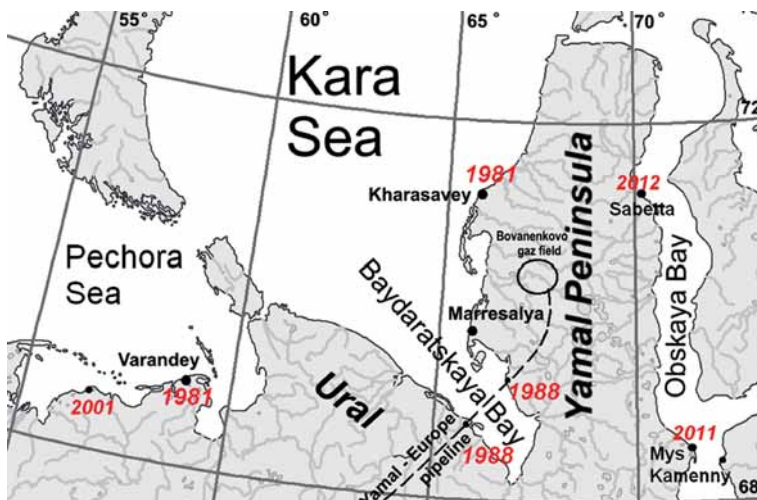


Fig. 1. Key sites of studies; years of the start of observations

leveling. An additional method of receiving an overview of multiannual coastal dynamics is studying multi-temporal aerial and satellite images of high and extra-high resolution.

An example of the results of such investigations and the analysis of the reasons of changes in the coastal retreat rates are provided for the Ural coast of the Baydaratskaya Bay; the hydrometeorologic factors are analyzed based on the data of the Marresalya hydrometeorologic station. Apart from that, the consequences of the unreasonable technogenic exploration are observed based on the examples of the coasts of Baydaratskaya Bay and of Varandey Island, Barents Sea.

#### FACTORS OF THE ARCTIC COASTAL DYNAMICS

For the Russian Arctic coasts, one of the crucial dangerous processes is thermal abrasion. According to its definition, thermal abrasion is the destruction of coasts and underwater slopes composed by frozen sediments. For the seas situated in the cryolithozone, thermal and thermo-mechanical abrasion is caused, on the one hand, by mechanical abrasion

induced by the wave action, and, on the other hand, by the thawing of the frozen grounds.

As a result of active thermal abrasion and thermal denudation, the coastline retreats up to several meters every year. Despite the short period of active dynamics, when the sea is ice-free, morpholithodynamic processes in the Arctic coastal zone are extremely intense because of the low stability of the cliffs composed by permafrost (Fig. 2). The mean multiannual retreat rates of thermal abrasion coasts vary from 0,5 to 2 m per year in natural conditions. Within sections with massive ice beds outcropping in the cliff, such destruction often reaches catastrophic velocities of up to 5–10 m per year or more.

Thermal abrasion of sea coasts has been studied relatively well in the XX century. However, in the XXI century, hydrometeorological features of the near-earth layer of the atmosphere will inevitably change under the conditions of global climate warming which will, in its turn, cause changes in the hydrosphere and lithosphere. The increase of the ice-free period will lead to the rising impact of the wave action, which, in its turn, will cause mechanical abrasion intensification.



**Fig. 2. Typical thermoabrasional coast of the Kara Sea**

Other changes of the hydrometeorologic characteristics, namely the occurrence of strong cyclones and storm surges, will also influence the coastal dynamics.

The dynamics of typical thermoabrasional coasts are generally determined by the combination and interaction of two factors: the thermal factor and the wave energy factor [Ogorodov, 2008, Ogorodov, 2011] (Fig. 3).

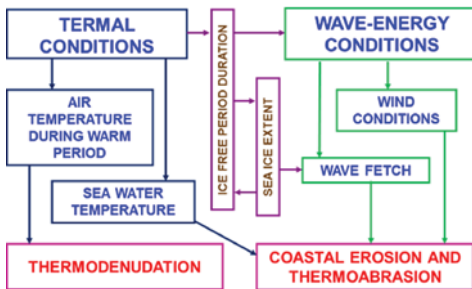


**Fig. 3. Hydrometeorologic factors of coastal dynamics**

The thermal impact is expressed in the transition of energy to the permafrost composing the cliff through its contact with air and water with the temperature above  $-1,8^{\circ}\text{C}$ . Correspondingly, the higher the air and water temperature is, and the longer the period with positive temperatures and the period of contact with sea water is, the more the thermal factor influences the coastal dynamics in permafrost areas.

The impact of the wave energy factor is expressed in the direct mechanical action on the coasts. Therefore the effect of this factor is determined by the intensity and duration of storms. The intensity of storms, in its turn, considerably depends on the length of the wave fetch (position of the sea ice border) and on the duration of the active dynamic period, when the water area is ice-free.

Under the conditions of global climate change and changes in the ice cover of the Arctic seas, forecasted for the XXI century, the influence of both the thermal and wave energy factors on the coasts will inevitably

grow. The increase of abrasion will occur not only due to the intensive thawing of the frozen ground under the action of higher air and water temperatures and possible precipitation, but also due to the increased impact of the wave action on the coast, the growth of which is determined by the repeated storm winds, sea level rise and ice-free period prolongation.

The changes of the last decades are not unique. In the Holocene, and in the years 30–40 of the XX century, there have been many cases when conditions in the Arctic area were similar to the modern ones, with rising air temperature. Fluctuations in the rates of natural processes, including thermoabrasion, corresponding to warmer periods, often lead to the damage of constructions designed without taking into account the features of coastal dynamics in the coastal areas. These consequences are, in most of the cases, determined by the ignorance of the natural environmental mechanisms in the cryolithozone.

## METHODS OF STUDY

### *Direct and remote sensing methods for coastal dynamics monitoring*

According to the Russian construction code of practice, no industrial facility can be constructed without a preliminary monitoring of natural exogenous processes, including coastal dynamics. The geotechnical safety of petroleum infrastructure objects under development, as well as the geocological safety of the surrounding areas, is highly dependent on the right choice of the most dynamically stable shore section, and on the implementation of the correct forecast of coastal dynamics for the facilities' lifetime.

A correct forecast of the coastal dynamics of thermoabrasional coasts is impossible without the understanding of the factors of their development. One of the most important parts is the monitoring of the cliff destruction

due to thawing (thermodenudation) and retreat due to wave action (wave abrasion). Only a proper sequence of repeated monitoring data can help to reconstruct the conditions of thermoabrasion and establish reliable correlations for active hydro- and meteorological factors that determine wave and temperature conditions.

Coastal dynamics monitoring from constant benchmarks is executed by direct measurements and by trigonometric leveling. The benchmarks are attributed to the Baltic-77 (Russian) system of heights. As a rule, 3 benchmarks are set (Fig. 4). The benchmark network for monitoring is usually set with respect to geomorphological and cryolithological composition of the shore. This helps to obtain integrative data on spatial and temporal variability of the processes of thermoabrasion at a relatively long coastal section.

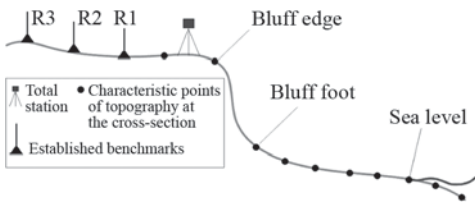


**Fig. 4. Coastal dynamics monitoring by trigonometric leveling**

A reliable method of studying coastal dynamics for relatively long time periods is the analysis of multitemporal aerial and space images [Ogorodov, Belova et al., 2011]. Among the archive space imagery, declassified Corona images shot between 1961 and 1970 are of particular interest, since they have medium resolution (4–7 m), good enough for coastal investigations. For a considerable part of the Arctic coast, modern space imagery of ultra-high resolution is available [Ikonos, QuickBird, Formosat 2].

The preparation of the obtained aerial and satellite imagery is the most important stage in the Arctic coastal dynamics investigations. Special attention should be paid to the spatial

reference of the data. Ikonos and QuickBird images are provided with the world-files (reference files) created by the satellite's orbit parameters. This kind of referencing is precise enough for coastal areas because the error between the heights on the terrain and the geoid level are negligible.

A more complicated task is the referencing of Corona satellite images which can only be obtained as a simple raster file. Ikonos and QuickBird images, as well as topographic maps and plans or field GPS-points can be used as benchmark data for these files. Because of their considerable coverage, Corona images have trapeze-like deformations in their peripheral part. For their referencing, special methods allowing the curvature of initial data (polynomial transformations, "rubber sheet" method) should be used. The main problem regarding the referencing of aerial and satellite imagery is the lack of stable points which is caused by little anthropogenic presence in the explored region. Consequently, hydrographic objects are often used in the georeferencing (rivers, lakes, ravines and hollows). By superimposing the received contours with the image and creating a set of verified reference points, precise enough correspondence can be reached.

After the referencing of all the multitemporal images available for the territory, the interpretation stage starts. One of the most wide-spread and well decipherable signs for thermoabrasion and accumulative coasts are the cliff line and the border of the continuous vegetation cover. Based on the satellite imagery, the cliff edge (for abrasion sections) and the continuous vegetation limit (for accumulative sections) are digitized. Sometimes, in case of aeolian processes influencing the beach and the littoral, for accumulative coasts, the border between the beach and littoral is digitized. It can either be determined visually by the difference in the color of these two landforms, or assessed based on the time and date when the image was taken, allowing calculating the height of

the tide at that moment. By superimposing the limits of landforms, vectorised with the help of multitemporal satellite images, it is possible to assess the deformations of these forms, as such coastal retreat or progradation for a set time period. By satellite images, we can also determine the location and evolution of the underwater bars which are quasi-ephemeral landforms and can completely change their position during several years. Basing on the analysis of multitemporal imagery, interpretative maps of coastal dynamics are created (Fig. 5).

### Methods of the wind-wave energy assessment

The wave energy flux is calculated using the Popov-Sovershaev [1981, 1982] wind-wave energy method [Ogorodov, 2002]. The method is based on the theory of wave processes and applies correlations between the wind speed and the parameters of the wind-induced waves.

For deep-water conditions, when the sea floor does not influence the formation of waves, the wave energy flux per second (for 1 m of the wave front) at the outer boundary of the coastal zone is calculated using the equation similar to the one used in V.V. Longinov's method [1966]:

$$E_{0dw} = 3 \cdot 10^{-6} V_{10}^3 x, \quad (1)$$

where  $V_{10}$  is the real wind speed measured by an anemometer at 10 m above sea level [m/s],  $x$  is the real or extreme distance of wave fetch [km] along the chosen wind direction. The dimension of the  $3 \cdot 10^{-6}$  coefficient corresponds to the dimensions of  $\rho/g$ , where  $\rho$  is density [gr./m<sup>3</sup>] (transformed into tons per cubic meter because of the big values, i.e. [t/m<sup>3</sup>]),  $g$  is gravitational acceleration [m/s<sup>2</sup>], i.e. is  $\frac{t/m^3}{m/s^2}$ . Thus,  $E_{0dw}$  has the dimension

of  $\frac{tm}{ms}$ , or  $t/s$ .

A similar equation for the shallow sea zone looks as follows:

$$E_{0sw} = 2 \cdot 10^{-6} \left( \frac{gH}{V_{10}^2} \right) V_{10}^5, \quad (2)$$

where  $E_{0sw}$  has the same dimensions as in equation (1). Equation (2) is applied if two conditions occur: 1) the kinematic index of shallowness  $\frac{gH}{V_{10}^2}$  is less than 3 ( $H$  is the sea

depth along the current wind direction expressed in meters); 2) the wave fetch  $x_{min}$  (in km) is great enough to generate waves:

$$\frac{x_{min}}{H} \geq 6.5 \left( \frac{gH}{V_{10}^2} \right)^{0.4}. \quad (3)$$

At  $\frac{gH}{V_{10}^2} < 3$  water depths hamper the formation of wind-induced waves. At  $\frac{gH}{V_{10}^2} = 3$

equation (3) becomes the following:

$$\frac{g x_{min}}{V_{10}^2} \geq 30. \quad (4)$$

From (4), the value of the extreme wave fetch for deep-sea conditions is obtained:

$$x_{lim} = 3V_{10}^2. \quad (5)$$

If any object like an island or a curve of the coastal line is closer than  $x_{lim}$ , the wave fetch is equal to the distance to this object, if not – it is determined by the formula (5).

Coastal wave abrasion is possible during the ice-free period. The longer it is, the greater the effect of wave action on coastal dynamics is. To calculate the energy coming to the shore from a given direction ( $E_d$ ) during the ice-free period, the instantaneous flux  $E_0$  is multiplied by the ice-free period duration expressed in seconds ( $n \times 86\,400$ , where  $n$  is the number of ice free days) and by the current wind speed ( $v$ ) and direction ( $d$ ) frequency ( $p_{dv}$  calculated over the ice-free period):

$$E_{dv} = E_0 \cdot n \cdot 86400. \quad (6)$$

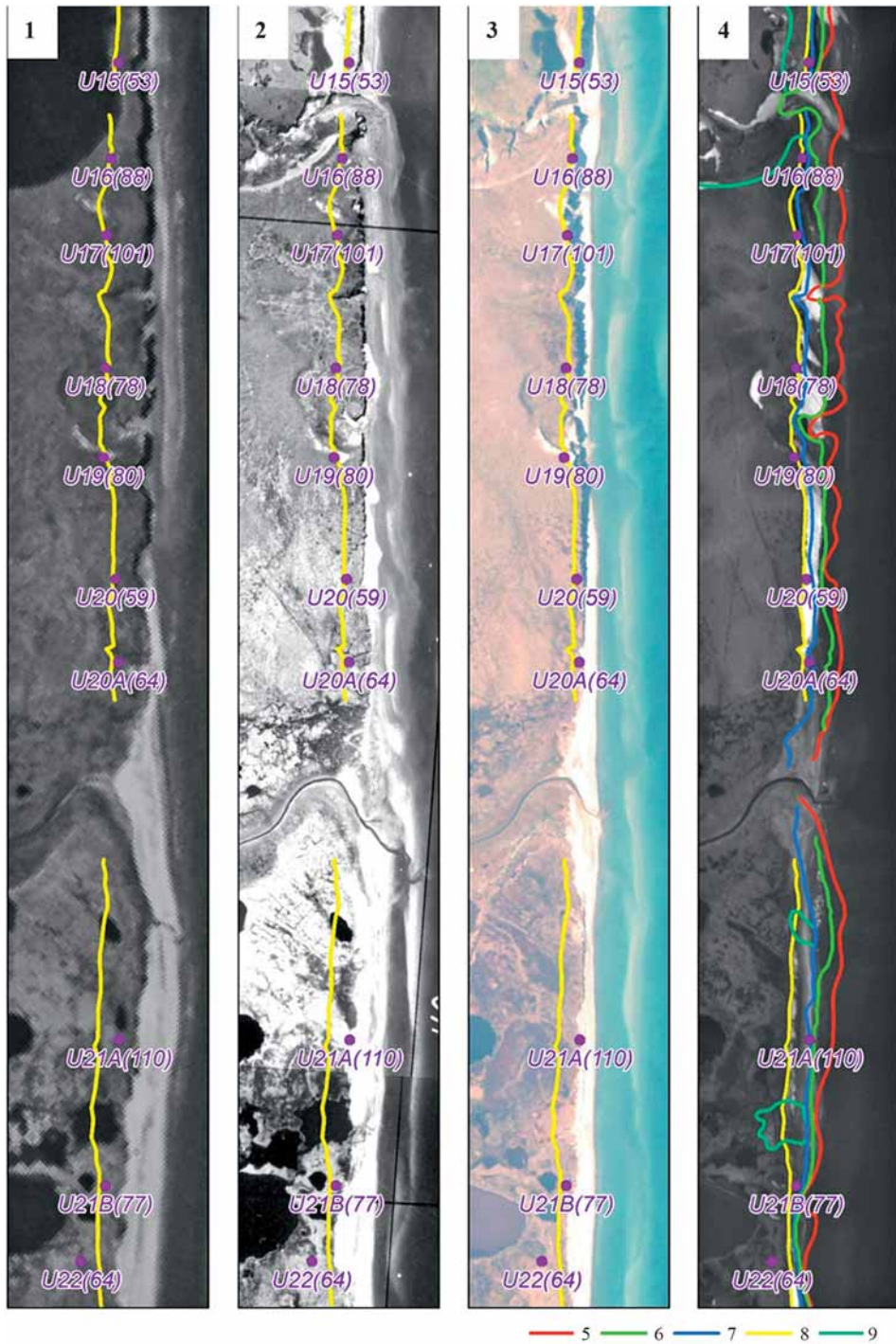


**Fig. 5. Interpretative scheme of coastal dynamics for the Ural coast of the Baydaratskaya Bay, Kara Sea:**

1 – Corona image 1964, 2 – aerial photo – 1988, 3 – QuickBird image – 2005, 4 – Formosat2 image -2012; coastal bluff in 2012; U8(110) – the number benchmark of the coastal dynamics monitoring network (the value of the coastal bluff retreat for 1964–2012, meters), 5 – coastline in 1964; 6 – coastline in 1988, 7 – coastline in 2005, 8 – coastline in 2012, 9 – contours of drained lakes

After that, the winds with all speeds which occurred are summarized:

$$E_d = \sum_{v=6}^{v_{\max}} E_{dv}. \quad (7)$$

It was shown in [Sovershaev, 1981, 1982] that the effect of weak winds (with velocities less, then 6 m/s) is negligible. That is why wind speeds higher than 5 m/s are taken into calculation.

The total amount of wind-wave energy (E) coming to a 1 meter long shore strap is calculated as the sum of  $E_d$  over all the wind-wave-dangerous directions, i.e. directions providing waves directed towards the coast:

$$E_d = \sum_{d=d_1}^{d_n} E_d = \sum_{d=d_1}^{d_n} \sum_{v=6}^{v_{\max}} E_{dv}. \quad (8)$$

The total energy flux vector is calculated as a geometrical sum of fluxes of wave-dangerous directions. It is divided into along- and across-shore components (Fig. 6).

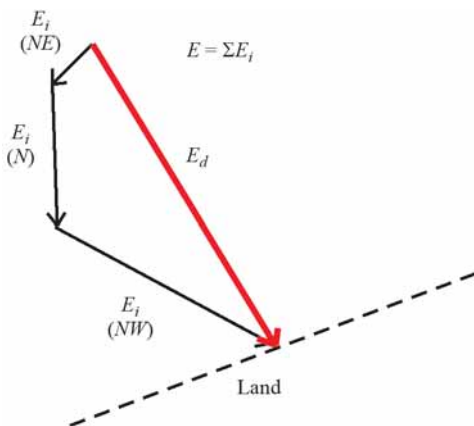


**Fig. 6. The illustration of the total energy flux vector (being a geometrical combination of energy fluxes of the wave-dangerous directions)**

## RESULTS AND DISCUSSION

### *Wind-wave energy interannual variations (the hydrometeorologic factor of coastal dynamics)*

The intensity of erosion of the sea shores and underwater slopes erosion is determined by the action of waves and excited currents. As far as waves in the Russian Arctic seas are generated mostly by wind, wind conditions are crucial in the formation of the wave energy flux. The waves act on the shores during the ice-free period. The seasonal coastal retreat rate is determined by the wave energy flux coming to the shoreline, which, in its turn, depends on the ice-free period duration. Storms provide the largest contribution to the total amount of wind-wave energy. The climate change of the latest decades is expressed both in ice and wind conditions changes. Satellite and ground-based ice observations show a reduction of the Arctic ice cover and an extension of the ice free period [<http://arctic.atmos.uiuc.edu/cryosphere/>; *Obzor...*, 2012].

The western Yamal region is good for the investigation of these processes because of its long observation history: the Marresalya station has held hydrometeorological observations (including ice monitoring) since 1914 and coastal dynamics monitoring is conducted from the beginning of the 80s (Fig. 1). As the climate of the Russian Arctic seas is characterized by a maximum of wind velocity and by the greatest number of storms in October-November, the shift of the end of the ice-free period towards winter would result in shoreline exposition to more and more severe storms. That would lead to coastal erosion intensification.

Using the Popov-Sovershaev's method [Sovershaev, 1980], the wind-wave energy of the ice-free period was calculated for the Marresalya station. The duration of the ice-free period in days is also shown on the graph (Fig. 7a). The analysis of the interannual variability of these values shows that the wind-wave energy flux generally increased

from 1977 to the present day, while the ice-free period experienced an extension (Fig. 7). However, these two parameters do not always show a direct agreement. For instance, in spite of the increasing ice-free period duration in 1998-2004, the wind-wave energy during this period, on the contrary, dropped due to a revealed period of weak wind activity [Ogorodov, 2011]. Combined retrospective analysis of storm events and interannual variability of the wave-energy flux can establish the presence and nature of their relation and, as a result, the potential of coastal erosion. In some years, in spite of high wind-wave energy, the ice-free period doesn't include the time of the Autumn storms, and therefore coastal destruction is minimal. However, with the increase of the ice-free period, these storms can dramatically increase the energy of waves affecting the coasts.

In Fig. 7b, it can be seen that the annual maximum of the wind-wave energy is usually referred to spring and autumn. If the sea is free of ice at that moment, the energy reaches the coast. This happened in the years 2005–2010, when the heaviest September and October storms fell into the ice-free period. As a result, a maximum of the wind-wave energy interannual variability was observed in this period. This occurred due to the high frequency of winds blowing from the open sea, generating the biggest waves, during that time. The frequency of north-westerly and west-north-westerly winds, providing the most part of the wind-wave energy flux, increased twice during the period of 2005–2010 compared to the previous years. As the wind frequency is governed by atmospheric circulation, such an anomaly shows global circulation changes in the Kara Sea region connected with the climate change.

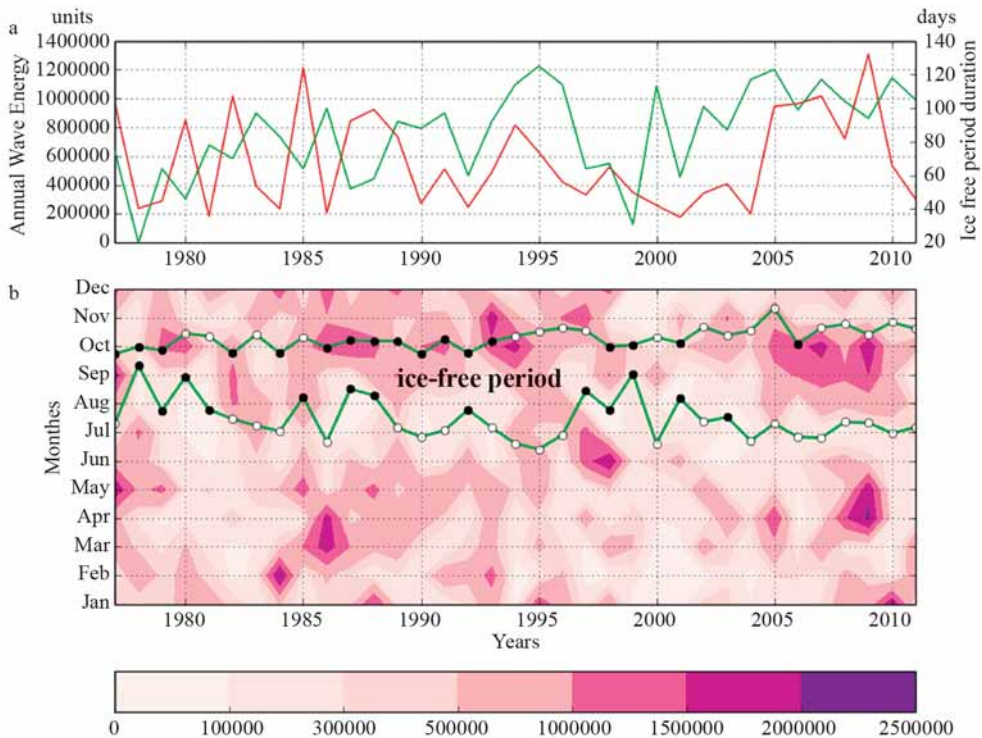


Fig. 7.

a) Marresalya annual wind-wave energy flux (standard units, red) and ice-free period duration (days, green);  
 b) values of potential wind-wave energy in standard units and ice-free period start and end dates (green line; black dot appears if the date reduces ice-free period duration in comparison to mean date, white – if extends)

The same patterns of wind-wave energy changes and consequent coastal retreat rates' increase were observed not only for the Kara Sea, but also for other parts of the Arctic, like the coasts of the Beaufort Sea in Alaska, where in 2007, in the conditions of an increased ice-free period, the rates of coastal retreat reached 25 m per ice-free season [Jones et al., 2009]. It has been noted that the duration of the open water season expanded from 45 days to 95 days during the period from 1979 to 2009 on the coasts of the Beaufort Sea, resulting in the fact that the exposure of the coastal cliffs to sea water increased by a factor of 2,5 [Overeem et al., 2011].

Climate change in the Arctic is also expressed in the wind speed decrease from the middle of XX to the beginning of XXI, especially noticeable at the Arctic shores [Vautard et al. 2010]. The reduction of the average wind speed occurs due to the decrease of strong winds frequency. At the same time, the number of calm days is getting lower too. At Marresalya station, changes in the ice-free period wind speed distribution are not related to the intensification or calming of the storm activity. There are periods of high and low storm activity (for the winds with the speed of more than 10 m/s). July–October of 1982–1996 are characterized by an increased number of storms. This is the case when the ice-free period end shifting towards winter extends the shore exposition to waves but does not necessarily result in the increase of the number of storms. The summers of 1997–2004 are the calmest. The wave energy minimum is caused both by small ice-free period duration (1998, 1999) and low storm frequency. The high values of wind-wave energy in 2000 appear because of high open water period duration and in 1980 – due to intensified storms in October. The same happened in 2005–2010, when, due to the extension of the ice-free period, the heaviest Autumn storms happened when the sea was ice-free. Data from the coasts of Alaska, based on time-lapse photography [Overeem et al., 2011] indicate that considerable erosion can happen even in one single storm; therefore

this increase of the ice-free period in Autumn can significantly influence the rates of thermoabration. The frequency of wave dangerous wind directions in October is higher than in November and September, and the wave dangerous storms' activity and the wind-wave energy values are the highest in October. That's why the presence of October in the ice-free period is crucial. In this way, the wave-energy flux and the related coastal retreat depend on several interconnected factors which may act separately or jointly enhancing or weakening each other.

#### *Interannual variations of coastal retreat rates (the Ural coast of the Baydaratskaya Bay)*

The Ural coast of the Baydaratskaya Bay is composed by permafrost and is retreating with the average rates of 0,5–4 m/year. The stationary observations of the coastal dynamics have been conducted here by the Laboratory of geocology of the North since 1988. In 2009, works on the construction of the underwater pipeline "Bovanenkovo-Uhta" crossing were made; therefore before that, coastal dynamics in natural conditions were observed, and after that they were affected by the influence of coastal constructions.

The profiles for the coastal dynamics monitoring are set in different geomorphological conditions (Fig. 8). In the north-west of the key area, a terrace with the heights of 10–18 m comes to the coast. In its central part, a low terrace of 4–10 m height with relatively high ice content is divided into several fragments by river valleys. In the south-eastern part, low laida (high water surge berm) with numerous lakes is situated. This laida can be covered by water during the highest surges and floods. As it can be seen from the retreat rate diagrams in Fig. 8, the coasts of the low terrace and laida generally experience a faster retreat. This retreat can be especially noticed in the last several years, with the increase of the wind-wave energy coming to the shores due to the prolongation of the ice-free period and changes in the wind patterns. The low coasts are, with all

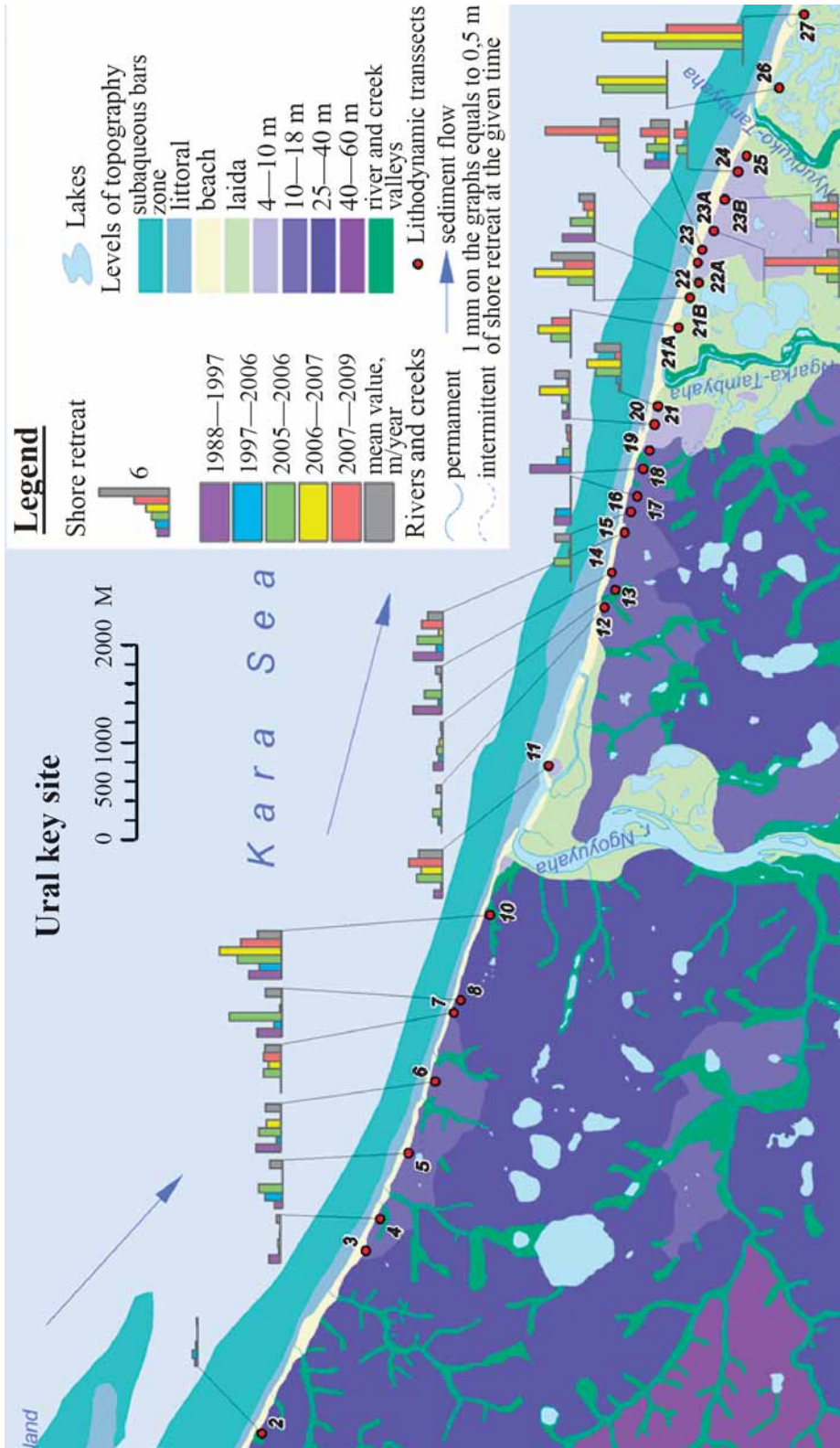
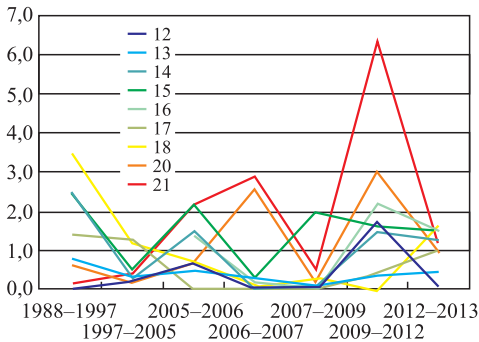


Fig. 8. Schematic map of the spatial and temporal variability of thermal abrasion coast of the Ural key area of Baidaratskaya Bay coast

other conditions being equal, less resistant to erosion than the high ones because with the same volume of material removed, the coast of, for instance, 20 m height will retreat by 1 m, while the coast of 1 m height will retreat by 20 m.

Not only spatial, but also temporal variability is characteristic for the retreat rates of the Ural coast. In general, two peaks of increase in retreat rates are observed: in 2005–2007 and in 2009–2012 (Fig. 9, 10).



**Fig. 9. Average rates of coastal retreat (m/year) for coastal dynamics monitoring profiles 12–21 within the Ural coast of the Baidaratskaya Bay key area (Y-axis – meters per year, X-axis – years)**

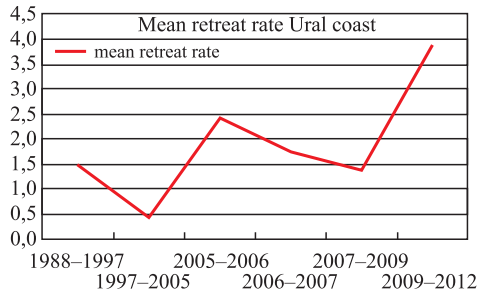


**Fig. 10. Mean rates of coastal retreat (m/year) for all coastal dynamics monitoring profiles within the Ural coast of the Baidaratskaya Bay key area (Y-axis – meters per year, X-axis – years)**

In 1997–2005, a negative peak is seen for all the profiles. It coincides with a minimum in wind-wave energy due to little occurrence of storm events, in spite of an increase of the ice-free period. After that, in 2005, 2006 and 2007, the increase of the ice-free period continued and coincided with an increase in the wind-

wave energy flux, which resulted in periods of Autumn storms and winds falling into the ice-free period, as mentioned above. As a result, most of the profiles show a 1,5–2 times increase of retreat rates compared to the average. The most affected were profiles 20 and 21, which showed a rate of 2,6 and 2,9 m/year in 2006–2007, respectively. These profiles are situated on a low terrace, which is, in natural conditions, destroyed quicker than the higher terraces. Probably, during the autumn storms of 2005 and 2006, most part of the low (4–10 m) cliff was directly affected by waves.

In 2007–2009, all the profiles show a negative peak in destruction rates again, although the wind-wave energy remained high. The negative peak, characteristic for the Ural coast for these years (unlike the Yamal coast, where higher retreat rates were observed) was caused by relatively low temperature during these years, which prevented ground ice and permafrost from thawing.

In 2009–2012, after the construction of the underwater pipeline crossing, a new, even more dramatic, peak of retreat rates is observed. The biggest retreat values were from 6 to 18 m/year, which is a record for the observations within the Ural coast. Profile 21, situated on low laida, reached a maximum retreat rate in 2009–2012, after the constructional works. Profile 28, which is situated within the coast of accumulative type and didn't retreat at all before 2009, showed a dramatic jump in the destruction rates in 2009–2013. The coast retreated by 55 m, which corresponds to an average rate of 18 m/year. The reason of such dramatic change lies in the road which came through the beach at this segment, with several heavy vehicles a day passing on the beach and littoral. In 2012–2013, this segment didn't retreat more than 3 m.

In general, there was a slight increase in the wind-wave energy in 2009–2012; however, it didn't exceed the typical values. Therefore the reason of erosion activation lies in processes connected with the technogenic impact.

In the last period of 2012–2013, rates of coastal retreat were, for most of the profiles, lower than the average values. Profile 17, 20 and 26 are an exception. The activation of abrasion for profile 20 is not extreme: the coast has already retreated here quicker in 2009–2012. In general, alteration of periods with high and low rates is characteristic for these profiles. For low rate periods (1988–2006, 2007–2009), typical values are 0,2–0,7 m/year, while for high rate periods (2006–2007, 2009–2013), 2,6–3,0 m/year are observed. It can be noted that average values were never observed. Such behavior is probably caused by the lithology of the coast within profile 20. Fine-grained sands here are overlain by peat. During “usual” years, the peat cover protects the bluff from erosion; this is why low retreat rates are observed. However, once every several years, a layer of peat falls from the edge of the cliff, which retreats several meters at once, providing a high erosion rate.

For profile 17, rates of retreat, close to those observed in 2012–2013, were noted before 2005. In 1991–1997, the average rate here was 1,4 m/year, and in 1997–2005 – 1,3 m/year. As both of these periods cover several years and an average rate is provided, it is highly probable that the retreat rate during some of these periods exceeded 1,6 m/year.

Therefore, the only area for the Ural coast of the Baidaratskaya Bay which experienced extreme retreat rates in 2012–2013, was profile 26. The coast retreated 12 m during 1 year, despite that, before, annual retreat rates didn't exceed 6 m/year. The coast here is accumulative, and the retreat is expressed not in cliff abrasion, but in displacement of the beach-slope landwards. Unlike the beach of full profile, which can migrate both seawards and landwards, a beach-slope retreats inevitably. The reason is that from the landward side, such beach transits into a laida, and therefore a washaway of such a beach will result in the laida destruction, not always even visible morphologically.

It should be noted that retreat was observed here even before the technogenic impact in 2005–2009. This testifies that coastal destruction is a natural process for this area, in spite of its accumulative morphology (the so-called retreating accumulative shore). However, the rate of retreat observed in 2012–2013, is not characteristic for the natural conditions of this coast. Such active retreat was caused by technogenic impact, and namely vehicles constantly driving on the beach as well as on adjacent laida.

It should be noted, that since the construction of the underwater pipeline, for areas where extreme abrasion rates were observed in 2009–2012, this trend didn't continue further on neither of the profiles. Interestingly, profiles 26, 27 and 28, situated in an area of alternation of thermoabrasional and accumulative coasts, are continuing to retreat in 2012–2013. This behavior can be connected with the movement of vehicles, because, before the latest time, coastal stability prevailed.

Average rates of coastal retreat on the coasts of the Kara Sea show steady growth (from 0,5 to 4 m/year on the average for all profiles, and up to 6 m/year for separate profiles). Similar values and trends were also noted for the eastern part of the Russian Arctic: erosion rates on Muostakh island, Laptev Sea increased from  $-1,8 \pm 1,3$  m/year since 1951 to  $3,4 \pm 2,7$  m a<sup>-1</sup> on average during the 2010–2013 observation period [Guenther et al., 2015]. However, in the American Arctic, greater velocities of coastal destruction were noted: the mean annual erosion rates at some locations of the Beaufort Sea coasts increased from 6,8 m/year in 1955–1979 to 13,6 m/year in 2002–2007 [Jones et al., 2009].

### *The human-induced factor of coastal dynamics*

The Varandey region is a negative example demonstrating the need for a well-developed, ecologically grounded approach to further exploitation of coastal regions. The main objects of oil transportation infrastructure

here have been built on a marine terrace with an average height of 3–5 m formed during the Holocene transgression. The terrace is represented by a series of barrier islands and barrier beaches. Its width reaches 2–6 km. The terrace is composed of fine sand unit underlain by peat-grass pillow. The cryogenic structure of the terrace sediments is characterized by low ice content [Novikov and Fedorova, 1989]. Frontal and seaward, part of the terrace is covered by an avandune (ridge-like dune belt) reaching 5–12 m asl. At the distal parts of the barrier beaches, the avandune turns into a series of ancient and young barrier ridges corresponding to different stages of the evolution of barrier beaches and barriers-spits. Barrier ridges have been considerably reworked by aeolian processes. The inner parts of the terrace behind the dune belt are laidas (surge flood plains) of up to 2,5–3 m high with two levels corresponding to the low and high surge.

At present, under natural conditions, most of the First terrace is being eroded at a rate of 0,5–2,5 m per year. The abrasion coast has an erosion scarp cut in aeolian-marine fine sands. During years with extraordinarily strong fall storms, the slope is eroded and

becomes steeper for a short period of time. Thermoabrasion does not, in fact, erode the slopes of the Holocene terrace. The latter is destroyed due to relatively high average annual ground temperatures, small ice content and a considerable thickness of the layer of seasonal melting. Coastal erosion is determined by a combination of different factors including the deficit of coarse-grained beach-forming material (the discrepancy between the grain size and hydrodynamic conditions), a poorly developed profile of the submarine coastal slope, and high gradient of the avandune slopes.

Active exploitation of the Varandey industrial area started in the 1970s. The Varandey Island experienced the strongest human impact. The main industrial base was formed here, and a new settlement for 3 thousand inhabitants, was built (Fig. 11). The well-drained dune belt of the Holocene terrace, composed of sand beds with low ice content, was chosen as the place for the settlement, oil terminal and storehouses, because it seemed to be more stable from the engineering-geological point of view than the surrounding swampy tundra lowland.

The construction of the settlement and industrial base practically at the edge of the



**Fig. 11. Aerial photo of the Varandey settlement at 1985; coastline of 2013**

abrasion cliff demanded repeated withdrawals of sand and sand-pebble sediments from the avandune and beach. This is extremely dangerous for the zones of wave energy divergence [Popov et al., 1988], especially in zones that have been eroded before. Within the zone of industrial exploitation, the coastal bluff and the coastal zone experienced considerable mechanical deformations of the landforms because of transport ramps, mechanical leveling of coastal declivities and other human disturbances [Ogorodov, 2005]. Uncontrolled use of transport and construction vehicles including caterpillars caused the degradation of soil and plant cover of the whole dune belt of Varandey Island. Under the conditions of deep seasonal melting, the dune belt formed of fine sands experienced deflation and thermoerosion. The extent and rate of these processes has been so great that in several places the surface of the island became 1-3 m lower than before the period of exploitation. Deflation hollows became widespread. Numerous deflation-thermoerosional gullies formed in the bluff. As a result, the bluff became lower, its homogeneity was disturbed, the volume of sediment supplied to the coastal zone decreased and, finally, the coasts became less stable, and their rates of retreat increased. Coastal protection at Varandey settlement caused a decrease in sediment supply to the adjacent areas and, hence, their erosion.

Under the existing conditions of intensive human impact, the coastal erosion rate increased considerably in the mid- to late seventies. In some years at some sites it reached up to 7–10 m/year. The rates of coastal retreat slightly decreased, down to 1,5–2 m/year, after the coastal-protection construction was built near the Varandey settlement. However, they remained high in the adjacent areas. Recent measurements have shown that the rate of coastal retreat in the region around the settlement increased and reached 3–4 m/year: that is twice and more as high as in the regions that are not affected by human activity. The acceleration of coastal and underwater slope erosion

has contributed to the self-excitation of the underwater pipeline to the surface. As a result, it was pulled out from the bottom by the sea ice impact [Chernikov, 2006]. After an earth-dam and a bridge were constructed in the eastern part of the Varandey Island, the height of storm surges increased. The latter is an important factor of coastal dynamics. Previously, during high surges corresponding in time with tides, water was partly flowing into the branches and channels, thus lowering the surge height and decreasing its influence on the coast. On July 24, 2010, an extreme storm surge completely flooded the Varandey Island, and penetrated several kilometers inland. Enormous damage was made for oil infrastructure.

The negative experience of Varandey area development was not taken into account during the construction of gas transportation facilities on the coasts of the Kara Sea. The section of the coast of the Yamal Peninsula (Baydaratskaya Bay) at the underwater crossing Yamal-Europe can be an example. The following types of direct human impact on the relief have been documented: construction of large artificial positive landforms, which leads to additional sediment income to the coastal area in a given place; construction of artificial concave landforms, removal of sand material from the beach, tide flats (Fig. 12) and from the underwater shore slope, which leads not only to erosion and narrowing of tide flats and of the beach, but also to changes in the position of submerged systems of bars; deformation of the surface of mud flats, beach, coastal barrier and laida during construction and during motion of heavy track machines or heavy vehicles as well as destruction or disturbance of soil and vegetation cover, which leads to intensification of erosion.

Among the results of human impact, the following changes are distinguished: appearance of anthropogenic accumulative forms in the coastal area connected with the change in the sediments drift; appearance of hollow forms on the beaches and tidal flats caused by the intensification of erosion



**Fig. 12. Yamal Coast of the Baydaratskaya Bay:  
traces of sandy sediment removal from the tide flat and beach**

resulting from the disruption of sediment transportation or from the change in the profile of the beach; intensification of deflation at the disturbed surfaces. Due to the fact that the places of extraction of constructional materials were not considered in advance from the perspective of morpholithodynamic situation, the extraction of sand material for constructional purposes is carried out without a certain plan and without consideration of the consequences. Sandy material is most actively extracted from the surface of the barrier beach between the nearest river mouth and the cofferdam. The surface deformation and the vegetation destruction at the barrier beach leads to the intensification of deflation. This creates sediments deficit in this coastal area, which leads to its erosion. The construction of the cofferdam where the pipeline lies resulted in the accumulation of sediments in the entrance corner to the south of the cofferdam and in the erosion of the coast to the north from it. In natural conditions, the barrier beach completely absorbs the wave energy even during extreme storms [Kamalov et al., 2006]. Changes in the barrier beach morphology cause the changes in the conditions of waves'

destruction and, therefore, changes in the entire morpholithodynamic regime that can lead to unfavorable and hazardous consequences. The coastal system will tend to reach a new equilibrium, which will cause off- and onshore topography reforming with the rates that were not considered in the construction project. In order to reduce the impact of the pipeline construction on coastal systems, the first required thing is stopping the removal of sediments.

As the Ural coast mentioned above, the Yamal coast also experienced an increase in the retreat rates in 2005–2010, right after the removal of sediments and the increase of the traffic of heavy vehicles of the beach. Unlike these two sites, at the Kharasavey area, where no considerable constructional works were executed in 2005–2010, the rates of retreat experienced only a slight increase. This proves again that such a dramatic peak in abrasion of the Ural and Yamal coasts of the Baydaratskaya Bay was caused not only by natural processes connected with climate change and wind-wave energy increase, but were enhanced by unreasonable human activity, which strengthened the negative natural effect.

## CONCLUSIONS

During the last decades, the Arctic coasts have experienced relatively quick changes. On the one hand, they are caused by the changing climate leading to higher summer air temperatures and longer ice-free period duration leading to sometimes dramatic increases of the wind-wave energy affecting the shores. On the other hand, unreasonable human activity can easily enhance the negative effect of the climate change, leading to redistribution of the natural morpholithodynamic systems causing catastrophic coastal retreat. Among this negative impact, the removal of sediment from the beach, tidal flat and lida, especially at low coasts, can be considered the most dangerous process.

A truly responsible decision-making towards the strategy of developing the northern coasts of Russia and constructing new facilities has to be based on integrated knowledge of the ongoing environmental processes, in particular coastal dynamics. The ignoring of this issue may cause irreversible damage to both the coastal geosystems and the facilities themselves, which, once they are destructed, may lead to enormous environmental implication.

## ACKNOWLEDGEMENTS

The work was executed with the financial support of the Russian Science Foundation project No. 16-17-00034. ■

## REFERENCES

1. Chernikov N.A. (2006) "Duga Barkova" (Barkov bow). Izdatelstvo "Smena", 238 p (in Russian).
2. Günther, F., Overduin, P.P., Yakshina, I.A., Opel, T., Baranskaya, A.V. and Grigoriev, M.N. (2015): Observing Muostakh disappear: permafrost thaw subsidence and erosion of a ground-ice-rich island in response to arctic summer warming and sea ice reduction, *The Cryosphere*, 9 (1), 2015, pp. 151–178. doi: 10.5194/tc-9-151-2015.
3. Jones, B.M., Arp, C.D., Jorgenson, M.T., Hinkel, K.M., Schmutz, J.A., & Flint, P. (2009). Increase in the rate and uniformity of coastline erosion in Arctic Alaska. *Geophys. Res. Lett.*, 36, L3503 doi: 10.1029/2008GL036205
4. Kamalov A.M., Ogorodov S.A., Biriukov V.Yu., Sovershaeva G.D., Tsvetsinskiy A.S., Arkhipov V.V., Belova N.G., Noskov A.I., Solomatin V.I. (2006) "Morfolitodinamika beregov i dna Baidaratskoi Guby na trasse perekhoda magistralnymi gazoprovodami" (Morpholithodynamics of the coasts and bottom of the Baydaratskaya Bay within the major pipeline crossing area). *Kriosfera Zemly (Cryosphere of the Earth)*, Vol. X, N 3, pp. 3–14 (in Russian).
5. Longinov V.V. (1966) Energeticheskiy metod ocenki vdolberegovikh perememsheniy nosov v beregovoy zone moria (Energetic method of estimating alongshore sediment drift in coastal zone). *Proceedings of SoyuzmorNIIproekt*, 12 (8), 13–28. (In Russian)
6. Novikov V.N. and Fedorova E.V. (1989) Razrushenie beregov yugo-vostochnoi chasti Barentseva Morya (Destruction of the coasts of the south-eastern part of the Barentz Sea), *Vestnik MGU, ser. 5, geogr*, N 1: 64–68 (in Russian).
7. Obzor gidrometeorologicheskikh protsessov v Severnom Ledovitom Okeane (Review of the hydrometeorologic processes in the Arctic Ocean) (2012) *Arkticheskii i Antarkicheskii nauchno-issledovatel'skii Institut, ROSGIDROMET*. 112 p. (in Russian).

8. Ogorodov S.A. (2002) Application of wind-energetic method of Popov-Sovershaev for investigation of coastal dynamics in the Arctic. In: Arctic Coastal Dynamic. Report of an International Workshop. Potsdam (Germany) 26–30 November 2001. Reports on Polar and Marine Research. Edited by V. Rachold et al. Bremerhaven. Vol. 413, 37–42.
9. Ogorodov S.A. (2005) Human impacts on coastal stability in the Pechora Sea, *Geo-Marine Letters*, Vol. 25, N 2–3, P. 190–195.
10. Ogorodov S.A. (2008) Vliyaniye izmenenii klimata i ledovitosti na dinamiku arkticheskikh beregov Evrazii (The impact of climate and ice extent change on the dynamics of the Eurasian Arctic coasts). *Problemy Arktiki i Antarktiki*, N 1 (78), pp. 123–128 (in Russian).
11. Ogorodov S.A. (2011) Rol' morskikh l'dov v dinamike reliefa beregovoy zony (The role of sea ice in the dynamics of the relief of the coastal zone). *Izdatelstvo Moskovskogo Universiteta* (The MSU Publishing House), 173 p. (in Russian).
12. Ogorodov S.A., Belova N.G., Kuznetsov D.E., Noskov A.I. (2011) Ispolzovanie materialov raznovremennykh aerokosmicheskikh syemok v tseliakh issledovaniya dinamiki beregov Karskogo moria (Using the materials of multitemporal aerospace imagery for the purpose of investigations of the Kara Sea coasts' dynamics). *Zemlia iz kosmosa-naibolee effektivnie resheniya* (Earth from space – most efficient solutions) № 10, p. 66–70 (In Russian)
13. Overeem, I., R.S. Anderson, C.W. Wobus, G.D. Clow, F.E. Urban, and N. Matell (2011), Sea ice loss enhances wave action at the Arctic coast, *Geophys. Res. Lett.*, 38, L17503, doi:10.1029/2011GL048681
14. Polar sea ice cap and snow – Cryosphere today [online]. Source. Available from: <http://arctic.atmos.uiuc.edu/cryosphere/> [Accessed date: 15.08.2015]
15. Popov B.A., Sovershaev V.A. (1981) Principi vybora ishodnikh dannikh dlia rascheta potokov volnovoy energii (Principles in distinguishing data for calculating wave energy fluxes). *Beregovaya zona morya* (Coastal zone). Moscow, Nauka, 47–53 (In Russian)
16. Popov, B.A., Sovershaev V.A., Novikov V.N. (1988) *Beregovaya zona Pechorsko-Karskogo regiona* (Coastal zone of the Pechora-Kara region). *Issledovanie ustoichivosti geosystem Severa* (Investigations on the sustainability of Northern geosystems), *Izdatelstvo Moskovskogo Universiteta* (The MSU Publishing House), pp. 176–201 (in Russian).
17. Popov, B.A., Sovershaev, V.A. (1982) Nekotoryie cherty dinamiki arkticheskikh beregov Azii (Some features of the coastal dynamics in the Asian Arctic). *Voprosy geografii*, 119. *Morskie berega* (Sea coasts). Moscow, Mysl', 105–116 (In Russian)
18. Sovershaev, V.A. (1980) *Beregoformiruyushie factory i zonirovaniye beregov morei Laptevykh, Vostochno-Sibirskogo i Chukotskogo po dinamicheskomu printsipu*. (The factors of coastal formation and zoning of the coasts of the Laptev. East Siberian and Chukchi seas based on the dynamic principle) *Dissertatsiya na soiskanie uchenoy stepeni kandidata nauk* (Ph. D. Thesis), MGU, 212 p (in Russian).
19. Vautard, R., J. Cattiaux, Yiou P., Thepaut J.N., and Ciais P. (2010), Northern Hemisphere atmospheric stilling partly attributed to an increase in surface roughness, *Nature Geosciences*, N 3, 756–761, doi: 10.1038/ngeo979.



**Stanislav A. Ogorodov** studied at the Lomonosov Moscow State University and commenced Ph. D. in 1999. Since 2004, he is a leading scientist at the MSU Faculty of Geography. In 2014, he habilitated as a full Doctor of Science. The area of his scientific interests is Arctic coastal dynamics and the ice effect on seabed. Main publications: The role of sea ice in the coastal zone dynamics of the Arctic Seas (2003); Human impacts on coastal stability in the Pechora Sea (2005); The Role of Sea Ice in Coastal Dynamics (2011).



**Alisa V. Baranskaya** graduated from the Lomonosov Moscow State University in 2010. In 2015, she received her Ph. D. in geomorphology at St. Petersburg State University. Since 2012, she is a research fellow at the Laboratory of Geoecology of the North, the MSU Faculty of Geography. Her research focuses on neotectonics and Quarternary geology of the Arctic and their influence on coastal dynamics in the cryolithozone. Main publications: Observing Muostakh disappear: permafrost thaw subsidence and erosion of a ground-ice-rich island in response to arctic summer warming and sea ice reduction (2015, with co-authors); New data on dislocations in the Quarternary deposits of the Yamal and Gydan peninsula and the latest tectonic movements associated with them by the results of the "Yamal-Arctic-2012" expedition (2013, with co-authors); Modern ice gauging relied of the western Yamal shelf: natural investigations and modeling (2013, with co-authors).



**Nataliya G. Belova** graduated from the Lomonosov Moscow State University in 2007; in 2012, she received her Ph. D. in cryolithology. She investigates the problems of the origin of massive ice beds in the Arctic, and their influence on modern coastal dynamics. Main publications: Buried and intrasedimental massive ice beds of the western coast of the Baydaratskaya Bay, Kara Sea (2015); The role of massive ice beds in the dynamics of the south-western coast of the Kara Sea (based on the data on monitoring of the coastal erosion within the sites of the HMS "Floks" and HMS "Kharasavey") (2011, with S.A. Ogorodov).



**Anatoliy M. Kamalov** graduated from the Lomonosov Moscow State University in 1982. His main research interests are the Arctic coastal dynamics. He currently works as an engineer in the Laboratory of Geoecology of the North of the MSU Faculty of Geography and investigates the morphology of the Russian Arctic coasts and their rates of retreat and accumulation. Main publications: Morpholithodynamics of the coasts and bottom of the Baydaratskaya Bay within the major pipeline crossing area (2006, with co-authors); Development of coastal accumulative forms in the conditions of the cryolithozone (1998, with co-authors).



**Dmitriy E. Kuznetsov** graduated from the Lomonosov Moscow State University in 2000. He currently works as an engineer in the Laboratory of Geoecology of the North. Dmitry's research focuses on GIS and remote sensing methods in coastal dynamics, as well as sea bottom morphology, bathymetry and sedimentology. Main publications: Assessing the sensitivity of Arctic coastal dynamics to climate change. (2014, with co-authors); Using the materials of multitemporal aerospace imagery for the purpose of investigations of the Kara Sea coasts' dynamics (2011, with co-authors)



**Pier Paul Overduin** studied at Wilfrid Laurier and York Universities in Canada, and completed a Ph. D. at the University of Alaska Fairbanks in 2005. Since 2006 he is a senior scientist in the Periglacial Research Department at the Alfred Wegener Institute for Polar and Marine Research in Potsdam, Germany. His research focuses on submarine permafrost and coastal dynamics in the Arctic. Main publications: Short and long-term thermo-erosion of ice-rich permafrost coasts in the Laptev Sea region (2013, with co-authors); Geoelectric observations of the degradation of near-shore submarine permafrost at Barrow (Alaskan Beaufort Sea) (2012, with co-authors); Evolution and degradation of coastal and offshore permafrost in the Laptev and East Siberian Seas during the last climatic cycle (2007, with co-authors).



**Natalya N. Shabanova** graduated from the Faculty of Geography, Lomonosov Moscow State University in 2011. Her area of interests lies in the meteorology and climatology of the Polar regions, especially Kara Sea. One of her major focuses is the Popov-Sovershaev wind-wave energy method and its implementation for the metocean constraints of the coastal dynamics. Main publications: Coastal Dynamics Monitoring at the Barents and Kara Seas (2013, with co-authors); Coastal Erosion Monitoring at the Barents and Kara Seas (2013, with co-authors)



**Alexey P. Vergun** works at the Laboratory of Geoecology of the North of the Lomonosov Moscow State University as an engineer-cartographer. In 2009, he graduated from the Department of Cartography, the MSU Faculty of Geography. His research interests are the GIS technologies allowing assessing the rates of coastal erosion of the Barents and Kara sea coasts, as well as the engineering geomorphology and general cartography. Main publications: Coastal Dynamics Monitoring at the Barents and Kara Seas (2013, with co-authors); Modern ice gauging relied of the western Yamal shelf: natural investigations and modeling (2013, with co-authors).

DOI: 10.15356/2071-9388\_03v09\_2016\_05

**Roman G. Zdorovenov<sup>1\*</sup>, Galina G. Gavrilenko<sup>1</sup>, Galina E. Zdorovenova<sup>1</sup>, Nikolay I. Palshin<sup>1</sup>, Tatyana V. Efremova<sup>1</sup>, Sergey D. Golosov<sup>1, 2</sup>, Arkady Yu. Terzhevik<sup>1</sup>**

<sup>1</sup> Northern Water Problems Institute, Petrozavodsk, Russia; Alexander Nevsky ave., 50, 185030, Tel. + 7 (814) 257-63-81

\*Corresponding author; e-mail: romga74@gmail.com

<sup>2</sup> Institute of Limnology, Russian Academy of Sciences; St-Petersburg, 196105, Sevastyanov st., 9, Tel. + 7 (812) 387-02-60

## OPTICAL PROPERTIES OF LAKE VENDYURSKOE

**ABSTRACT.** We conducted a field study on light conditions in a small boreal Karelian Lake Vendyurskoe over two years. Albedo of ice-covered lake varied from 0.9 to 0.1, and the euphotic zone depth exceeded 3.5 m during the melting stage. The Secchi disc depth changed from 2.5 m after ice-break to 3.7 m at the stage of early summer. The vertical distribution of the photosynthetically active solar radiation (PAR) attenuation coefficient for water  $K_w$  was characterized by high spatial (vertical) and temporal (seasonal and interannual) variability which can be connected with the dynamics of plankton cells. The highest values of  $K_w$  reached 2–2.8  $m^{-1}$  in the upper 0.5 m layer of a water column, and decreased to 0.5–1.5  $m^{-1}$  with increasing depth. The highest values of  $K_w$  were marked in the end of ice-covered period.

**KEY WORDS:** ice-covered lake, albedo, photosynthetically active radiation, under-ice irradiance, PAR attenuation coefficient.

### INTRODUCTION

Solar radiation is one of the most important parameters in functioning of the lake ecosystem. Radiative heating of water, spring under-ice convection, photosynthesis, the daily activity of the plankton and fish community – all of these processes are determined by the flux of solar radiation penetrating into a water column [Zaneveld et al., 1981; Mironov & Terzhevik, 2000; Mironov et al., 2002; Reynolds, 2006]. Snow-ice cover, high water color and turbidity, and large concentrations of phytoplankton in the surface layers of the reservoir are the key factors that limit the penetration of solar radiation into a water column [Chekhin, 1987; Arst et al., 2008]. The attenuation of the solar flux within the snow-ice cover has been studied quite well [Petrov et al., 2005; Arst et al., 2006, 2008; Lei et al., 2011; Zdorovenova et al., 2013]. At the same time under-ice light measurements

are rare and often limited to the upper meter of a water column [Leppäranta et al., 2003; Arst et al., 2006]. Thus, parameterization of attenuation of the solar radiation within ice-covered lakes is an important task of modern physical limnology.

In order to obtain a better knowledge on the distribution of light in shallow ice-covered boreal lakes, we performed field measurements of solar radiation fluxes at the upper and lower boundary of ice and within a water column of Lake Vendyurskoe (Karelia, Russia). The aim of research was to study the spatial and temporal dynamics of PAR flux in a water column during late winter, spring, and early summer.

### MATERIALS AND METHODS

Measurements of solar radiation fluxes were carried out on a small Lake Vendyurskoe located in the south of Karelia (62°10'N,

33°10'E). Lake Vendyurskoe is a shallow lake of glacial origin. Surface area of the lake is 10.4 km<sup>2</sup>, volume is 54.8 · 10<sup>6</sup> m<sup>3</sup>, maximal and mean depths are 13.4 and 5.3 m, respectively. The duration of the ice season is 5–6.5 months: the ice-period starts between the first half of November and the beginning of December, and the ice-break occurs in the first half of May [Petrov et al., 2005; Zdorovenov et al., 2013].

Measurements of solar radiation fluxes at the surface of snow-ice cover and PAR-fluxes into a water column were conducted on 21–24 April 2013 and 26–31 March 2014 when the radiatively-driven convection under ice was in progress. Also PAR fluxes were measured during open water on 8 May 2013, 17–18 June 2013, 20–21 May 2014, and 11–15 June 2014. All measurements were performed at 1-min intervals.

The measuring station with a depth of 7.2 m was located at a distance of 300 m from the northern shore of the lake (Fig. 1, A). During the ice-covered period pyranometers were mounted on a special holder at a height of about one meter above the ice surface (Fig. 1, B). The downwelling and upwelling planar irradiance at the surface of snow-ice cover were measured with a "Star-shaped" pyranometer (Theodor Friderich & Co, Meteorologische Geräte und Systeme, Germany). Downwelling planar irradiance at the lower boundary of ice was measured with M-80m universal pyranometer (Gydrometpribor, USSR).

Measurements of PAR flux at the lower boundary of ice and within a water column were performed using sensors JFE Alec MkV-L ("Alec Electronics", Japan, 390–690 nm, range 0–2000 μmol · m<sup>-2</sup> · s<sup>-1</sup>, accuracy ±4 % FS, resolution 1 μmol · m<sup>-2</sup> · s<sup>-1</sup>). The PAR sensors were attached to the fishing line at intervals of 0.5–1 m to the depth of 7.2 m. The top sensor was located directly under the ice or at the depth of 0.2 m during open water measurements. A scheme of the observational site during ice-period is shown in Figure 1, B. The Secchi disk depth was measured during

open water surveys in May and June 2013. The thickness of the snow and ice at the station of radiation was measured twice a day during 21–24 April 2013 and 26–31 March 2014.

The albedo  $\alpha$  was calculated as a ratio of downwelling  $E_d(0)$  and upwelling  $E_u(0)$  global irradiances at the surface of the snow-ice cover:

$$\alpha = \frac{E_u(0)}{E_d(0)}. \quad (1)$$

Assuming exponential decay of PAR in a water column, the PAR attenuation coefficients for water  $K_w$  was calculated using the measured values of PAR at the top sensor and at different depths in water:

$$K_w(z, z_1) = -\frac{1}{z_1 - z} \ln \left( \frac{E_d(z_1)}{E_d(z)} \right). \quad (2)$$

The depth of the euphotic zone (the euphotic zone is a layer of the water column at the lower boundary of which irradiance drops to 1 % of the surface value and less [Jerlov, 1976; Chekhin, 1987]) was estimated based on the measurements of irradiance on the upper and lower boundaries of the snow-ice cover taking into account the albedo and calculated values of  $K_w$ , as in [Kirillin et al., 2012]:

$$z(1\%) = \ln[100(1 - \alpha)\tau]/K_w \quad (3)$$

where  $\tau$  is the light transmittance of the snow-ice cover, defined as the ratio of transmitted irradiance to incident irradiance,

$$\tau = \frac{E_d(z)}{(1 - \alpha)E_d(0)}. \quad (4)$$

Here  $E_d(z)$  is the downwelling planar irradiance at the lower ice boundary.

Data from the weather station "Petrozavodsk" closest to Lake Vendyurskoe were used in the analysis of the weather conditions. Visual observations of cloud cover were conducted every three hours daily throughout the measurement period.

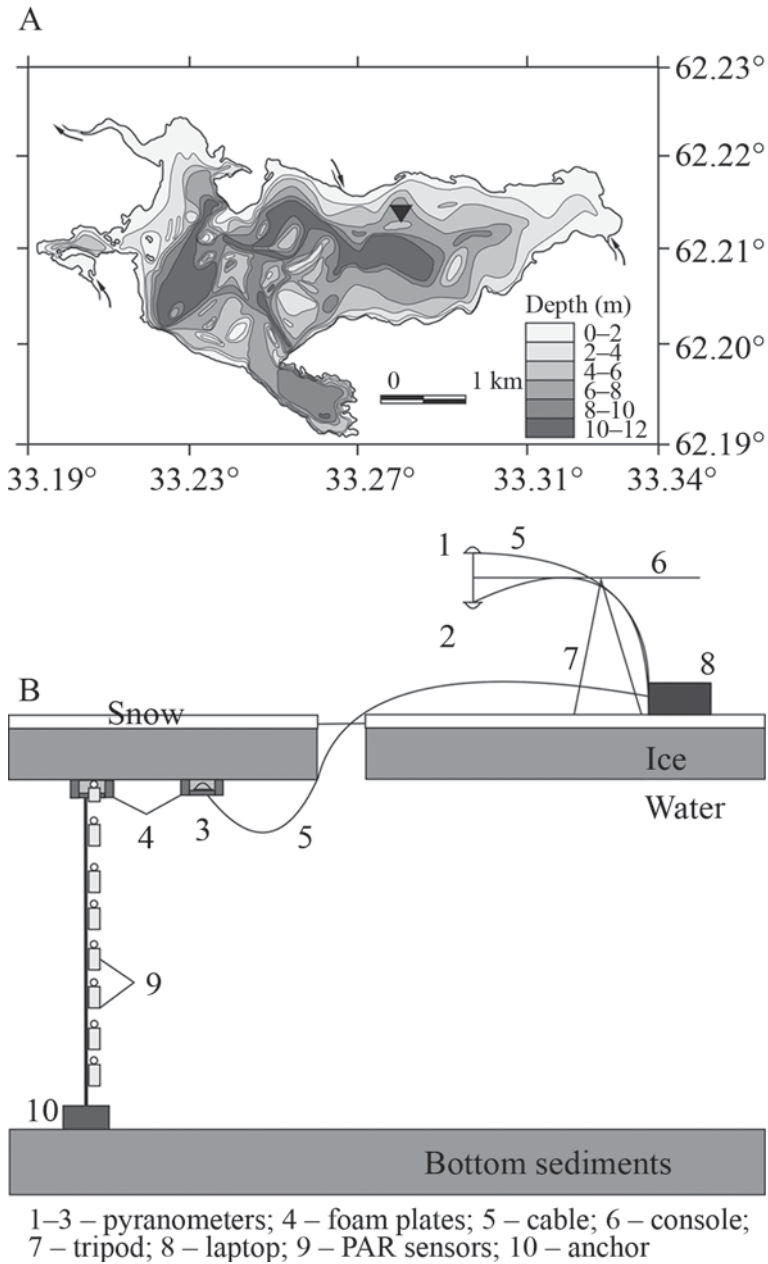


Fig. 1. Bathymetric map of Lake Vendyurskoe with the measurement station (black triangle) (A). A scheme of the observational site in April 2013 and March 2014 (B).

## RESULTS AND DISCUSSION

### *Ice cover period*

Weather and ice conditions differed significantly in April 2013 and March 2014. Intensive ice melting caused by the warm overcast weather (the air temperature reached +13 °C at daytime and decreased to -3 + 4 °C at night) was observed from 21 to 24 April 2013: the thickness of the ice-sheet decreased by 10 cm over four days (from 41 to 31 cm). The thickness of the white ice on 21 April was 6 cm, and that of congelation ice 35 cm. During the four days of observations, white ice melted completely, and the thickness of congelation ice decreased by four cm. The albedo of the lake's surface reduced from 0.35 to 0.13 over the same period, and light transmittance ranged between 0.4–0.5.

In contrast, the weather was cold on 26–31 March 2014. The air temperature increased to +4...+7 °C at daytime on 26 and 27 March, and +1 °C on 28–30 March. The night air temperature dropped to -1...-7 °C. It was clear on 26–28 March, it was cloudy on 29–30 March, and it snowed. The thickness of white ice was 10 cm and of the congelation ice 30 cm at the first day of observation. Each layer has decreased by one cm during the measurement period. The albedo was 0.35–0.45 during the first three days of measurements. On 29 March after the snowfall, there was a sharp increase in albedo to 0.85–0.9; albedo remained at a high level of 0.75–0.8 during the next three days. The light transmittance in the first days of measurements reached 0.3–0.4; after the snowfall, it decreased to 0–0.05.

The daytime maxima of downwelling planar irradiance at the surface of the snow-ice cover reached 550–800 W·m<sup>-2</sup> on the background of clear or slightly overcast sky, and did not exceed 350 W·m<sup>-2</sup> under completely overcast during both surveys. The downwelling planar irradiance at the lower ice boundary reached 100–200 W·m<sup>-2</sup> during measurements of

April 2013, and did not exceed 100 W·m<sup>-2</sup> on 26–28 March 2014. After the snowfall on 29 March 2014, the flux of solar radiation on the lower boundary of ice was significantly reduced.

The daily maxima of PAR flux reached 1500–2000 μmol·s<sup>-1</sup>·m<sup>-2</sup> at the lower boundary of ice on 21–23 April, and 900–1000 μmol·s<sup>-1</sup>·m<sup>-2</sup> on 26–28 March 2014; after a snowfall on 29 March, it fell down to 200 μmol·s<sup>-1</sup>·m<sup>-2</sup> and did not exceed 50 μmol·s<sup>-1</sup>·m<sup>-2</sup> on 30–31 March. The PAR flux decreased rapidly with depth: it was close to zero at a depth more than 3–4 m during both surveys.

On 21–24 April 2013, the depth of the euphotic zone, z(1 %), ranged within 3–3.8 m. On 26–28 March 2014, z(1 %) reached three meters and then, after a snowfall, rapidly decreased to zero.

Since the PAR flux at different depths of a water column was characterized by high variability, the PAR attenuation coefficient for water  $K_w$  was calculated using the 10-minute averaged PAR data. The maximal values of  $K_w$  2–2.8 m<sup>-1</sup> were confined to the under-ice layer 0–0.5 m during 21–24 April 2013 (Fig. 2, A). On 26–28 March 2014,  $K_w$  reached 2 m<sup>-1</sup> in a layer of 0–1 m (Fig. 2, B), and dropped to 1–1.2 m<sup>-1</sup> after 29 March. Values of  $K_w$  rapidly decreased to 1.4–1.8 m<sup>-1</sup> (average 1.6 m<sup>-1</sup>) at a depth of 0.5–1 m during April survey and to 0.5–1.4 m<sup>-1</sup> (average 1.1 m<sup>-1</sup>) at a depth of 1–2 m during March survey. Below, up to a depth of 3–4 m,  $K_w$  values were gradually reduced to 1.2 m<sup>-1</sup> (with extremes 0.6–1.6 m<sup>-1</sup>) during the April survey and to 0.5–0.7 m<sup>-1</sup> during the March survey.

### *Open water period*

Ice-off occurred on 3 May 2013. The measurements were performed on 8 May 2013 from 9:00 to 15:00. The weather was clear, warm, and windy: the air temperature varied from +9 to +16 °C during the measurement period, northwest wind reached 4–6 m·s<sup>-1</sup>

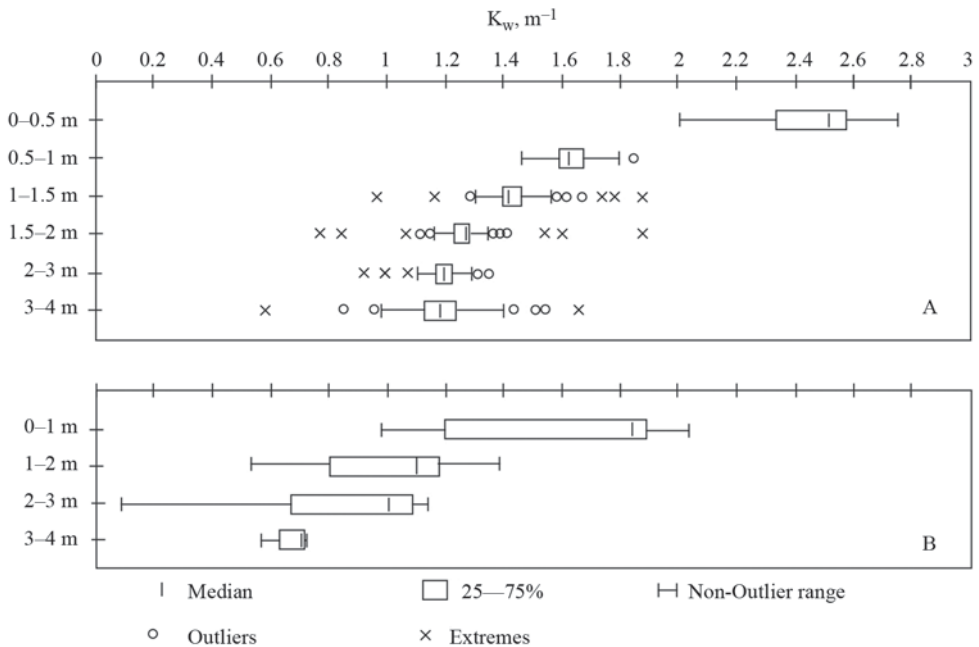


**Fig. 2. Variability of PAR attenuation coefficient for water  $K_w$  (10-min averaging) in different layers of a water column on 21–24 April 2013 (A) and 26–31 March 2014 (B).**

with gusts of up to  $10 \text{ m} \cdot \text{s}^{-1}$ . Likely due to the waves, the upper PAR-sensor (located at a depth of 0.2 m) periodically reached the surface of the lake. Consequently, its records had a strongly fluctuating nature: the PAR flux varied in the range of  $500\text{--}3000 \mu\text{mol} \cdot \text{s}^{-1} \cdot \text{m}^{-2}$ , with an average value of  $1500 \mu\text{mol} \cdot \text{s}^{-1} \cdot \text{m}^{-2}$ . The flux of PAR decreased rapidly with increasing depth: to  $500 \mu\text{mol} \cdot \text{s}^{-1} \cdot \text{m}^{-2}$  at a depth of 0.7 m, to  $100 \mu\text{mol} \cdot \text{s}^{-1} \cdot \text{m}^{-2}$  at a depth of 1.7 m, and to  $25 \mu\text{mol} \cdot \text{s}^{-1} \cdot \text{m}^{-2}$  at a depth of 3.2 m. It was close to zero deeper than 3.2 m. The Secchi disk depth varied 2.5–2.8 m.

The weather was cloudy and warm on 17–18 June 2013: the air temperature reached  $+18 \text{ }^\circ\text{C}$  at daytime and  $+9 \text{ }^\circ\text{C}$  at night; cloudiness was 50–100 %; southwest wind was  $1\text{--}3 \text{ m} \cdot \text{s}^{-1}$ . The flux of PAR reached  $3000 \mu\text{mol} \cdot \text{s}^{-1} \cdot \text{m}^{-2}$  at a depth of 0.2 m; its average value was  $850 \mu\text{mol} \cdot \text{s}^{-1} \cdot \text{m}^{-2}$  at daytime. The transparency of the water column increased, compared with the May survey: the Secchi disk depth was 2.9–3.7 m.

The PAR flux at a depth of 1.7 m periodically exceeded  $500 \mu\text{mol} \cdot \text{s}^{-1} \cdot \text{m}^{-2}$ , at a depth of 3.2 m reached  $100 \mu\text{mol} \cdot \text{s}^{-1} \cdot \text{m}^{-2}$ , at a depth of 4.2 m reached  $35 \mu\text{mol} \cdot \text{s}^{-1} \cdot \text{m}^{-2}$ , and deeper it was close to zero.

The weather was extremely hot on 19–20 May 2014: the air temperature reached  $+32 \text{ }^\circ\text{C}$  at daytime and  $+20 \text{ }^\circ\text{C}$  at night; cloudiness was variable; southwest wind was  $1\text{--}4 \text{ m} \cdot \text{s}^{-1}$ . The flux of PAR reached  $2000 \mu\text{mol} \cdot \text{s}^{-1} \cdot \text{m}^{-2}$  at depth of 0.5 m; its average value was  $650 \mu\text{mol} \cdot \text{s}^{-1} \cdot \text{m}^{-2}$  at daytime. The transparency of a water column was higher than in May 2013: the flux of PAR at a depth of 3, 4 and 5 m reached 90, 35 and  $10 \mu\text{mol} \cdot \text{s}^{-1} \cdot \text{m}^{-2}$ , and deeper it was close to zero.

The weather was cool, windy and cloudy on 11–15 June 2014: the air temperature not exceeded  $+21 \text{ }^\circ\text{C}$  at daytime and dropped down to  $+5\text{--}9 \text{ }^\circ\text{C}$  at night; cloudiness was variable (4–8 points on the 8-point scale); northeast wind reached  $1\text{--}5 \text{ m} \cdot \text{s}^{-1}$ . The flux of PAR exceeded  $3000 \mu\text{mol} \cdot \text{s}^{-1} \cdot \text{m}^{-2}$  at a

depth of 0.5 m on 12 and 13 June; but its value was less than  $600 \mu\text{mol} \cdot \text{s}^{-1} \cdot \text{m}^{-2}$  on 14 June under overcast. The transparency of a water column was higher than in May 2014: the flux of PAR at a depth of 3, 4 and 5 m reached 150, 70 and  $20 \mu\text{mol} \cdot \text{s}^{-1} \cdot \text{m}^{-2}$  and deeper it was close to zero.

The values of the PAR attenuation coefficient  $K_w$  during the open water in May and June 2013 and 2014 widely varied from 0.2 to  $2.6 \text{ m}^{-1}$  (Fig. 3). The highest values of  $K_w$  were observed in the surface layer of a water column at depth of 0.2–0.7 m in May 2013 ( $1.5\text{--}2.4 \text{ m}^{-1}$  with average  $1.9 \text{ m}^{-1}$ ) (Fig. 3, A) and in June 2013 ( $1.3\text{--}2 \text{ m}^{-1}$  with average  $1.7 \text{ m}^{-1}$  and with extremes up to  $2.5 \text{ m}^{-1}$ ) (Fig. 3, B), when the transparency of a water column was minimal. Exactly as during ice measurements,  $K_w$  rapidly decreased with increasing depth in the top-meter layer: its values were  $0.8\text{--}1.8 \text{ m}^{-1}$  (average  $1.4 \text{ m}^{-1}$ , sporadic outlier to  $2.6 \text{ m}^{-1}$ ) at depth of 0.7–1.2 m in May 2013 and  $0.9\text{--}1.4 \text{ m}^{-1}$  (average  $1.1 \text{ m}^{-1}$ , extremes  $0.4\text{--}1.8 \text{ m}^{-1}$ ) at the same depth in June 2013. Below, to depth of 3.2 m the average values of  $K_w$  were close to  $1.2 \text{ m}^{-1}$  in May 2013 and to  $1 \text{ m}^{-1}$  in June 2013.

In May and June 2014  $K_w$  did not exceed  $2.2 \text{ m}^{-1}$  with average values  $1.4\text{--}1.5 \text{ m}^{-1}$  in the surface layer of 0.5–1 m (Fig. 3, C and D). The average values of  $K_w$  decreased to  $1\text{--}1.1 \text{ m}^{-1}$  at depth of 1.5–4 m during both surveys. During the May 2014 survey, the vertical distribution of  $K_w$  was more arranged, while it was characterized by a large number of extremes and outliers in June 2014.

A wide variability of parameters describing the snow-ice cover optical properties of small shallow lakes is the main feature of late winter. The albedo decreased rapidly, and ice transparency increased during melting of snow and ice. At same time, varying weather conditions, e.g., snowfall, led to a sharp increase of albedo and lower light transmittance. Our estimates of albedo and light transmittance during early spring are in

good agreement with the results of previous measurements on Lake Vendyurskoe [Petrov et al., 2005; Leppäranta et al., 2010] and measurements on other lakes [Bolsenga & Vanderploeg, 1992; Arst et al., 2006; Lei et al., 2011].

If the snow layer is thick, the flux of solar radiation penetrating the ice underneath is negligible [Malm et al., 1997]. During intensive spring melting, the radiation flux in the under-ice layer rises, the depth of the euphotic zone also increases. Our estimations of the euphotic zone depth (from 3.5 m for clear ice to technically zero values after snow fall) are in a reasonable agreement with the results of other researchers. The estimates of the euphotic zone for different boreal lakes when ice is covered with snow are in the range of 0–1.3 m, and in the absence of snow within 0.5–4.7 m [Arst et al., 2006; Jakkila et al., 2009].

We have defined the range of variability of the PAR attenuation coefficient for water  $K_w$  from 0.5 to  $2.8 \text{ m}^{-1}$  for late winter period. Our estimations of  $K_w$  are in a good agreement with the data presented recently [Leppäranta et al., 2003; Arst et al., 2006, 2008]: according to the measurements in the Estonian and Finnish lakes, the diffuse PAR attenuation coefficient for under-ice water varied from 0.5 to  $2.6 \text{ m}^{-1}$ .

In our measurements, we found significant spatial and temporal variability of  $K_w$ . The increase in values of  $K_w$  occurs with the decrease in water transparency. In late winter, one of the probable reasons of lowering the water transparency is intensification of photosynthesis and increasing algal biomass. Measurements on the different types of lakes revealed that primary production in a water column is well correlated with the penetration of PAR through the ice [Tulonen et al., 1994; Fritsen & Priscu, 1999]. The melt water coming to the under-ice layer of the lake from the catchment area may be significantly less transparent and also cause fluctuations of  $K_w$ . In addition, increasing values of  $K_w$  after melting snow may be explained by the

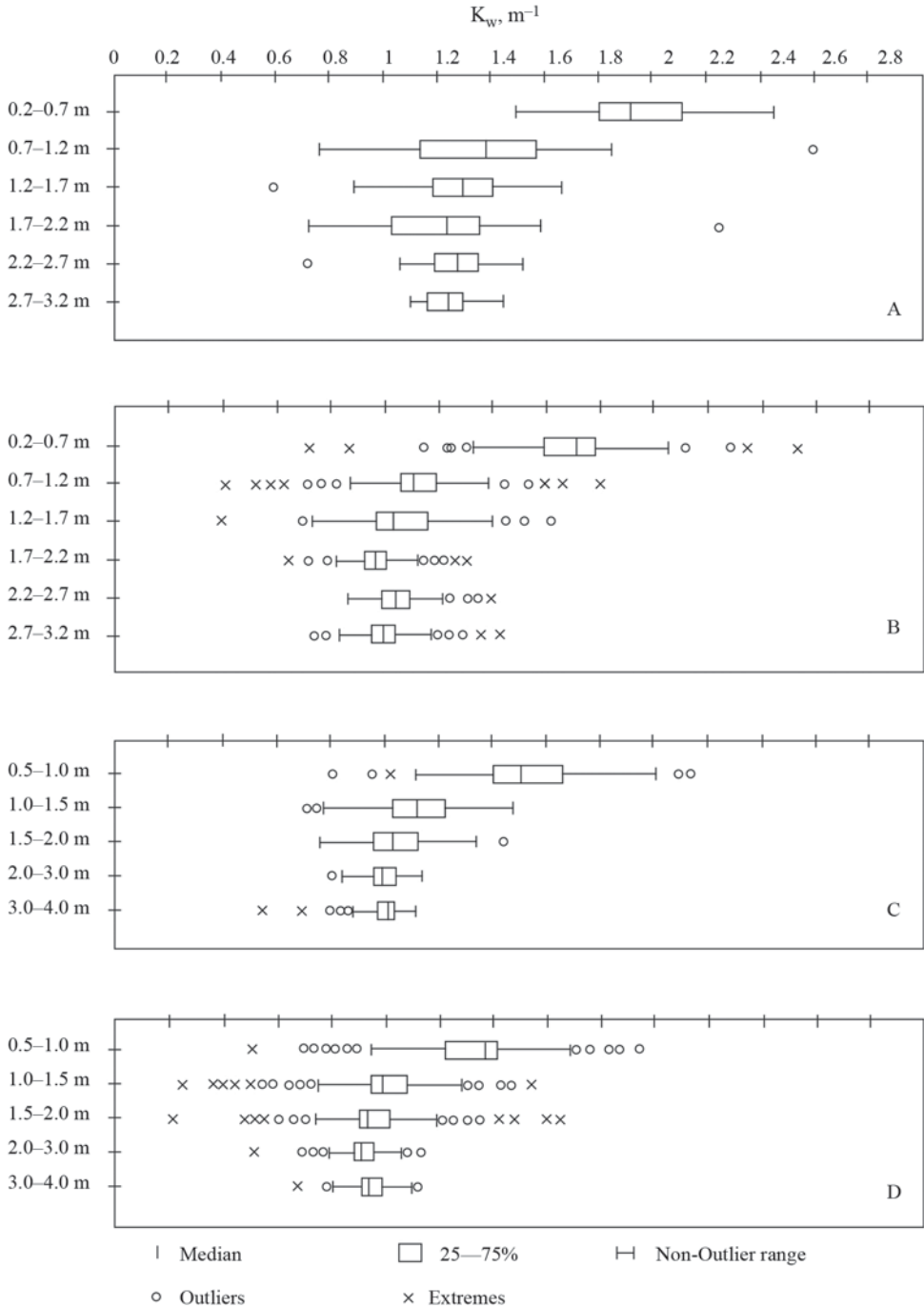


Fig. 3. Variability of PAR attenuation coefficient (10-min averaging) in different layers of a water column during May 2013 (A), June 2013 (B), May 2014 (C), and June 2014 (D).

difference in the spectral composition of irradiance below the snow-ice cover or clear ice [Arst et al., 2008].

Decreasing values of  $K_w$  along increasing depth is a sign that water transparency is minimal in the under-ice layer and increases in the underlying water. Apparently, this is due to the maxima of phytoplankton cells concentrated in the under-ice water layer where light conditions are most favorable. The vertical distribution pattern of algal biomass with a maximum in the under-ice layer has been observed in the different types of lakes during the development of the radiatively-driven convection [Belzile et al., 2001; Twiss et al., 2012]. On the other hand, it is known that the high level of illumination can lead to inhibition of photosynthesis in the sub-ice layer. In that case, the maximum concentration of plankton is located at a certain depth with the optimal light conditions [Vanderploeg et al., 1992; Jewson et al., 2009].

In our measurements, the values of  $K_w$  always decreased with increasing depth. Such a vertical variation of this parameter is described as typical in the study [Leppäranta et al., 2003]. The authors also describe the opposite situation, when the minimum value of  $K_w$  ( $0.8\text{--}1\text{ m}^{-1}$ ) was confined to a 0.2 m layer of under-ice water of mesotrophic Lake Ülemiste, and at the depth of 1.2 m, the coefficient values increased twofold.

In our investigations, the highest values of  $K_w$  were observed in the 0.5-m under-ice layer of a water column in April 2013 ( $2.5\text{--}2.8\text{ m}^{-1}$ ) and in the first days of measurements in March 2014 ( $1.9\text{ m}^{-1}$ ) at the stage of the active ice melting, when the snow was absent, and the thickness of white ice did not exceed a few centimeters. Apparently, the amount of phytoplankton cells in the under-ice layer during the active stage of ice melting and favorable light conditions was significantly higher than on 29–31 March 2014 when after the snowfall the PAR penetration was limited.

The values of  $K_w$  in April, May and June 2013 were visibly higher than in March, May and June 2014. Presumably, this was due to a more active under-ice phytoplankton development in April 2013. Furthermore, in both years there was a gradual decrease in the coefficient values for three consecutive surveys: from the melting stage through homothermy to the stage of thermocline formation. Such a change of  $K_w$  should correspond to a gradual increase in water transparency, which was confirmed by measurements of a Secchi disk depth in May and June 2013. Possibly, the seasonal variation of phytoplankton concentration has a decisive influence on the transparency of the surface layer of Lake Vendyurskoe.

We have shown that the  $K_w$  value significantly changes not only during the transition period from winter to summer, but from year to year. Extensive analysis of optically active substances, light attenuation, and a Secchi depth were performed based on 10-year measurements on 14 Estonian and 7 Finnish lakes [Arst et al., 2008]. Significant seasonal and interannual variability of the PAR attenuation coefficient for water was noted, but no systematic temporal change could be detected.

The diffuse PAR attenuation coefficient for water  $K_w$  is used in the numerical modeling for a wide range of tasks: from heat-budget models of a mixed layer (see, e.g., Zaneveld et al., 1981) and under-ice convection [Matthews & Heaney, 1987; Mironov et al., 2002] to weather prediction (see, e.g., Mironov et al., 2010). It must be admitted that the variability of  $K_w$  is much better studied for open water as compared to the ice season.

There are a number of parameterizations for  $K_w$  in a water column [Henderson-Sellers, 1984]: from simple, taking into account the depth of the Secchi disk [Williams et al., 1981], to complex, using multiple coefficients, which vary depending on the level of turbidity of the reservoir [Zaneveld et al., 1981]. All of them assume a constant  $K_w$  value for a water

column. From our estimates, it is particularly noteworthy to mention that a sharp decrease of  $K_w$  with depth is present in the most of calculated  $K_w$  profiles, demonstrating its spatial heterogeneity.

Analysis of our PAR measurements in a water column for two consecutive years, significantly different in weather and ice conditions, revealed that the coefficient values vary widely. The vertical profiles of  $K_w$  calculated from the instant values of the PAR flux at different depths, are characterized by significant variability. Two important consequences can be formulated: (1) instant PAR profiles are not suitable to calculating reliable estimates of  $K_w$ , and (2) existing approximations do not allow us to describe the spatial and temporal dynamics of this coefficient. To obtain realistic values of  $K_w$  it is necessary to measure the radiation fluxes at different depths in water column with a possibly small time interval for a few hours, and then to average obtained values for each depth.

Erroneous values of  $K_w$  may strongly affect results of numerical modeling. Given  $K_w = 2 \text{ m}^{-1}$ , about 87 % of solar radiation penetrated into water would be "arrested" in the uppermost 1-m layer. In a case  $K_w = 1 \text{ m}^{-1}$ , this value decreases to 63 %, resulting in artificial over-warming of underlying waters. In turn, a decrease of the density jump may develop comfortable conditions for deeper mixing.

## CONCLUSIONS

The present study focuses on light conditions in a shallow lake at the stage of late winter, spring, and early summer and demonstrates the significant temporal variability of optical properties of the snow-ice cover and PAR attenuation coefficient for water  $K_w$ .

To study the temporal dynamics of the lake's optical properties during the transition from ice-covered period to open water, three surveys were carried out: (1) during the melting stage at the end of the ice-covered

period (21–24 April 2013 and 26–31 March 2014), (2) shortly after ice-off at the stage of homothermy (8 May 2013 and 20–21 May 2014), and (3) early summer at the stage of formation of thermal stratification (17–18 June 2013 and 11–15 June 2014).

Analysis of observational data, containing downwelling and upwelling planar irradiance at the surface of snow-ice cover, downwelling irradiance at the lower ice boundary and PAR-flux at the lower boundary of ice and within a water column at different depths was performed. Weather conditions have a great impact on the optical properties of snow-ice cover, and, consequently, on the under-ice irradiance at the stage of active melting. As snow melts, albedo decreases, the light transmittance rises, and the depth of the euphotic zone gradually increases, reaching several meters. The presence of a snowfall invokes the sharp decrease in light amount under the ice. Only a few cm of fresh snow lead to a sharp increase in albedo, decreasing light transmittance to negligible values and reducing the depth of the euphotic zone to zero.

Measurements for two consecutive years revealed that the highest values of  $K_w$  were confined to the surface layer thickness of about 1 m; with increasing depth the coefficient typically decreased. Such a pattern of  $K_w$  vertical distribution represents an increase in water transparency with depth, presumably caused by the vertical distribution of phytoplankton cells with a maximum in the most illuminated surface layer. Significant spatial and temporal variability of  $K_w$  can be connected to the dynamics of plankton cells.

The observations have demonstrated that the coefficient values vary widely, thus the single PAR profiles are hardly acceptable to get reliable estimates of  $K_w$  for the practical use, e.g., in numerical simulations. The presence of strong gradients between  $K_w$  in the uppermost water layer and that in the rest of a water column requires the development

of the depth-dependent  $K_w$  parameterization. These two conclusions can be considered as the novelty of our work.

Further research is expected to be focused on the parameterization of  $K_w$  as a function of depth during late winter and open-water periods.

## ACKNOWLEDGEMENTS

The study was partially supported by the Russian Foundation for Basic Research (projects 13-05-00338, 14-05-91761, 14-05-00787) and by the European Commission (grant Marie Curie IRSES: GHG-LAKE № 612642). ■

## REFERENCES

1. Arst H., Erm A., Leppäranta M. & Reinart A. (2006) Radiative characteristics of ice-covered fresh- and brackish-water bodies. *Proc. of the Estonian Academy of Sciences, Geology*. 55 (1): 3–23.
2. Arst H., Erm A., Herlevi A., Kutser T., Leppäranta M., Reinart A. & Virta J. (2008) Optical properties of boreal lake water in Finland and Estonia. *Boreal Env. Res.* 13: 133–158.
3. Belzile C., Vincent W.F., Gibson J.A.E. & Van Hove P. (2001) Bio-optical characteristics of the snow, ice, and water column of a perennially ice-covered lake in the High Arctic. *Can. J. Fish. Aquat. Sci.* 58: 2405–2418.
4. Bolsenga S.J. & Vanderploeg H.A. (1992) Estimating photosynthetically available radiation into open and ice-covered freshwater lakes from surface characteristics; a high transmittance case study. *Hydrobiologia*. 243/244: 95–104.
5. Chekhin L.P. (1987) *Svetovoi rezhim vodoemov* [Light Regime of Water Bodies]. Petrozavodsk: Karel'skii filial AN SSSR. 130 p. [in Russian].
6. Fritsen C.H. & Priscu J.C. (1999) Seasonal change in the optical properties of the permanent ice cover on Lake Bonney, Antarctica: consequences for lake productivity and phytoplankton dynamics. *Limnol. Oceanogr.* 44: 447–454.
7. Henderson-Sellers B. (1984) *Engineering Limnology*. Boston: Pitman Advanced Publishing Program.
8. Jakkila J., Leppäranta M., Kawamura T., Shirasawa K. & Salonen K. (2009) Radiation transfer and heat budget during the melting season in Lake Pääjärvi. *Aquatic Ecology*. 43 (3): 681–692.
9. Jerlov N.G. (1976) *Marine optic*. Elsevier Oceanography Series 5, Elsevier, Amsterdam–Oxford–New-York.
10. Jewson D.H., Granin N.G., Zhdanov A.A. & Gnatovsky R.Yu. (2009) Effect of snow depth on under-ice irradiance and growth of *Aulacoseira baicalensis* in Lake Baikal. *Aquatic Ecology*. 43(3): 673–679.
11. Kirillin G., Leppäranta M., Terzhevik A., Granin N., Bernhardt J., Engelhardt C., Efremova T., Palshin N., Sherstyankin P., Zdorovenova G. & Zdorovenov R. (2012) Physics of seasonally ice-covered lakes: a review. *Aquatic Sciences*. 74 (4): 659–682.

12. Lei R., Leppäranta M., Erm A., Jaatinen E. & Pärn O. (2011) Field investigations of apparent optical properties of ice cover in Finnish and Estonian lakes in winter 2009. *Estonian Journal of Earth Science*. 60 (1): 50–64.
13. Leppäranta M., Reinart A., Erm A., Arst H., Hussainov M. & Sipelgas L. (2003) Investigation of Ice and Water Properties and Under-ice Light Fields in Fresh and Brackish Water Bodies. *Nordic Hydrology*. 34 (3): 245–266.
14. Leppäranta M., Terzhevik A. & Shirasawa K. (2010) Solar radiation and ice melting in Lake Vendyurskoe, Russian Karelia. *Hydrology Research*. 41 (1): 50–62.
15. Malm J., Terzhevik A., Bengtsson L., Boyarinov P., Glinsky A., Palshin N. & Petrov M. (1997) Temperature and Hydrodynamics in Lake Vendurskoe during Winter 1995/1996. Department of Water Resources Engineering, Institute of Technology. University of Lund, № . 3213. 203 p.
16. Matthews P.C. & Heaney S.A. (1987) Solar heating and its influence on mixing in ice-covered lakes. *Freshwater Biology*. 18: 135–149.
17. Mironov D.V. & Terzhevik A.Y. (2000) Spring convection in ice-covered freshwater lakes. *Izvestiya Atmospheric and Oceanic Physics*. 36 (5): 627–634.
18. Mironov D., Terzhevik A., Kirillin G., Jonas T., Malm J. & Farmer D. (2002) Radiatively-driven convection in ice-covered lakes: observations, scaling and a mixed-layer model. *J. Geophys. Res.* 107 (C4): 7-1-7-16.
19. Mironov D., Heise E., Kourzeneva E., Ritter B., Schneider N. & Terzhevik A. (2010) Implementation of the lake parameterization scheme FLake into the numerical weather prediction model COSMO. *Boreal Env. Res.* 15: 218–230.
20. Petrov M.P., Terzhevik A.Y., Palshin N.I., Zdorovenov R.E. & Zdorovenova G.E. (2005) Absorption of Solar Radiation by Snow-and-Ice Cover of Lakes. *Water Resources*. 32 (5): 496–504.
21. Reynolds C.S. (2006) *The Ecology of Phytoplankton*. Cambridge University Press.
22. Tulonen T., Kankaala P., Ojala A. & Arvola L. (1994) Factors controlling production of phytoplankton and bacteria under ice in a humic, boreal lake. *J. of Plankton Res.* 16 (10):1411–1432.
23. Twiss M.R., Smith D.E., Cafferty E.M. & Carrick H.J. (2012) Diatoms abound in ice-covered Lake Erie: An investigation of offshore winter limnology in Lake Erie over the period 2007 to 2010. *J. Great Lakes Res.* 38: 18–30.
24. Vanderploeg H.A., Bolsenga S.J., Fahnenstiel G.L., Liebig J.R. & Gardner W.S. (1992) Plankton ecology in an ice-covered bay of Lake Michigan: utilization of a winter phytoplankton bloom by reproducing copepods. *Hydrobiologia*. 243–244 (1): 175–183.

25. Williams D.T., Drummond G.R., Ford D.E. & Robey D.L. (1981) Determination of light extinction coefficients in lakes and reservoirs. Proc. ASCE Symp. On Surface Water Impoundments. Minneapolis, Minnesota. 2: 1329–1335.
26. Zaneveld J.R.V., Kitchen J.C. & Pak H. (1981) The influence of optical water type on the heating rate of a constant depth mixed layer. Journal of Geophysical Research. 86 (C7): 6426–6428.
27. Zdorovenov R., Palshin N., Zdorovenova G., Efremova T. & Terzhevik A. (2013) Interannual variability of ice and snow cover of a small shallow lake. Estonian Journal of Earth Science. 61 (1): 26–32.
28. Zdorovenova G., Zdorovenov R., Palshin N. & Terzhevik A. (2013) Optical properties of the ice cover on Vendyurskoe lake, Russian Karelia (1995–2012). Annals of Glaciology. 54 (62): 121–124.

**Received 12.11.2015****Accepted 29.08.2016**

**Roman E. Zdorovenov** is Senior Research Scientist at the Northern Water Problem Institute of the Karelian Research Centre of the Russian Academy of Sciences. He graduated from St. Petersburg State University, Geography and Geoecology Faculty, in 1996. He received his Ph. D. degree in Oceanology in 2004. His main research fields are hydrodynamics of the White Sea and hydrophysical processes in lakes. He is a permanent member of the NWPI fieldworks and the author and co-author of more than 40 papers.



**Galina G. Gavrilenko**, is a second-year postgraduate student at the Northern Water Problem Institute of the Karelian Research Centre of the Russian Academy of Sciences. She graduated from St. Petersburg State University, Geography and Geoecology Faculty, in 2009. Her research interests are associated with shallow lakes and their regimes, thermodynamics and seasonal variability. She is the author and co-author of 6 papers. She participated in a number of international conferences and workshops in hydrology and geography.



**Galina E. Zdrovennova** is Senior Research Scientist of Laboratory of Hydrophysics at the Northern Water Problem Institute of the Karelian Research Centre of the Russian Academy of Sciences. She graduated from St. Petersburg State University, Geography and Geoecology Faculty, in 1996. In April 2007, she received her Ph. D. degree in Hydrology. Her main research fields are: thermal, dynamic, ice, radiation and oxygen regimes of shallow lakes. In February 2010, she has been trained on the software package MATLAB and has been writing programs in the same programming language at the Institute of Freshwater Ecology (IGB), Berlin. She is the author and co-author of more than 20 papers.



**Nikolay I. Palshin**, is Senior Research Scientist at the Northern Water Problem Institute of the Karelian Research Centre of the Russian Academy of Sciences. He graduated from Leningrad Hydrometeorological Institute in 1975. In 1991, he received his Ph. D. degree at Moscow State University. His research interests: thermal and hydrodynamic processes in lakes (dilution and mixing of waste water in the lakes, the effects of sealing, with stirring, ice and thermal regime of lakes, climatic variability, oxygen regime of lakes, optical properties of natural waters). He is a member of the Russian Geographical Society. He is the author and co-author of more than 40 papers.



**Tatyana V. Efremova** is Senior Research Scientist at the Northern Water Problem Institute of the Karelian Research Center of the Russian Academy of Sciences. She graduated from St. Petersburg State University, Geography Faculty, in 1979. She defended the thesis in 2005 at the Institute of Limnology of RAS. Her main research fields: thermal and ice regime of lakes. She is the author and co-author of more than 30 papers.



**Sergey D. Golosov** is Senior Research Scientist at the Northern Water Problem Institute of the Karelian Research Center of the Russian Academy of Sciences. He graduated from Leningrad Hydrometeorological Institute in 1982. In 1993, he received his Ph. D. degree. His research interests are associated with hydrophysical and chemical and biological processes in lakes and mathematical modeling of aquatic ecosystems. He is a member of the editorial board of the series "Limnology" journal and "Proceedings of the Karelian Research Centre of Russian Academy of Sciences". He is the author and co-author of more than 30 papers.



**Arkady Yu. Terzhevik** is a Head of Laboratory of Hydrophysics of the Northern Water Problem Institute of the Karelian Research Center of the Russian Academy of Sciences. In 1991, he received his Ph. D. degree in technical sciences. His main research fields: hydrodynamics of shallow lakes with environmental applications. He is the author and co-author of more than 40 papers.

DOI: 10.15356/2071-9388\_03v09\_2016\_06

**Alexander F. Finaev<sup>1, 2\*</sup>, Liu Shiyin<sup>1\*</sup>, Bao Weijia<sup>1</sup>, Jing Li<sup>1</sup>**

<sup>1</sup> State Key Laboratory of Cryospheric Science, Cold and Arid Regions Environmental and Engineering Research Institute, Chinese Academy of Sciences

<sup>2</sup> Institute of Water Problems, Hydropower and Ecology of Tajikistan AS

\* **Corresponding authors;** e-mail: finaeff@gmail.com, liusy@lzb.ac.cn

# CLIMATE CHANGE AND WATER POTENTIAL OF THE PAMIR MOUNTAINS

**ABSTRACT.** The Pamir region supplies water for most countries of the Central Asia. Discussions and arguments with regard to reduction of water resources related to climate change are popular today among various governmental and international institutions being a great concern for modern society. Probable decrease of the Pamirs runoff will affect downstream countries that can face water deficiency. However, there is no scientific rationale behind such disputes. The Pamir region is a remote, high-mountainous and hard-to-access area with scarce observation network and no reliable data. It is not sufficiently investigated in order to perform any assessment of climate change. This article represents results of study of climate parameters change (such as temperature, precipitation and river discharge) in the Pamirs. The study area covers all countries included in this mountain region (Tajikistan, China, Afghanistan and Kyrgyzstan). Observation records, remote sensing data and GIS modeling were used in the present work. Chronological data series were divided into two equal time intervals and were treated as climatic periods. Further analysis of climate change helped to estimate its influence on change of water potential in the Pamirs. The paper considers issues of liquid and solid precipitation change in the study area.

**KEY WORDS:** Pamirs, water resources, climate change, glaciers, glacial areas, river discharge, mountain precipitation.

## INTRODUCTION

The Pamir Mountains are bordering the north-west of the Tibetan Plateau and stretch through the territories of Tajikistan, Kyrgyzstan, Afghanistan and China. High elevated mountain ranges make a great barrier to air streams coming from the west. This results in intense precipitation in the western part of the whole area and windward slopes of high ranges. The most extensive contemporary glaciers are found in the Central Pamir of Tajikistan and in the Kashgar mountains of China. The Pamirs, being a source of major rivers in Central Asia and China, is divided into two large watersheds – the Amu Darya river in the west and upper reaches of the Tarim river in the east. Global warming of climate undoubtedly impacts the snow cover, glaciers'

dynamics and water potential of this area. Change of water resources has direct influences on irrigation sector in Central Asian countries and northwestern China. A comprehensive description of the Pamir glaciers was done by Schetinnikov [1998]; theoretical basis of glacial study for this area was developed by Glazyrin [1991]. Estimation and forecast of glacial changes for that part of the region in case of various scenarios have been done by several scientists [Glazyrin and Finaev, 2003]; the Book of articles "Glacial areas of the Pamir-Alay" [1993]; Finaev [1999]. Such estimations were generally done on the basis of records obtained from some glaciers of Tajikistan before 1980. The recent development of remote sensing and geo-information technologies (GIS) allows estimation of glacial changes on a large scale, for instance the Chinese part of the Eastern

Pamirs [Liu and others, 2008] or the Western Pamirs in Tajikistan [Finaev, 2013]. A thorough review made by some researches [Unger-Shayesteh and others, 2013] proved that Central Asia has experienced accelerated warming since the 1970s which resulted in shrinkage of glaciers in the Pamirs and Tieng Shan.

In the paper published by Tandong Yao and other [2012], the authors have shown that glacial areas of the Himalayas were shrinking due to change of atmospheric circulation and precipitation decrease, while in the Pamirs precipitation increase was observed from 2006 to 2010. It should be noted that Yao et al, [2012] studied only Chinese part of the Pamirs (the Kashgar ridge) which included the highest peak of Muztagh Ata. However, the greatest glacial areas here stretch to the west and can be found in the Central Pamirs of Tajikistan.

Modeling of climate change and glacial areas under the ADB project TA-7599 [Climate Resiliency for Natural Resources Investments, 2011] has shown that the Pamir glaciers were tending to reduce. There are many earlier works proving degradation of some glaciers [Schetinnikov, 1998]. The catalogue of the Pamir glaciers located in the USSR was published based on aerial photography performed in 1968 [Catalogue of glaciers of the USSR, 1968]. It described parameters of glaciers for 1955–1960. Information provided in the second catalogue of glaciers included the period through 1980 [Catalogue of Pamir and Hissar-Alay glaciation for 1980, 2011]. These data proved reduction of glaciers compared to the information from the first catalogue. No glacial inventory and assessment were done afterwards in the Pamirs. All mentioned studies include only the Tajik side of the Pamirs, although glacial areas are distributed over the territories of China and Afghanistan as well.

The present paper represents an updated review of climate change in the Pamirs based on meteorological and hydrological records, space images and modeling results with the help of GIS. Analyses of different parameters' change such as air temperature, precipitation,

snow cover and snow accumulation thickness (in water equivalent) for glacial areas across the whole Pamirs and particular basins of large rivers have been performed in the present study.

## STUDY REGION

Usually “the Pamirs” describes the mountains located between the Pyanj and the Vakhsh rivers (the conditional boundaries are identified along these two rivers). However, this approach is not correct from the hydrological point of view, because river basins include mountain ranges which are not part of the Pamirs by the above definition. Thus, the study area covers the entire basins of the Vakhsh, the Pyanj and the Tarim rivers (including ranges adjacent to the Pamirs). Therefore, the present study considers the area which is larger than the total area of the Pamirs typically mentioned in the scientific literature.

### *The topography and river systems*

The study area is located at altitudes from 1100 m up to above 7700 m asl. Particular features of the Pamir highland allow dividing the whole territory into two parts – the Eastern and the Western Pamirs.

The land forms of the Western Pamirs vary and can be characterized by separate high ridges (up to 3.0–4.0 km) alongside with flat river valleys affected by erosion. The main ridges of the Western Pamirs stretch from the southwest to the northeast, where the highest peak is Somoni (Communism) with an elevation of 7495 m asl. Catchment areas of the Western Pamirs belong to the Pyanj and Vakhsh river basins.

The Eastern Pamirs is a high mountain plateau located at the elevation of 3.8–4.5 km. Small mountain ridges rise over flat valleys at the height of 0.5–1.5 km, and some ranges reach 6.2–6.9 km. This high elevated region is covered with permafrost due to low temperatures. The Kashgar ridge with the highest peaks of Muztag-Ata (7546 m asl.) and Kongurt (7719 m asl.) is located eastward. In

the central part of the Eastern Pamirs there is an orographic depression with a closed (drainless) basin of the Karakul lake. This territory is protected by mountains from penetration of damp air masses, thus receiving very small amount of precipitation. High mountain plateaus are characterized by wide and flat river valleys. The catchment areas of the Eastern Pamirs belong to the Pyanj and Tarim river basins (Fig. 1). Altitudes of main river basins are presented in Table 1.

**Table 1. Altitudes of river basins (according to ASTER DEM, resolution 0.028 km)**

Basin	Max altitude, masl	Min altitude, masl	Mean altitude, masl	Area, km <sup>2</sup>
Tarim	7630	1231	3748	44157
Karakul	6721	3859	4501	4543
Pyanj	7339	1200	4163	71648
Vakhsh	7445	1144	3547	29005
Total				149353

*The climate*

The most frequently repeated synoptic processes during the cold part of the year are the southwest anticyclone periphery and intrusion of cyclones from the territories of Iran and Afghanistan. Cyclones are the reason for warm and moist air masses. Back of cyclones in the Pamirs are usually characterized by cold air intrusions from the west and the north resulting in temperature decrease and precipitation increase. Clear anticyclone weather is associated with rapid temperature decrease.

During the warm part of the year, anticyclone is the reason for temperature increase. During this period, air masses usually penetrate from temperate zones of the west and from the north. In mountain areas, such intrusions are accompanied by precipitation and decrease of temperature.

Decrease of temperature in mountains depends on elevation. The high-elevated

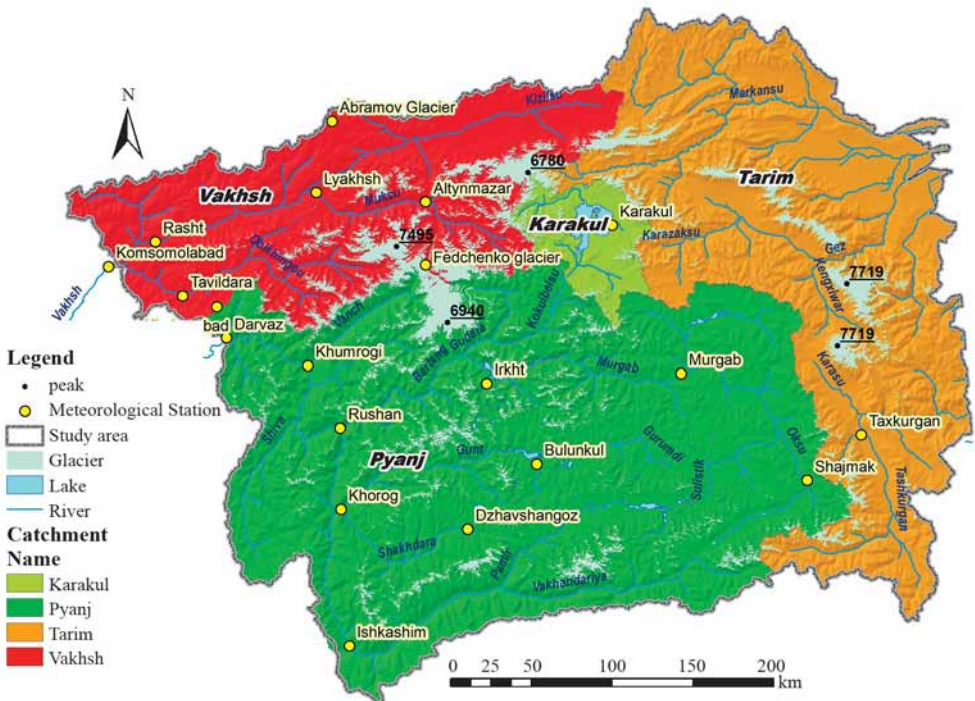


**Fig. 1. The main river basins in the study area**

plateaus are very dry. When moving up over windward slopes air masses lose considerable quantity of moisture, and flat land forms do not promote precipitation. Plenty of precipitation usually occurs in upper reaches of valleys open to moisture-containing air streams from the southwest and the south.

### *Snow cover and glaciers*

Snow cover in the Pamirs can be observed from September to March at the elevation of more than 4–5 km asl. Snow stays all the year round on slopes of northern exposition. The period of the maximum snow cover accumulation throughout the whole area varies from January to May depending on elevation. Melting of steady snow cover could be observed from March to July depending on relief features and surface elevation. The greatest thickness of snow cover varies from 60 cm at the elevation of 1.0–1.5 km to 118 cm at the altitudes higher than 3.5 km.

The highest part of the Pamir mountains contains many glaciers with the total glacial area of more than 10000 km<sup>2</sup>. The biggest glacial zones can be found in the Central Pamirs (the highest part of the Western Pamirs) and on the Kashgar ridge (Kongur-Muztag Ata). The largest is the Fedchenko glacier. According to recent studies, its length is 75.4 km [Finaev, 2013] and its thickness is about 1000 m [Aizen and other, 2009].

## DATASETS AND METHODS OF RESEARCH

### *Climate data*

Monthly mean air temperature (1927–2008) and monthly precipitation (1927–2009) records from 20 meteorological stations located in the Pamirs were collected for the present study (Figure 1). It is obvious that density of climate stations is low, and they are not evenly distributed over different catchments. For instance, in the Tarim river basin there is only one station, and only one is also in the Karakul lake basin. These two stations are located at altitudes 3930 and 3090

m asl. In the Vakhsh river basin there are 7 stations ranging from 1258 up to 4169 m asl. In the Pyanj river basin there are 11 stations; the highest one is Shaimak (3840 m asl.) and the lowest one is Darvaz (1284 m asl).

Station measurements do not hold the common starting time with the earliest in 1927. Besides, gaps can be found in records of some stations. In order to get rid of such discrepancies, all data series have been corrected to match common time interval from 1927 to 2009 using well-known techniques in climatology. Such methodology implies correlation of short-term and long-term station records [Narovlyanskiy, 1968; Pedhazur, 1982; Drozdov and others, 1989; The international meteorological dictionary, WMO, 1992]. In the present study this procedure was done by tools of multiple linear regression available in Microsoft Excel 2010. In order to improve calculation results, 16 stations outside the Pamir territory from Tajikistan, China, Afghanistan, Kyrgyzstan and Pakistan have been included in the study. Totally, records from 36 stations for temperature and records from 35 stations for precipitation have been included.

The term “climate” implies average weather conditions (meteorological parameters) for the period of 30 years and longer. In the present study the total investigated interval is 83 years. In order to estimate probable climate change, the whole time interval has been divided into two climatic periods (CP): from 1927 to 1969, and from 1970 to 2008/2009. Thus, it became possible to analyze real climate change in two climatic periods with the average time interval of 42 and 43 each, instead of estimating trends of meteorological elements, which is usually done based on annual data, and then treated as climate change.

The average altitude of stations is 2740 m asl, which is 1020 m lower than the average elevation of the Pamirs according to the Shuttle Radar Terrain Mission (SRTM) digital elevation model (DEM). In conditions of complicated

mountain relief and big variety of altitudes, records obtained from valley stations cannot correctly illustrate change of climate in high glacial areas. In order to analyze climate change in the Pamirs, it is necessary to have fields of meteorological parameters throughout the investigated territory taking into account surface elevation. Calculations of monthly temperature and precipitation fields for two CP have been done for this purpose.

Despite the fact that all meteorological stations are located in mountain valleys, they are at different altitudes. Since the whole area is not big, change of temperature in case of altitude increase is more significant than its variations related to the stations' locations. Thus, the altitude gradient was used to calculate spatially distributed monthly air temperatures for the Pamir area, which is presented in the formula below:

$$T = a \cdot H + b,$$

where  $a$  and  $b$  – coefficients of regression equation for each month in two climatic periods;  $H$  – elevation of the station extracted from the DEM;  $T$  – average monthly air temperature. DEM resolution was 0.833 km.

Distribution of precipitation in mountains does not depend on elevation change, but relates more to land forms and air masses movement. Thus, the method used for calculation of temperature is not applicable for precipitation modeling. Information from the World Climate Database (WCD) [Hijmans and other, 2005; www.worldclim.org] was used for calculation of precipitation fields throughout the Pamirs. Time intervals used in the present study (1927–1967 and 1970–2009) and the period represented in the WCD (1950–2000) did not match. This fact causes differences between precipitation grid from the WCD and the average monthly records from the meteorological stations. However, the advantage of the WCD is that it can characterize relative distribution of precipitation over a particular territory taking

into account surface elevation and various climate conditions. In order to have reliable precipitation distribution throughout the Pamirs, calibration between data from the WCD and the stations records have been done for each month in both CP. Error ( $Er_{st}$ ) between precipitation data from WCD ( $P_{wcd}$ ) and records at each station was calculated for this purpose.

$$Er_{st} = P_{wcd} - P_{st}$$

where  $Er_{st}$  – the WCD error at the station;  $P_{wcd}$  – precipitation at the station according to WCD;  $P_{st}$  – actual precipitation at the station.

The field of errors ( $F_{Er}$ ) for the entire territory has been calculated according to the obtained error results  $Er_{st}$ . Then the WCD field has been calibrated using the error field ( $F_{Er}$ ).

$$WCD_{correct} = F_{WCD} + F_{Er}$$

where  $WCD_{correct}$  – the WCD corrected field;  $F_{WCD}$  – the WCD field;  $F_{Er}$  – the error field.

As a result, the corrected precipitation grids for each month in both climatic periods were calculated. Assessment of grids and volume of solid precipitation (snow) has been done for conditions when temperature was below or equal to zero ( $T \leq 0$ ).

### *Hydrological and glaciological data*

Available observation records obtained from hydrological stations of Tajikistan have been used for water discharge analysis (Fig. 2). Using the abovementioned methodology, all observation records have been equalized to one time interval from 1932 to 2009. Records from hydrological stations of other countries were not available.

The Darbant hydrological station is located right on the border of the investigated area, thus it observes water discharge of the Vakhsh river basin which is located in the Pamirs. The Shidz hydrological station represents only

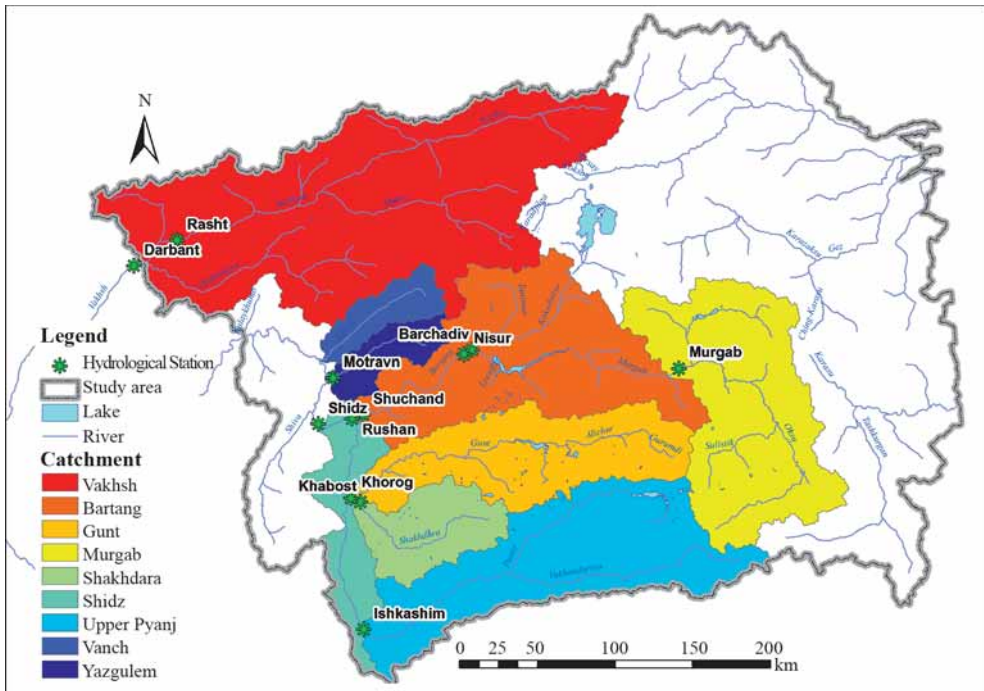


**Fig. 2. Hydrological stations and river basins**

part of the entire Pyanj river basin. It was impossible to obtain discharge records for the entire Pyanj river basin. Thus, assessment of runoff change in the Pamirs was done using data from two hydrological stations – Darbant and Shidz. Hydrological records from the drainless Karakul lake basin and the Tarim river basin are absent, because there are no observations in these areas.

Change of open ice area depends on climate change and can characterize glacial fluctuations. It is necessary to have long-term space images of the entire Pamirs to perform assessment. Unfortunately, such data are not available. The present study uses Landsat images covering the whole Pamir region for different time intervals. It helps to do the mosaic of debris-free ice areas. In the Pamirs, the proportion of ice covered with debris and stone fragments (moraines) is 10 % on average [Schetinnikov, 1998]. Areas without debris are clearly identified and outlined on space images.

## RESULTS AND DISCUSSION

Analysis of changes in climate data is based on the calculated temperature and precipitation fields.

### *Temperature*

The analysis of temperature records from meteorological stations showed that average air temperature during the second CP has increased by  $0.42^{\circ}\text{C}$  (Table 2). It proves positive temperature trend with the rate of  $1.01^{\circ}\text{C}/100$  years.

The analysis of simulated air temperature fields in the Pamirs showed that average temperature has increased by  $0.44^{\circ}\text{C}$  (or  $1.06^{\circ}\text{C}/100$  years) in the second CP. That value is  $0.02^{\circ}\text{C}$  higher than the values calculated using the observation records from the stations. Maximum warming occurred in autumn and winter seasons (up to  $1^{\circ}\text{C}$ ), and minimum warming was observed during summertime ( $0.3^{\circ}\text{C}$ ). Decrease of temperature by  $0.1^{\circ}\text{C}$  was observed in March (Table 3).

Table 2. Air temperature and precipitation from meteorological stations in the Pamirs

WMO	Station	H, m	T <sub>ave</sub> 1927–1969	T <sub>ave</sub> 1970–2008	ΔT	P 1927–1969	P 1970–2009	ΔP, mm	ΔP, %
38840	Komsomolabad	1258	11.0	11.6	0.6	867	904	37	4.3
38856	Darvaz	1284	13.9	14.4	0.5	508	473	-36	-7.0
38851	Rasht (Garm)	1316	10.6	10.8	0.2	724	762	38	5.2
38852	Tavildara	1616	8.7	9.0	0.3	918	964	47	5.1
38867	Khumrogi	1737	11.9	12.3	0.4	200	201	1	0.5
38951	Rushan	1981	9.5	9.9	0.4	245	273	28	11.5
38744	Lyakhsh	1998	6.2	6.3	0.1	401	417	16	4.0
38954	Khorog	2075	8.6	9.3	0.7	280	337	56	20.0
38957	Ishkashim	2524	6.7	7.3	0.6	108	114	6	5.1
38748	Altynmazar	2787	3.3	3.6	0.2	153	173	20	13.2
51804	Taxkurgan	3090	–	–	–	70	73	3	4.7
38869	Irht	3290	0.9	1.3	0.4	130	132	2	1.3
38853	Khaburabad	3347	-1.4	-1.2	0.2	696	688	-8	-1.2
38956	Dzhavshangoz	3410	-2.1	-1.6	0.5	139	137	-2	-1.3
38878	Murgab	3576	-1.6	-1.2	0.3	80	70	-10	-13.0
38953	Bulunkul	3744	-5.6	-5.6	0.1	102	98	-4	-3.9
38707	Abramov Glacier	3840	-4.3	-4.0	0.3	723	758	36	4.9
38966	Shaimak	3840	-3.6	-3.0	0.6	135	141	6	4.5
38871	Karakul	3930	-4.1	-2.8	1.2	75	76	1	1.3
38862	Fedchenko- Glacier	4169	-7.1	-6.7	0.3	1234	1285	51	4.1
T & P year			3.2	3.7	0.42	389	404	14	3.2

Table 3. Air temperature for average elevation in the Pamirs (3760 m asl)

Month	Temperature 1927–1969	Temperature 1970–2008	dT
Jan	-17.74	-16.99	0.8
Feb	-14.97	-14.88	0.1
Mar	-9.55	-9.68	-0.1
Apr	-3.46	-2.73	0.7
May	1.59	2.05	0.5
June	5.61	6.13	0.5
July	9.05	9.45	0.4
Aug	9.10	9.37	0.3
Sept	4.45	4.71	0.3
Oct	-2.22	-1.82	0.4
Nov	-9.43	-8.47	1.0
Dec	-14.65	-14.03	0.6
T average	-3.52	-3.07	0.44

Induced by temperature growth, the elevation (asl) of the zero degree isotherm increased. The altitude of zero degree isotherm increased by 66 m on average in the second CP. The average elevation of the zero degree isotherm was 3220 m asl in the first CP, and 3286 m asl in the second CP. In July, the zero degree isotherm was 5090 m asl during the first CP, and 5168 m asl during the second CP. Thus, the temperature below zero is higher than this level within the whole year.

### Precipitation

Atmospheric precipitation at all stations has increased by 3.2 % on average during the second CP (Table 4). Analysis of simulated precipitation fields showed that the average amount of precipitation over the territory was 372 mm/year during the first CP, and

Table 4. Annual precipitation in the Pamirs (water equivalent)

Parameters	1927–1969	1970–2009	Delta	Delta, %
Average precipitation, mm	372	379	6	1.69
Maximum precipitation, mm	1337	1371	34	2.52
Total precipitation, km <sup>3</sup>	58.08	59.05	0.97	1.67
Water (liquid precipitation), km <sup>3</sup>	16.87	18.14	1.27	7.54
Snow (solid precipitation), km <sup>3</sup>	41.21	40.91	-0.30	-0.74
Water (liquid precipitation), %	29.0	30.7		1.7
Snow (solid precipitation), %	71.0	69.3		-1.7
Snow accumulation volume, km <sup>3</sup>	14.08	13.62	-0.46	-3.28
Average snow accumulation thickness, mm	685	689	4	0.63
Maximum snow accumulation thickness, mm	1306	1357	50	3.85
Snow accumulation volume in glacial areas, km <sup>3</sup>	5.81	5.85	0.05	0.85
Precipitation volume in glacial areas, km <sup>3</sup>	6.72	6.91	0.20	2.91
Precipitation volume on grounds, km <sup>3</sup>	51.4	52.1	0.77	1.51
Average snow area, km <sup>2</sup>	97569	95132	-2438	-2.50
Minimum snow area, km <sup>2</sup>	9291	6871	-2420	-26.05

379 mm/year during the second one. Volume of precipitation changed from 58.08 km<sup>3</sup> to 59.05 km<sup>3</sup>, which illustrates increase by 1.7 % in the second CP. Volume of snow over the territory decreased by 0.74 %. However, in the glacial area amount of snow was 2.91 % higher during the second CP compared to the first one (Table 4).

Thickness of snow accumulation in water equivalent for the glacial areas varied from 49 mm/year to 1306 mm/year on average in the first CP. Maximum thickness of snow accumulation increased by 3.9% and reached 1357 mm/year in the second CP.

Two ice cores taken during a field study (summer 2005) in the upper reaches of the Fedchenko glacier proved that average thickness of snow accumulation in water equivalent was 1380 mm/year and 2080 mm/year, accordingly [Aisen and others 2009]. Thickness of snow accumulation for the same two ice core sites, based on our model, was 1230 mm/year and 1260 mm/year, accordingly. Thus, the difference between real measurements and calculations is 10.9% and 39.7%, accordingly. There are three reasons for

such variance. Firstly, different time intervals were used when comparing available data. Ice cores characterize only from 5 to 6 years period, which is obviously less than the climatic period of around 40 years determined for the present study. Secondly, snow distribution is usually uneven in mountain areas, especially aggravated by wind, frequent snowstorms, variety of land forms and other factors; however, in simulation the pixel is considered as flat surface. Thirdly, the ice core is taken from a particular point, but the model shows average precipitation over the area of one pixel (0.8 km<sup>2</sup>).

Maximum of precipitation occurs in the highest part of the Pamirs (up to 1371 mm/year), and this is the reason for big concentration of glaciers here. In the Eastern Pamirs, precipitation is less than 100 mm/year. Eastward moving air streams are obstructed by the Kashgar ridge located in China, and that induces up to 400-500 mm of precipitation per year over mountains (Fig. 3).

Balance between liquid and solid precipitation (rainfall and snow) varies within a year. In winter season, snow is observed over the

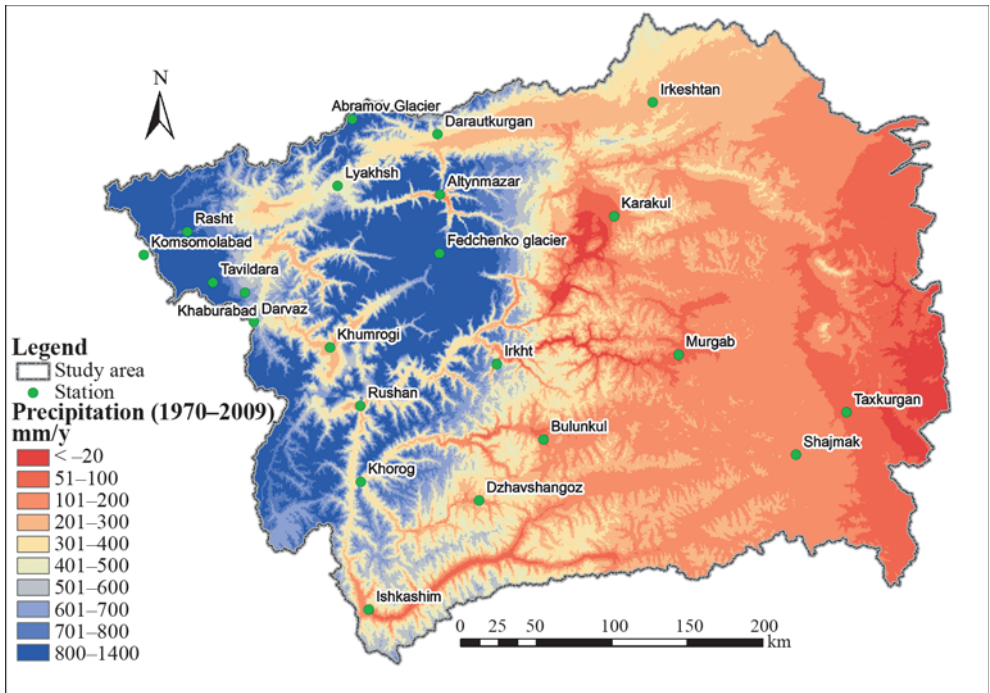


**Fig. 3. Annual precipitation in the Pamirs (1970–2009)**

entire Pamirs, while during summer it occurs only in high mountains. In the second CP such balance changed due to temperature growth, thus increasing rainfall and decreasing snowfall (Fig. 4).

In the first CP, precipitation varied from 5.6 mm/year to 1337 mm/year. In the second CP, the range of precipitation extended from 0.3 mm/year to 1371 mm/year (see Table 3). Change of precipitation throughout the study area was not similar. In the second CP, precipitation increased by 40 mm/year in some high mountain areas, and decreased by 20 mm/year over other territories (Fig. 5).

Precipitation in the glacial area in the first CP was 6.72 km<sup>3</sup>/year, and in the second CP, it was 6.91 km<sup>3</sup>/year showing an increase of 2.91 %. Precipitation over the territory without glaciers was 51.4 km<sup>3</sup>/year during the first CP, and 52.1 km<sup>3</sup>/year during the second CP (see Table 4). Maximum of snow accumulation occurred in April. In the first CP, it was 30.6 km<sup>3</sup>/year, and in the second CP, it decreased by

2.85 % to 29.8 km<sup>3</sup>/year (Fig. 6). The maximum area of snow cover occurs in January when the whole Pamir region is covered with snow.

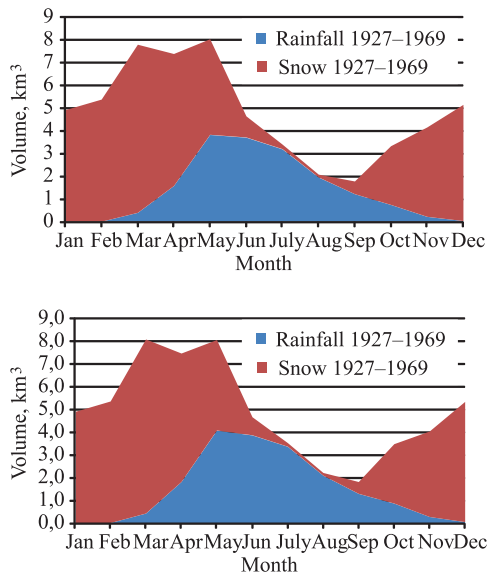


**Fig. 4. Annual course of solid and liquid precipitation in the Pamir area calculated for the two periods (1927–1969 and 1970–2009)**

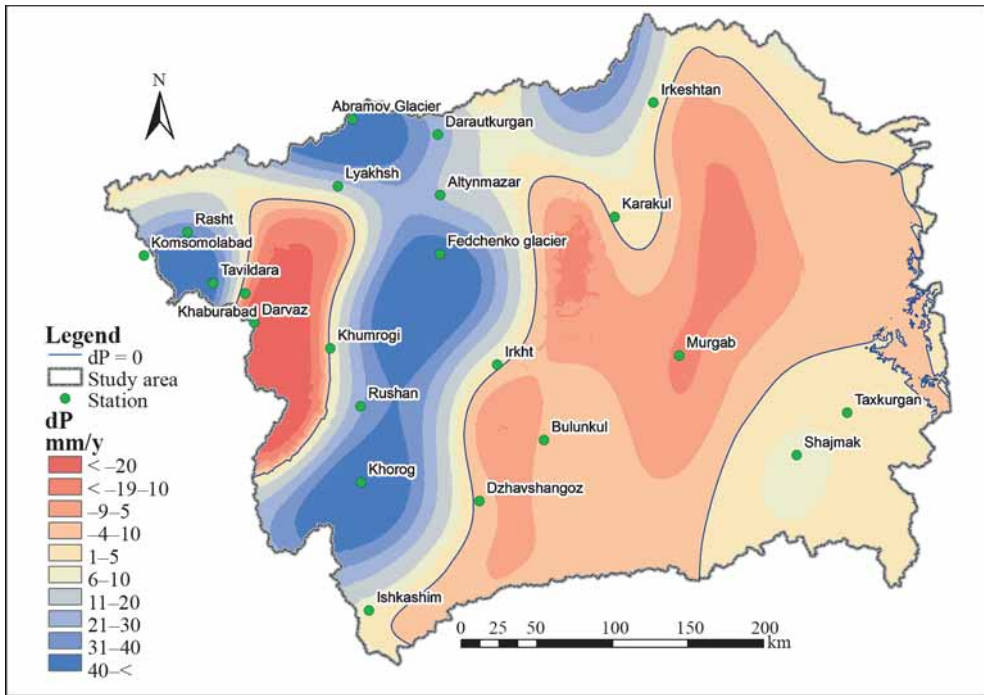


Fig. 5. Change of annual precipitation in the Pamirs during the second CP (mm/year)

Minimum volume of accumulated snow of less than 0.5 km<sup>3</sup> (0.48 km<sup>3</sup> in the first CP and 0.46 km<sup>3</sup> in the second CP) is observed in August, and the minimum area of snow cover is observed in July (9291 km<sup>2</sup> in the first CP and 6871 km<sup>2</sup> in the CP). In July snow cover volume decreased by 21 % due

to area reduction (Fig. 6). The minimum area of snow accumulation in the same month decreased by 26.05 % during the second CP. The maximum thickness of snow cover increased by 3.85 %. However, the average annual snow accumulation volume decreased by 3.28 % in the second CP (see Table 4).

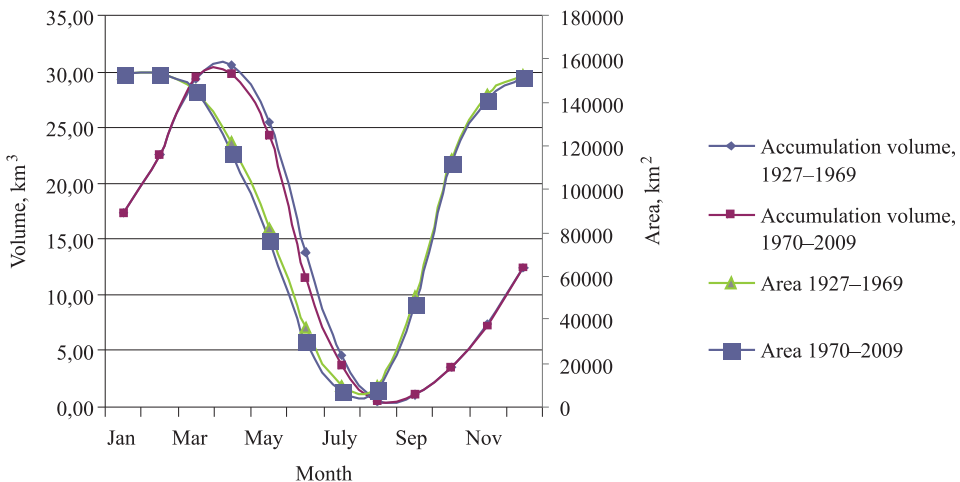


Fig. 6. Change of the snow cover area and water volume in snow on the Pamirs

For a better understanding of climate change, calculation of the seasonal precipitation changes for the three decades from 1981 to 2010 has been made.

Analysis of precipitation change over decades showed the following picture. During the period of 1981–1990, amount of precipitation was 55.9 km<sup>3</sup>/year. In the next period of 1991–2000, precipitation increased up to 59.8 km<sup>3</sup>/year. In the period of 2001–2010, precipitation decreased again to 57.7 km<sup>3</sup>/year. In winter season continuous increase of precipitation was observed. During spring and summer seasons precipitation increase occurred in the second decade (1991–2000) (Fig. 7).

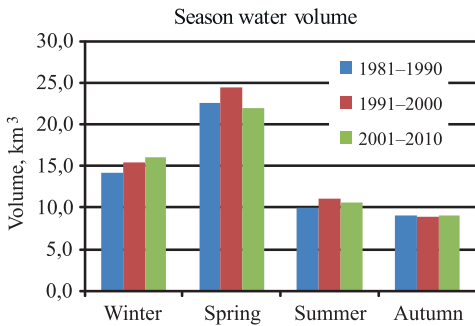


Fig. 7. Seasonal change of precipitation over decades

### Glacial zone

The area of open ice calculated based on Landsat images was 10382 km<sup>2</sup> or 7 % of the total area of the entire Pamirs (Table 5). The greatest glacial areas can be found in the Pyanj river basin (3702.82 km<sup>2</sup>); however,

the share of glaciers in the total basin is only 5.2 %. The biggest share of glacial areas can be found in the Vakhsh river basin, which is 12.2 % of the total catchment. Mean annual snow cover area across the Pamirs decreased by 2.5 % during the second CP. Maximum reduction of mean annual snow cover area by 2.7 % occurred in the Vakhsh river basin.

### Distribution of precipitation throughout river basins

Assessment of precipitation distribution throughout river basins showed increase from 1.3 % (the Vakhsh river) to 2.4 % (the Pyanj river) in western part of the Pamirs during the second CP (1970–2009). In the Karakul lake basin precipitation increased by 4.1 %, and in Chinese part of the Pamir it decreased by 0.9 % (Table 6). Precipitation increased by 1.7 % or 0.97 km<sup>3</sup>/year across the entire Pamirs in the second CP.

**The Tarim river basin.** During the first CP precipitation varied from 30 mm/year to 609 mm/year in the Tarim river basin near the Kashgar ridge, and the average value was 164.9 mm/year. During the second CP precipitation varied from 30 mm/year to 613 mm/year, and the average value was 163.5 mm/year (Table 7). Thus, a small reduction of precipitation volume (–0.9 %) with increased range was observed.

Despite decrease of snow cover area in the Tarim river basin by 4.9 % during the second CP, snow volume in glacial zone of the Kashgar ridge increased by 1.8 % (see Table 6).

Table 5. Distribution of glacial areas in river basins of the Pamirs

Basin	River basins & glaciation areas			Average snow area, km <sup>2</sup> /year		
	Basin area, km <sup>2</sup>	Glacial area, km <sup>2</sup>	Glacial area, %	1927–1969	1970–2009	Delta, %
Tarim	44157	2743.42	6.2	27481	26754	–2.6
Karakul	4549	407.19	9.0	3488	3411	–2.2
Pyanj	71648	3702.82	5.2	49673	48506	–2.3
Vakhsh	28964	3528.89	12.2	16890	16425	–2.7
Total	149318	10382.32	7.0	97532	95096	–2.5

**Table 6. Average annual precipitation in river basins (water equivalent)**

Basin	Precipitation, km <sup>3</sup> /year			Snow, km <sup>3</sup> /year			Snow in glacial areas, km <sup>3</sup> /year		
	1927–1969	1970–2009	Change, %	1927–1969	1970–2009	Change, %	1927–1969	1970–2009	Change, %
Tarim	7.28	7.22	–0.9	3.56	3.39	–4.9	0.61	0.63	1.8
Karakul	0.91	0.95	4.1	0.74	0.75	2.3	0.20	0.21	4.0
Pyanj	30.85	31.59	2.4	24.00	24.09	0.3	2.76	2.87	3.9
Vakhsh	19.05	19.30	1.3	12.91	12.68	–1.8	3.14	3.21	2.2
Total	58.08	59.05	1.7	41.21	40.91	–0.7	6.72	6.91	2.9

**Table 7. Average annual precipitation in river basins of the Pamirs**

Basin	Precipitation, mm/y		dP, mm/y	dP,%
	1927–1969	1970–2009		
Tarim	164.93	163.48	–1.45	–0.9 %
Karakul	199.79	207.96	8.17	4.1 %
Pyanj	430.52	440.86	10.35	2.4 %
Vakhsh	657.57	666.35	8.78	1.3 %
Total	388.99	395.48	6.49	1.7 %

The share of average annual precipitation in the Tarim river basin relative to the entire Pamirs was 12.5 % during the first CP, and 12.2 % during the second one. The share of snow in the glacial areas did not change and was 1.06 % (Table 8).

**The Karakul lake basin.** Annual precipitation in the Karakul lake basin increased by 4.1 % during the second CP, i.e. from 199,8 mm/year to 208 mm/year, or from 0.91 km<sup>3</sup>/year to 0.95 km<sup>3</sup>/year (see Table 6,

Table 7). Quantity of snow throughout the entire basin increased by 2.3 %; amount of snow in glacial areas increased by 4 %. The share of annual precipitation in the Karakul lake basin relative to the entire Pamirs remained constant at 1.6 %. The share of snow in the total precipitation was 1.3 %, and the share of snow in the glacial area was 0.35 %.

**The Pyanj river basin.** Average precipitation in the Pyanj river basin was 430.5 mm/year during the first CP and 440.9 mm/year

**Table 8. Share of basin total precipitation, solid precipitation (snow) and solid precipitation in glaciated areas in total precipitation over the Pamirs**

Basin	Precipitation, %		Snow, %		Snow in glacial areas, %	
	1927–1969	1970–2009	1927–1969	1970–2009	1927–1969	1970–2009
Tarim	12.5	12.2	6.1	5.7	1.06	1.06
Karakul	1.6	1.6	1.3	1.3	0.35	0.35
Pyanj	53.1	53.5	41.3	40.8	4.75	4.85
Vakhsh	32.8	32.7	22.2	21.5	5.41	5.44
Total	100.0	100.0	71.0	69.3	11.57	11.71

during the second one (see Table 7), i.e., 30.85 km<sup>3</sup>/year and 31.59 km<sup>3</sup>/year, accordingly (see Table 6). Amount of snow increased by 0.3 % reaching 24.09 km<sup>3</sup>/year during the second CP. In the glacial area, snow volume increased by 3.9 % reaching 2.87 km<sup>3</sup>/year during the second CP. The share of precipitation in the Pyanj river basin in the total area was 53.1 % in the first CP, and 53.5 % in the second one (Table 8). The share of snow in the total precipitation decreased from 41.3 % to 40.8 %, and in the glacial areas it increased from 4.75 % to 4.85 % during the second CP.

**The Vakhsh river basin.** The most intensive precipitation was observed in the Vakhsh river basin – from 657.57 mm/year in the first CP to 666.35 mm/year in the second one (see Table 7). Volume of precipitation increased from 19.05 km<sup>3</sup>/year during the first CP to 19.30 km<sup>3</sup>/year during the second one (see Table 6). The average annual amount of snow throughout the basin decreased by 1.8 % in the second CP. During the first CP, the amount of snow was 12.9 km<sup>3</sup>/year, and during the second one it was 12.7 km<sup>3</sup>/year. In the glacial area, snow was 3.14 km<sup>3</sup>/year during the first CP and 3.21 km<sup>3</sup>/year during the second one, which is 2.2 % greater. The share of precipitation relative to the total amount for the entire Pamirs was 32.8 % in the first CP and 32.7 %

in the second one; the amount of snow was 22.2 % and 21.5 % respectively. The share of snow in the glacial area of the Vakhsh river basin relative to the total precipitation for the entire Pamirs was 5.41 % in the first CP and 5.44 % in the second one.

The share of snow in the first CP throughout the entire Pamirs was 71 % (Table 8); in the second one it was 1.7 % smaller. However, in the glacial area, the amount of snow was 0.14 % greater during the second CP compared to the first one.

### River discharge

As it was mentioned above, the Vakhsh river basin discharge is characterized by records obtained from the Darbant station. The area of the Vakhsh river basin upstream from this station is 29005 km<sup>2</sup>. The area of the Pyanj river basin, upstream of the Shidz station, is 60044 km<sup>2</sup>. Historical data show a slight tendency for water discharge decrease during the entire observation period. However, increase of water discharge in the Vakhsh river can be noticed since 1974 (Fig. 8).

In the second CP precipitation increased by 2,8 % in the Vakhsh river basin, and by 1,7 % in the Pyanj river basin. However, river discharge in the second CP decreased by 5,1 % in the

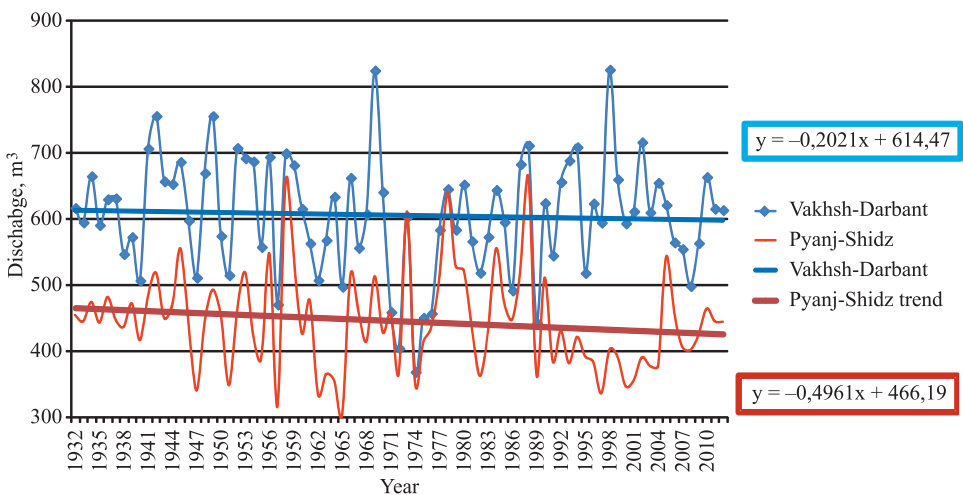
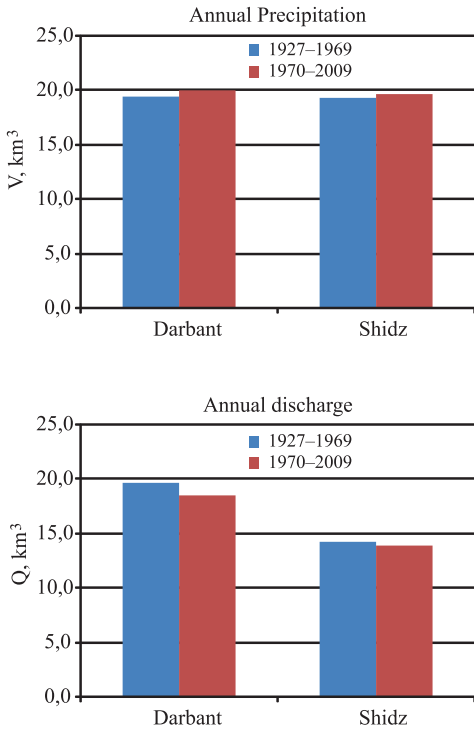


Fig. 8. Water discharge in the Vakhsh-Darbant and Pyanj-Shidz rivers

Vakhsh river basin, and by 1,8 % in the Pyanj river basin (Fig. 9).



**Fig. 9. Change of precipitation and water discharge in the Vakhsh (Darbant) and Pyanj (Shidz) basins.**

Reduction of water discharges while precipitation grows can be explained by two factors. Firstly, rise of temperature increases evaporation. Secondly, in high mountains precipitation grows without thawing, which results in snow accumulation increase.

*Circulation Index and climate fluctuation in the Pamirs*

The Pamir Mountains lie between 36 and 39 degree of the northern latitude. The Polar front zone is supposed to be at the same latitude which separates tropical and moderate air masses. Displacement of this front northwards or southwards affects weather over the Pamirs. Apart from seasonal shifts, front disposition is influenced by a long-term change of cyclones and anticyclones related to polar fronts. It

results in change of atmospheric circulation with subsequent long-term variations of temperature and precipitation cycles in the Pamirs. When such variations last over several decades, they can be considered as climatic periods.

In the middle of the XX<sup>th</sup> century Prof. B.L. Dzerdzeevsky and his colleagues published number of studies about global circulation features in the Northern hemisphere (Dzerdzeevsky and others, 1946; Dzerdzeevsky, 1975). Later the same scientists developed Classification of atmospheric circulation features in the Northern hemisphere, which became useful for identifying of 41 Elementary Circulation Patterns (ECP). The researchers proved that during a long-time interval (of several years) there are certain types of circulation which influence cyclones or anticyclones shifting latitudinally or longitudinally. Thus, variable air stream routes can significantly impact on climate change in particular regions.

In the present study, the authors have tested the mentioned Classification of circulation patterns and periods in the Northern hemisphere (<http://atmospheric-circulation.ru>) for climate change assessment in the Pamir region. Thus, the total circulation index for decadal moving average has been used together with mean annual precipitation in the Pamirs for the same decades (Fig. 10). Approximation by a polynomial of the sixth order showed nearly synchronically change of precipitation and circulation. Such correlation illustrates impact of global circulation processes on climate change in the Pamirs. It reflects the influence of global circulation processes on climate of the Pamirs

**CONCLUSION**

The present work allowed estimating climate change and its impact on water resources of the Pamir region during the observation period (1927-2009). The findings revealed average increase of air temperature and precipitation in the second half of the whole chronological

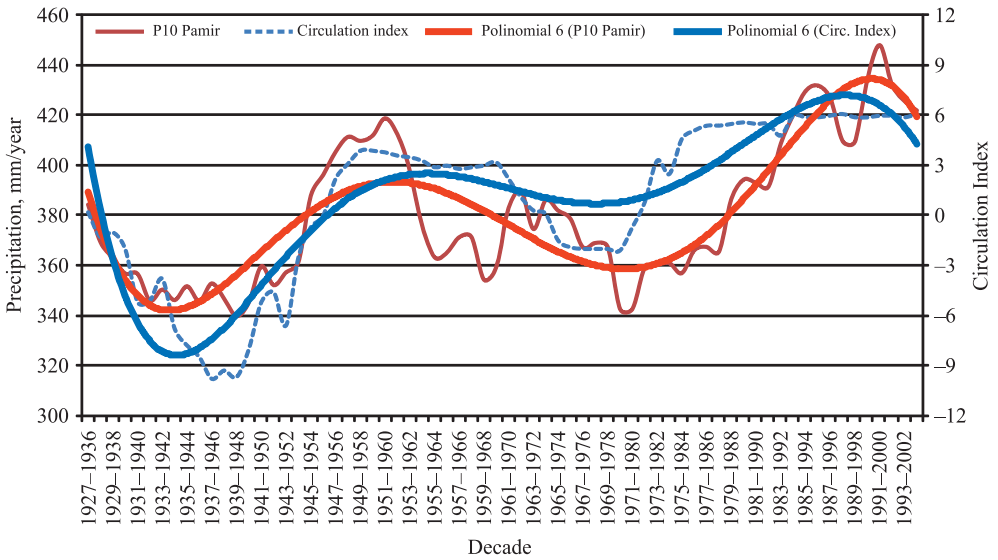


**Fig. 10. Total circulation index and average annual precipitation in the Pamirs**

*Legend: P10 Pamir – total annual precipitation in the Pamirs per 10 years; Circulation Index =  $Z + Vz + Mn + Ms$  ( $Z$  – zonal circulation index;  $Vz$  – zonal circulation disturbance index;  $Mn$  – northern meridional circulation index;  $Ms$  – southern meridional circulation index).*

interval. In the western and northern areas of the Pamirs precipitation increased, while in the eastern part a small decrease was observed. Snow accumulation increased by 2.9 % in the upper reaches of glaciers. Despite this, winter snow stocks decreased due to reduction of the entire snow area by 2.5 %. It can be assumed that in the next period glaciers located below 3200 m asl will continue to shrink until they gain mass balance. Thawing of glaciers will slightly increase at the elevation between 3200 m and 5100 m asl. At the same time, snow will be accumulated in the areas higher than 5100 m asl. When getting a critical mass, it is likely for glaciers to start shifting downwards. Thus, the glacial area at high altitudes can be extended. Hydrological characteristics in rivers of the Pamirs varied within several percent. Therefore, no trends of discharge change were revealed in the upper parts of the Pyanj and Vakhsh river basins.

Climate change in the Pamirs can, probably, be related to global circulation processes in the atmosphere. This point of view is supported by good correlation between the atmospheric circulation index and long-term variations in precipitation.

#### ACKNOWLEDGEMENTS

The authors express their gratitude to the State Key Laboratory of Cryospheric Sciences, Cold and Arid Regions Environmental and Engineering Research Institute of the Chinese Academy of Sciences for providing good environment and all possible assistance in the abovementioned joint research. This study was partially supported by the Ministry of Science and Technology (grant № 2010DFA92720-23), the Chinese Academy of Science (KZZD-EW-12-1) and the Natural Science Foundation of China (41130641). ■

#### REFERENCES

1. Aizen V., Mayewski P., Aizen E., Joswiak D., Surazakov A., Kaspari S., Grigholm B., Krachler M., Handley M., Finaev A. (2009). Stable-isotope and trace element time series from Fedchenko glacier (Pamir) snow/firn cores. *Journal of Glaciology*, Vol. 55, No. 190, 2009, pp. 275–291.

2. Katalog lednikov SSSR. [USSR Glacier Inventory]. (1968). Tom 14. Srednjaja Azija. Vypusk 3. Chasti 4–18. Gidrometeoizdat. Leningrad. 64 p. (in Russian).
3. Catalogue of Pamir and Hissar–Alay glaciation for 1980 (database of A.S. Schetinnikov). (2011). Ed: M. Glazirina. UNDP. 564 p.
4. Climate Resiliency for Natural Resources Investments. (2011) Asian Development Bank. Project TA 7599-TAJ. 158 p.
5. Drozdov O.A., Vasil'ev V.A., Kobysheva N.V., Raevskij A.N., Smekalova L.K., Shkol'nyj E.P. (1989) Klimatologija [Climatology]. Leningrad. Gidrometeoizdat. 568 p. (in Russian).
6. Dzerdzeevskij B.L. (1975). Obshhaja cirkuljacija atmosfery i klimat [General atmospheric circulation and climate]. Izbrannye trudy. M. Nauka. 287 p. (in Russian)
7. Dzerdzeevskij B.L., Kurganskaja Z.M., Vitvitskaja Z.M. (1946) Tipizacija cirkuljacionnykh mehanizmov v Severnom polusharii i kharakteristika sinopticheskikh sezonov. [Classification of atmospheric circulation features in the Northern hemisphere including typifying of synoptic seasons]. Trudy NIU GUGMS. Gidrometeoizdat. 80 p. (in Russian).
8. Finaev A.F. (1999) Climatic Changes in the Mountain Glacier Area of Pamir. In NATO ASI Series I, Vol. 56. Ice Physics in the Natural Environment. (Eds. Wettlaufer/Dash/Untersteiner). Springer-Verlag. Berlin, Heidelberg, pp. 289–294.
9. Finaev A.F. (2013) Dinamika oledeneniya nekotorykh rajonov Pamir-Alaja [Glaciation dynamics in some areas of the Pamir and Pamir-Alay]. Voprosy geografii i geojekologii. TOO "Institut geografii". Almaty. № 3. pp. 32–42. (in Russian).
10. Oledenenie Pamiro-Alaja [Glacial areas of the Pamir-Alay]. (1993). Editor V.M. Kotlyakov M., "Nauka". 256 p. (in Russian).
11. Glazyrin G.E. (1991). Gornye lednikovye sistemy, ih struktura i jevoljucija [Glacial mountain systems, their structure and evolution]. L., GIMIZ. 109 p. (in Russian).
12. Glazyrin G.E., Finaev A.F. (2003). Prognoz izmeneniya oledeneniya gor Zapadnogo Tadzhikistana [The forecast of mountain glaciation change in Western Tajikistan]. MGI Moskva. 2003. Vypusk 95, pp. 102–106. (in Russian).
13. Hijmans R.J., Cameron S.E., Parra J.L., Jones P.G. and Jarvis A. (2005) Very high resolution interpolated climate surfaces for global land areas. International Journal of Climatology 25: 1965–1978 (2005), pp. 1965. [http://www.worldclim.org/worldclim\\_IJC.pdf](http://www.worldclim.org/worldclim_IJC.pdf)
14. Liu Shiyin, Ding Yongjian. (2008) Glacier changes in West China. In Book: Concise glacier inventory of China. Editor: Shi Yafeng. Shanghai Popular Science Press, pp. 174–181.
15. Narovljanskij G.Ja. (1968) Aviacionnaja klimatologija [Aviation climatology]. L. Gidrometeoizdat. 268 p. (in Russian).
16. Pedhazur Elazar J. (1982) Multiple regression in behavioral research: Explanation and prediction (2nd ed.). New York: Holt, Rinehart and Winston. ISBN 0-03-041760-0.

17. Shhetinnikov A.S. (1998) Morfologija i rezhim lednikov Pamiro-Alaja [Morphology and mode of glaciers in the Pamir-Alay]. Red. G.E. Glazyrin. SANIGMI. Tashkent. 220 p. (in Russian).
18. Tandong Yao, Thompson L., Wei Yang, Wusheng Yu, Yang Gao, Xuejun Guo, Xiaoxin Yang, Keqin Duan, Huabiao Zhao, Baiqing Xu, Jiancheng Pu, Anxin Lu, Yang Xiang, Dambaru B. Kattel and Daniel Joswiak. (2012) Different glacier status with atmospheric circulations in Tibetan Plateau and surroundings. *Nature Climate Change Letters*. Published online 15 July 2012. Macmillan Publishers Limited.
19. The international meteorological dictionary. WMO, (1992).
20. Unger-Shayesteh K., Vorogushyn S., Farinotti D., Gafurov A., Duethmann D., Mandychev A. and Merz B. (2013) What do we know about past changes in the water cycle of Central Asian headwaters? A review. *Global and Planetary Change*, 110: 4–25.

Received 03.03.2016

Accepted 29.08.2016



**Alexander F. Finaev** obtained the Ph. D. in Geography in 1988 from the Leningrad Hydrometeorological Institute (LHMI), which he had graduated earlier as an engineer-meteorologist. At present, he is the Head of Laboratory for Climatology and Glaciology of the Institute of Water Issues, Hydropower and Ecology, Academy of Sciences of the Republic of Tajikistan. The current scientific interests are in the field of climate change and its impact on the environment. He studied the radiation balance, aerosol pollution, bio climate, climate and glaciation change, hydro-meteorological observations and assessment of the synoptic processes in Tajikistan. He published more than 60 papers.



**Shiyin Liu** is Professor of the Cold and Arid Regions Environmental and Engineering Research Institute, the Chinese Academy of Sciences (CAREERI, CAS). He graduated from the Lanzhou University and received his master and Ph. D. degrees in 1989 and 1996 at the Lanzhou Institute of Glaciology and Geocryology, CAS. He studied mass balance modeling of glaciers and is now working in remote sensing of glaciers, glacier hazards and glacier hydrology. He has led projects for the new glacier inventory of China and the monitoring of mass changes of glaciers in China. He has authored and coauthored over 100 papers in international journals and some book chapters. He is an editorial board member of some English and Chinese journals.



**Bao Weijia** is a doctoral student of the Cold and Arid Regions Environmental and Engineering Research Institute, the Chinese Academy of Sciences (CAREERI, CAS) and studies glacier change remote sensing monitoring and modeling. Education Background: 2008–2011: Anhui Normal University (The College of Territorial Resources and Tourism), Master Degree. 2003–2007: Changchun Normal University (The College of City Planning and Environment Engineering), Bachelor Degree.



**Jing Li** is Assistant Researcher of the Cold and Arid Regions Environmental and Engineering Research Institute, the Chinese Academy of Sciences (CAREERI, CAS). He graduated from the Hengyang Normal University and received his PhD degree in 2011 at the CAREERI, CAS. He has worked in snow and glacier hydrology, especially in the modeling of the glacier-snow melt in the mountainous area of Northwest China. He studied the process of ice-snow melt, ice-snow surface energy balance, method of the glacier-snow modeling and application of melt models. He has authored and coauthored over 10 papers in international journals. He has also been invited as reviewer for several journals

DOI: 10.15356/2071-9388\_03v09\_2016\_07

**Emmanuel Oriola\*, Cynthia Chibuike**

Department of Geography and Environmental Management, University of Ilorin,  
P.M.B. 1515, Ilorin. Nigeria

\*Corresponding author; e-mail: lolaoriola@gmail.com

# FLOOD RISK ANALYSIS OF EDU LOCAL GOVERNMENT AREA (KWARA STATE, NIGERIA)

**ABSTRACT.** This study examines flood risk propensity of communities in Edu Local Government Area of Kwara state, with a view to classifying the area into risk zones for better and proper management of the environment for the sustainable living of the people. The three administrative districts of Edu Local Government area were identified as pragmatic areas for the study. In each of the districts, Geographical Information System data capture and analytical tool were used to harvest and treat the data for subsequent interpretation. The coordinates of various locations of interest were taken, contour and slope maps of the area were generated to produce flood risk map for the area. The results revealed three distinct risk zones; High, Moderate, and low-risk areas. Three settlements fall into a low-risk area with elevations above 196 m, two settlements located at between 110 m and 196 m are within moderate risk zone and six settlements in High-risk area with elevations below 110 m. This paper concludes that the people of the riverine communities in Edu LGA are culturally attached to the environment. The study, therefore, recommends public enlightenment on the trend in climate and weather about the flood and its implications, environmental education and then resettlement of these communities. When and where resettlement scheme proves very difficult due to strong cultural attachment, flood prevention mechanism via engineering construction such as dykes, embankments and ditches should be adopted.

**KEY WORDS:** flood risk, information, resettlement, planning, sustainable development.

## INTRODUCTION

Floods were observed as one of the effects of global warming ravaging both the coastal cities and riverine communities in the hinterland. Dilley et al. [2005] reported that floods are among the most devastating natural disaster that has a serious impact on life and properties of the people. As rightly observed and reported by Drogue [2004], the frequency at which flood occur is on the increase in many parts of the world Nigeria inclusive. Flood experience in Nigeria has been towing the world trend. Widespread flooding across the country claimed many lives, displayed millions of people and destroyed properties worth billions of naira.

Eludoyin et al. [2007] reported disasters in 1985, 1987 and 1990 in Ibadan, Oyo state, 1992, 1996 and 2002 in Oshogbo Osun state. The flood years in Akure Ondo state were 1996, 2002, 2004 and 2006 just to mention a few of such occurrences in Nigeria.

PrimeTimes Nigeria [2013] estimated the total value of Infrastructure, physical and durable asset destroyed by the flood was put at N1.5 trillion, 2.3 million people displaced, 363 people killed, and 597,474 houses destroyed. It was reported to be the worst in Nigeria History.

Oriola [1994] was of the opinion that flood in coastal regions might not be unexpected,

but an incessant flood in the hinterland and riverine communities has become worrisome. Especially when people are social, culturally and economically attached to such environment. Therefore, it is expedient to probe into how such people and community can have a sustainable environment that will secure their sustenance and life in general.

Flood risk analysis is a crucial element of flood risk management which often provides maps – Flood hazard maps and Flood risk maps. Such analysis also assists in providing flood alert or flood warning if flood water level is rising.

Many times the maps generated from the analysis will show or locate places at higher levels to escape from floods or in flood rescue/ flood relief operation. The analysis has been found to be of help in planning irrigation system and water management. Finally, mapping flood-prone areas in developing countries are to provide planners and disaster management institutions with a practical and cost-effective way to identify floodplains and other susceptible areas and to assess the extent of disaster impact [OAS, 1991]. It can be used in sectoral planning activities and integrated planning studies, and for damage assessment.

Embarking on flood risk analysis will help in regulating development in the floodplain; identify the areas that are exposed to flood risk and their level of severity. Then, serves as a template for evaluating streams vulnerability to flood in order to improve the social and economic well-being and sustain the livelihood of the people in general.

Many researchers have carried out flood analysis which yielded relevant results. For instance, Ogunorisa and Abawua [2005] reviewed some of the techniques of flood risk assessment. These techniques are meteorological especially those involving the rainfall data; hydrological parameters involving the use of runoff data; socioeconomic factors, and a combination of hydrometeorological parameters and socio-economic factors,

and the use of Geographical Information System (GIS) tool. The study recommended the use of GIS technique for risk assessment of flooding as it is capable of integrating the geomorphological, hydrological, meteorological and socio-economic variables.

Oriola and Bolaji [2012] identified areas at risk of urban flood along Aluko river Basin in Ilorin and provided information on flood risk implications on the city dwellers. Data sets on roads, rivers, dump sites and contour lines were extracted from Ikonos Imagery and Topographical map of Ilorin. The study area was eventually classified as high, moderate and low flood risk zones, based on approved setbacks and previous flood range. Buffering, Overlay Operations, Digital Terrain Modelling, Flow Accumulation and Spatial Search were the spatial analyses carried out using ArcGIS 9.3b. The study provided information that would be of help in regulating development in a flood plain, identified the number of buildings that are exposed to flood risk and their level of severity. It also serves as a template for evaluating urban streams vulnerability to flood. Abah [2013] similarly applied Geographic Information Systems (GIS) in mapping flood risk zones in Makurdi Town. His study draws its relevance from the importance of a GIS database in tackling flood-related problems. He employed ArcView GIS package to digitize a topographic map and other relevant themes of the study area and through GIS overlay and manipulative functions, he created a Digital Elevation Model of the study area; and a classification map of flood risk zones in Makurdi town. The map generated shows that Makurdi town is susceptible to flooding, and physical development is still going on in the 'highly susceptible' areas. The study, therefore, recommended the need for town planners to be proactive in their duty to avoid disaster. Njoku et al. [2013] applied the concept of integrated data analysis, using GIS to determine the implications of flooding in Aba metropolis. The Digital Elevation Model developed for the area showed the variation in height as the areas ranging from 35 m–39

m, and 43 m–48 m are likely to be prone to flooding, being that runoff from the areas of higher elevations tends to concentrate on the areas of lower elevations. He, therefore, recommended that some stormwater routes should be rerouted in Aba metropolis.

The goal of this paper is to generate adequate and relevant data on the physical environment which the people have been culturally attached, analyzed them to determine the level of flood risk the people are exposed to. Such information will be relevant for planning and developing the area and ensure an enabling environment for sustainable livelihood.

### THE STUDY AREA

Edu, the study area, is located between longitude  $4^{\circ}54'15''$  East and  $50^{\circ}31'00''$  East of the Greenwich meridian and latitude  $8^{\circ}35'38''$  North and  $9^{\circ}15'00''$  North of the Equator (Fig. 1). It covers an area of  $2,542 \text{ km}^2$ . Edu is one of the sixteen Local Government Areas in Kwara State with Lafiagi as headquarter (Fig. 1). The Local Government Area has a population of 201,469 as reported in the 2006 population census. It has three administrative districts: Lafiagi, Tsaragi, and Shonga, Bello and Makinde [2007], reported that the study area has a mean annual rainfall and temperature of 300 mm and  $29^{\circ}\text{C}$  respectively. The Average

Relative Humidity is about 78.6 % and this varies seasonally with the lowest reaching as low as 69.99 %. The study area is characterized by the alternate dry and wet season, the rainy season starts towards the end of March and lasts till October while dry season commences in November and ends in early March.

The study area falls within the penplain of the river Niger trough, which stretches from Jebba to Eggan on a topography that is relatively flat, lying near the River Niger and rises to the crystalline upland in the south to an elevation of less than 150 m above sea level [Bello and Makinde, 2007]. The River Niger and its tributaries, Oyi and Oro, drain the land. An overflow of the Niger and its tributaries during rain often floods the area and on recess deposits sediments on the flood plain.

Edu LGA is dominated by Nupe speaking people, they live close to river banks and engage in agriculture as the major economic activity. Fish farming and rice cultivation are the two major activities of the people in the study area.

### MATERIALS AND METHODS

Handheld Global Positioning System (GPS) was used to take the location coordinates of each sampled settlements [see Oriola and Chibuke, 2016]. These are settlements

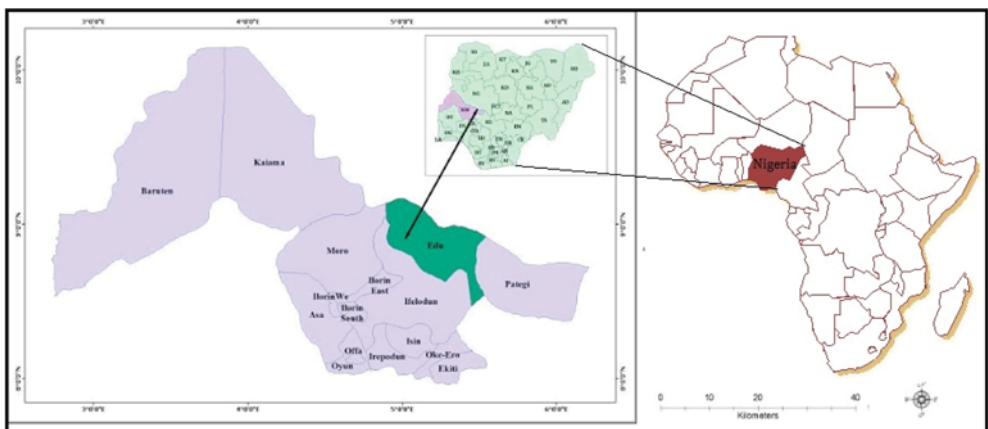


Fig. 1. Map of Kwara State Showing the Study Area, Edu Local Government

that fall within the riverine area of the Local Government Area. Data acquired through the GPS were used to map the area and risk zones were demarcated.

### *Geo-referencing and extraction of study area location*

The Satellite Image of Edu Local Government Area was georeferenced, and supervised classification carried out on the image identifies six (6) different land use classes: water bodies, built-up areas, cloud cover, shrubs (vegetation), unclassified and bare surfaces (see Fig. 2). The built-up areas are comprised of lands where varying degree of anthropogenic activities are being carried out and have modified the natural vegetal cover of the study area; such activities include farmlands, schools, houses, rural roads among others.

The digitized Satellite image highlighted prominent features in the area. They include

locations, districts, settlements, rivers (River Niger and streams Oyi & Oro), main roads among others displayed (see Fig. 3). The River Niger trough that stretches from Yelwa to Edogidukun presents a relatively flat topography. While Rivers Oro and Oyi, present in this area flow North-easterly to join River Niger.

### *Methods of Data Analysis*

The satellite image of Edu Local Government Area was georeferenced and re-sized. The study area was then extracted using the ArcGIS Arc-toolbox. Furthermore, the Satellite Image was classified to ascertain the different land use classes in the area. Digitizing of the satellite imagery was also done to highlight prominent features such as settlements, rivers, and roads.

The elevation coordinates were used to prepare a contour, relief and slope maps as well as a 3D elevation image of the study area.

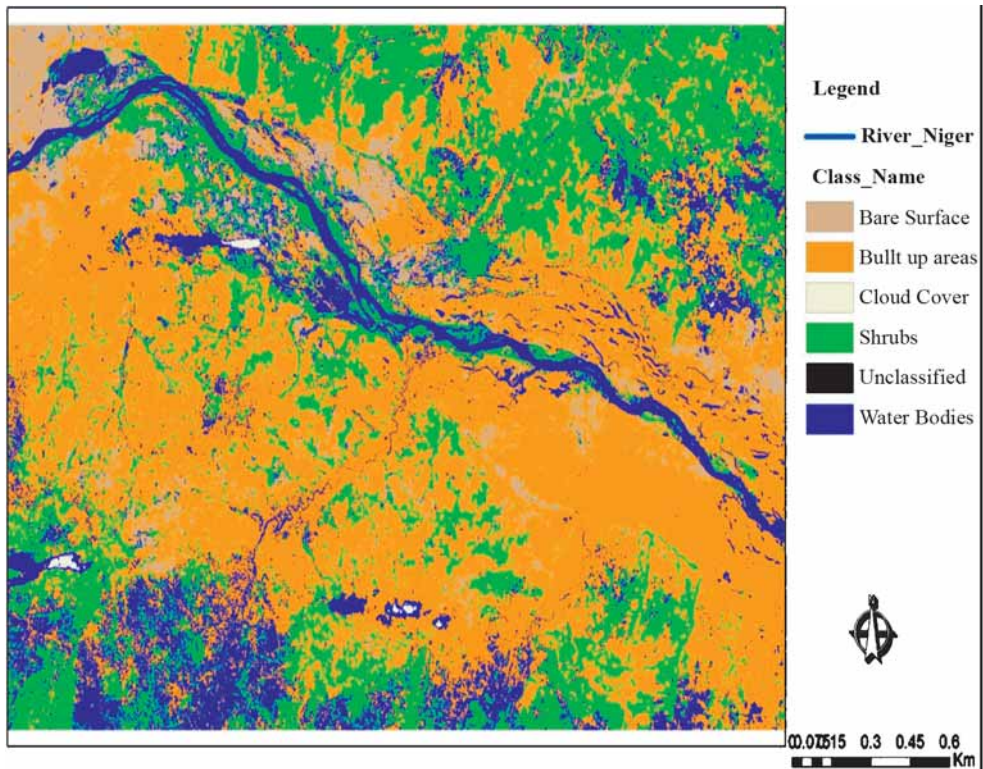


Fig. 2. Land use Map of the Study Area including River Niger.

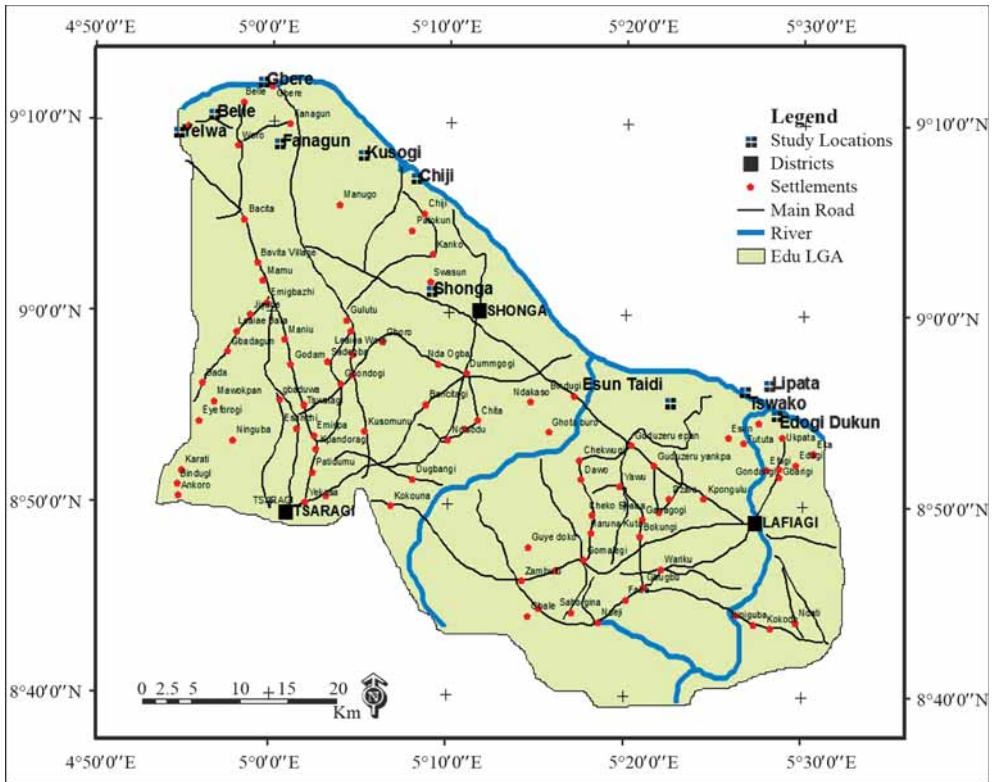


Fig. 3. Settlement map of Edu Local Government Area

- Contour Map of Edu LGA Riverine Areas was developed, using the Shuttle Radar Thematic Map (SRTM) Image obtained from Geotech Consults in Abuja.
- Similarly, slope Map of the study area was created to measure the changes in surface value over distance, to ascertain the angle of curvature using the hydrological analysis tools in ArcGIS 10.1.
- Surfer 8 software and 3D Analytical tool in Arc GIS10.1 was used to develop the Digital Elevation Model.

Finally, Flood risk mapping of the study area was done using overlay, buffer and hotspot analysis tools of Arc 10.1 Spatial Analyst Software to show and identify areas liable to flood. Spatial Queries were carried out to determine the risk zones using proximal search; phenomena search (features within

zones) and susceptibility analysis. The map of flood risk zones was prepared using the DEM [Abah, 2013] and proximity to water bodies. Different parts of Edu Local Government Area were mapped, and the three risk zones were demarcated and classified.

**RESULTS AND DISCUSSION**

*Determination of Flood Prone Areas*

a. Contour Map of Edu LGA: Fig. 4 presents the surface analysis of the terrain of the study area. The contours range from 30 m–330 m. The legend shows the contour lines of spots from 241–330 m as areas that are free and have no probability of flooding while the contour lines joining locations from 30–60 has the highest probability and a concentration of flood and floodable areas, followed by 61–120 m, 121–180 m, 181–240 m. A similar

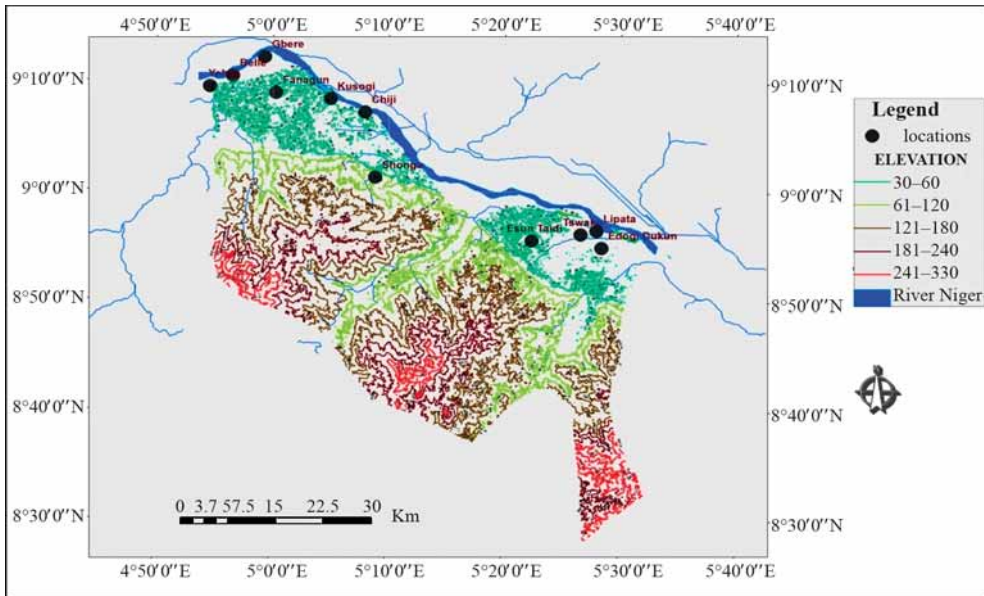


Fig. 4. Contour Map of Edu Local Government Area

result was recorded and reported by Njoku et.al, [2013] in Aba metropolis.

b. Slope Map of Edu LGA Riverine Areas: Areas of depression and those of elevation in the study area were shown on the Slope Map of

Edu LGA Riverine Areas with contour map displayed in tandem. Therefore, areas that are within 0 – 2.2 degrees of the slope are low terrain while the areas of 11.76–46.57 degrees of the slope are high (Fig. 5). The nature of the slope in terms of the degree

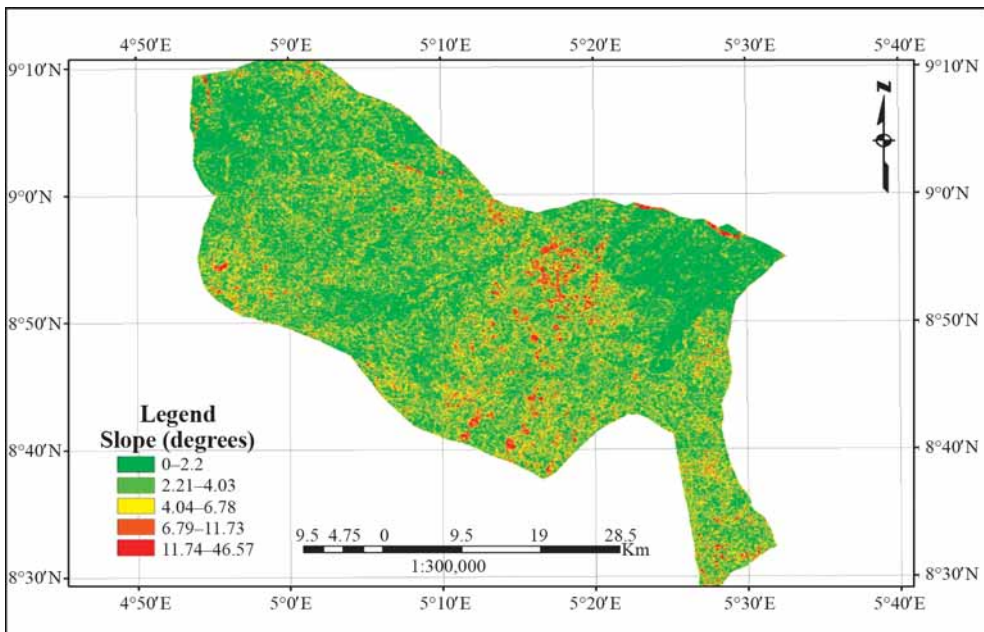


Fig. 5. Slope Map of Edu Local Government Area.

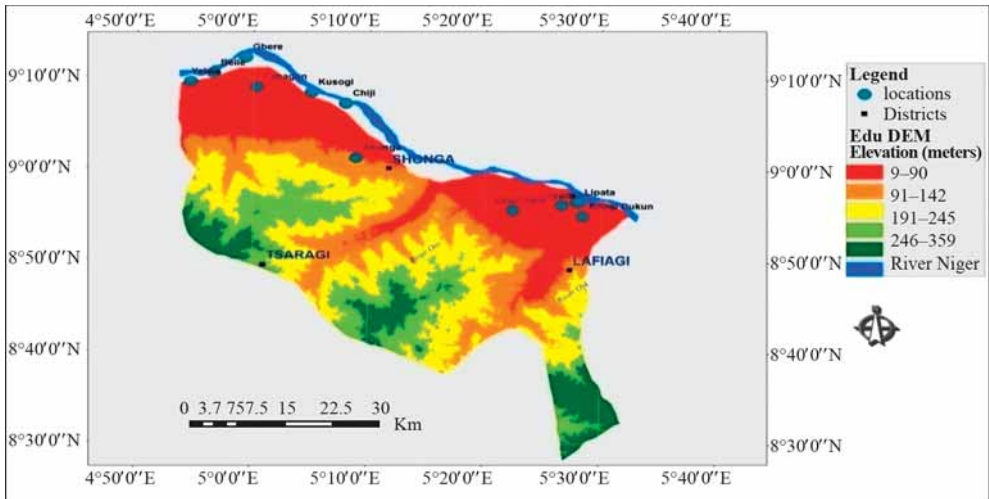


Fig. 6. Digital Elevation Model (DEM) of Edu Local Government Area

has a direct implication on how high or low the plain is and their vulnerability to flood. Most of the communities in the study area are within the low terrain (0–2.2 and 2.21–4.03 degrees of slope), indicating that the communities are at high risk and vulnerable to flooding (Fig. 5). This observation is in line with the work of Abu and Mursheda [2013] in Sirajganj, Bangladesh where they reported downward movement of water to areas of low terrain.

c. Digital Elevation Model of Edu Riverine Areas: The Digital Elevation Model (DEM) of Edu Local Government Area presented in Fig. 6 enhances the chromatic and ophthalmic view of the study area. The result revealed that riverine areas in Edu LGA are areas of flat, featureless (peneplain) plain. The figure shows elevation in meters, with the highest point between 246–359 meters, while the point of entry into the riparian communities is between 9–90 meters and this is the hub and crux of the River Niger. The decreasing nature of the elevation of the floodplain according to [Oriola and Bolaji, 2012] has a direct implication on speed, intensity and erosive capacity of the flood water along the plain as shown in Fig. 6. Apart from Shonga district and its communities that fall within a height range of 91–142 m, other communities in the study area fall within the height range

of 9–90 m. Areas around 91–142 meters may be prone to flood while areas within 143–190 meters and 191–245 meters are slightly elevated region but may also be liable to flood risk. The only safe zones in the study area are between 246–359 meters and none of the settlements selected for the study fall within this height range.

The 3D Flood Inundation Model presented in Fig. 7, reveals that when the water level is at 130 m, the whole eleven sampled communities will be submerged due to the fact that their elevations are below 110 m. It also shows that the study area is liable to flood due to its surface characteristics.

#### *Flood Risk Classification and Zones*

Edu LGA can be classified into three risk zones as presented in the flood risk maps (Fig. 8 and 9). The high-risk zones are areas that are likely to be inundated in a flooding event while the low-risk areas are the least liable to flood. Obviously, this could be explained by the geomorphology, slope, and steepness of the area. A further explanation could be because of the slight slope angles of the area which suggests that all fields are situated very close to water levels.

The flood risk map produced based on the elevation of the study area presented in Fig. 8

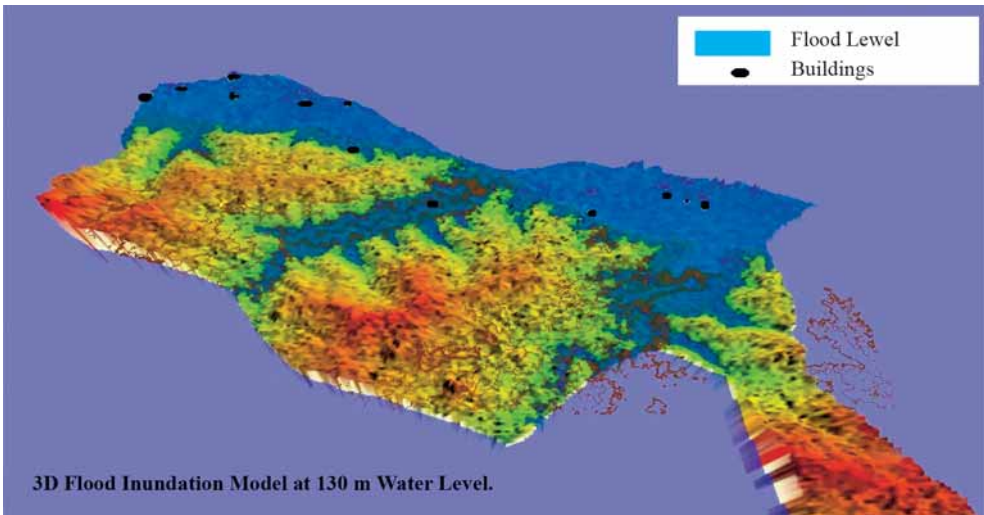


Fig. 7. 3D Flood Inundation Model of Edu Local Government Area

clearly shows three (3) zones with the level of risk and their proneness to disasters. All locations with height less or equal to 110 meters above sea level are considered to have a very high risk. Coincidentally, all the sampled communities fall within this elevation while the areas that fall between 110 and 196 meters are as areas of moderate flood risk

and the land areas from 196 to 360 meters above sea level are considered to be in a low-risk zone. By implication, these last two zones are prone to flooding, but they are not likely to experience a severe flood that the high-risk areas are liable to experience. However, areas above 360 meters above sea level are considered safe with varying degrees of safety

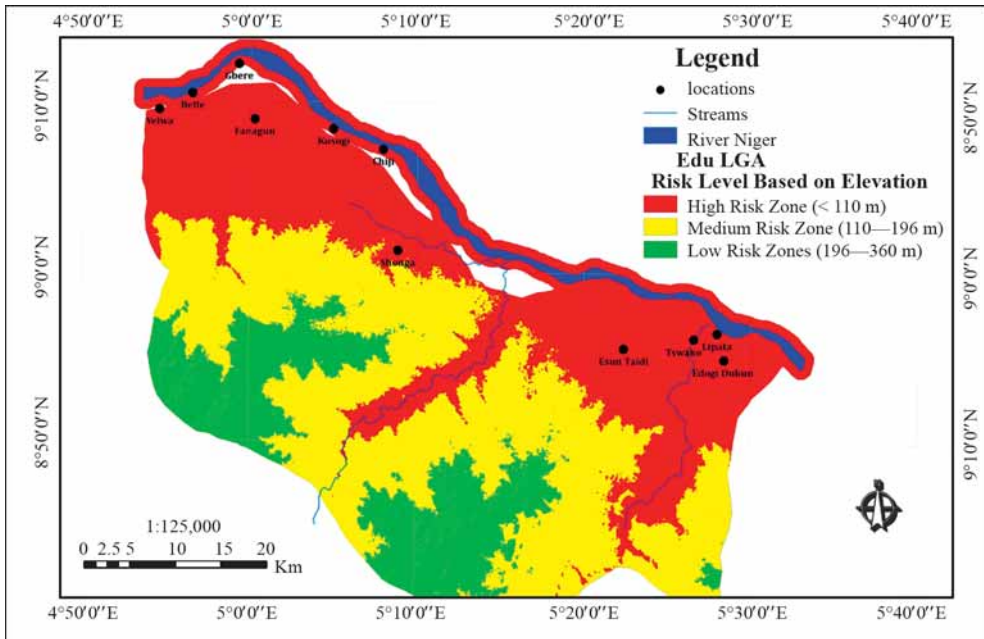


Fig. 8. Flood Risk Level based on Elevation

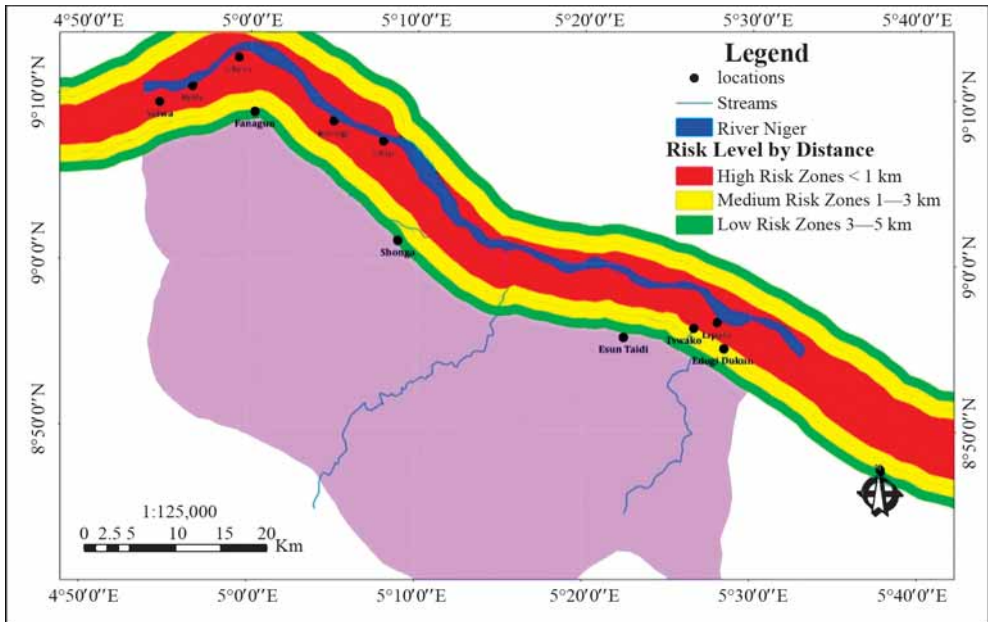


Fig. 9. Flood Risk Level based on Proximity to Water Bodies

attached to them, based on their height above sea levels. Decreasing nature of the elevation of the floodplain according to Oriola and Bolaji [2012] had a direct implication on speed, intensity and erosive capacity of the flood water along the plain. This was also observed and reported by Njoku et al. [2013] in their study of the flood in low elevation areas in Aba, Nigeria.

### Proximity Analysis

Based on proximity to water bodies, floods risk areas were also demarcated [Oriola and Chibuikwe, 2016] (Fig. 9). This was made possible with a buffer distance of less than 1 kilometer, 1–3 kilometers and 3–5 kilometers benchmarks. The map revealed that Yelwa, Belle, Gbere, Kusogi Chiji, Lipata fall within the High-Risk Zone; Tswako and Edogi Dukun are within the Medium Risk Zone, the low-risk zone has Fanagun, Shonga and Esun Taidi settlements (Fig. 9) as observed and reported by Oriola and Chibuikwe [2016]. The location of Tswako and Shonga beside Oro and Oyi Rivers respectively may increase their susceptibility despite the fact that they are considerably far from the main river (River Niger) if the plain is not properly managed and protected. Oriola

and Bolaji [2012] made this observation in their study of river Aluko in Ilorin metropolis, Nigeria. In the study, they reported the high risk of residential, commercial, educational and religious buildings along the river channel in Ilorin. A similar observation was made by Abah [2013] in Makurdi where areas closest to the River Benue and characterized by very low relief (0 to 72 m), are highly susceptible to flooding.

### CONCLUSION

This study utilized Geographic Information System to analyze flood hazard in riverine communities of Edu Local Government Area of Kwara State for a better understanding of the phenomena and proactive steps in mitigating flood hazard in such environment. The paper recommends public enlightenment on the trend in climate and weather about the flood and its implications, environmental education and then resettlement programs for the communities. When and where resettlement scheme proves difficult due to strong cultural attachment, flood prevention mechanism via engineering construction such as dykes, embankments and ditches should be adopted. ■

## REFERENCES

1. Abah, R.C. (2013). An Application of Geographic Information System in Mapping Flood Risk Zones in a North Central City in Nigeria. *African Journal of Environmental Science and Technology*. 7 (6): 365–371.
2. Abu, Z.S. and Mursheda, R. (2013). Spatial strategies for flood vulnerability analysis and long term scenario with geographic information system (GIS) in Sirajganj, Bangladesh. *International Journal of Water Resources and Environmental Engineering*. 5 (9): 546–555.
3. Bello, A. and Makinde, V. (2007). Delineation of the Aquifer in the South- Western Part of the Nupe Basin, Kwara State, Nigeria *Journal of American Science*, 3 (2): 36–44.
4. Chibuke (2015). Assessment of the Impacts of Seasonal Flood on the Riverine Communities in Edu Local Government Area, Kwara State. Unpublished M. Sc. Dissertation Department of Geography and Environmental Management, University of Ilorin, Ilorin. Nigeria.
5. Dilley, M., Chen, R.S., Deichmann, U., Lerner-Lam, A.L. and Arnold, M. (2005). *Natural Disaster Hotspots: A Global Risk Analysis*. The World Bank, US, 150: 9.
6. Drogue, G., Pfister, L., Leviandier, T., El Idrissi, A., Iffly, J.F., Matgen, P., Humbert, J. and Hoffmann, L. (2004). Simulating the Spatio-temporal Variability of Stream flow Response to Climate Change Scenarios in a Meso Scale Basin. *Journal of Hydrology*, 293: 255–269.
7. Eludoyin, A.O., Akinbode, M.O. and Okuku, E. (2007). Combating Flood Crisis with Geographical Information System: An Example from Akure Southwestern Nigeria. *International Symposium on New Direction in Urban Water Management UNESCO, Paris 12–14 September 2007*.
8. Njoku, J.D., Amangabara, G.T. and Duru, P.N. (2013). Spatial Assessment of Urban Flood Risks in Aba Metropolis, using geographical information systems techniques. *Global Advanced Research Journal of Environmental Science and Toxicology* 2 (3): 086–092.
9. Organization of American States (1991) *Flood Plain Definition and Flood Hazard Assessment in Primer on Natural Hazard Management in Integrated Regional Development Planning*. Department of Regional Development and Environment Executive Secretariat for Economic and Social Affairs Organization of American States. Washington. D.C. Retrieved from <https://www.oas.org/dsd/publications/Unit/oea66e/ch08.htm>
10. Ologunorisa, E.T. and Abawua, A.J. (2005). Flood Risk Assessment: a Review. *Journal of Applied Science and Environmental Management*. 9 (1): 57–63.
11. Oriola, O. (1994). Strategies for Combating Urban Flooding in Developing Countries: A Case Study from Ondo. *The Environmentalist*. 14 (1): 57–62.
12. Oriola, E. and Bolaji S. (2012). Urban Flood Risk Information on a River Catchment in a Part of Ilorin Metropolis, Kwara State, Nigeria. *IISTE Journals* 2, (8): 70–83. [www.iiste.org](http://www.iiste.org)
13. Oriola, E. O and Chibuke, C.C. (2016) GIS for Sustainable living in the riverine Communities in Edu Local Government Area of Kwara State, Nigeria *Geografia: Malaysian Journal of Society and Space*. 12 (1): 1–7.
14. Premium Times, Nigeria (2013). Nigeria lost N2.6 trillion to 2012 floods. *The Premium Times, Nigeria*. May 26, 2013.



Dr. **Emmanuel Oriola** is an Associate Professor in the Department of Geography and Environmental Management, University of Ilorin, Nigeria. He started his academic career with M. Sc. Degree (in Physical Geography) from University of Ibadan in 1985 as a Lecturer at Oyo State College of Education, Ilesha (now Osun State), Nigeria. He was appointed an Assistant Lecturer in the Department of Geography Adeyemi College of Education, Ondo, Nigeria in 1987 and joined the services of the University of Ilorin as Lecturer I in 1995. He obtained his Ph. D. Degree (Geography) in 2004 at the University of Ibadan, Nigeria. He also obtained Master's Degree in Business Administration from Obafemi Awolowo University Ile-Ife, Nigeria in 1995 and Advanced Certificate in Geographic Information Systems from Federal School of Surveying, Oyo, Nigeria in 2000. He has teaching and research experience of 30 years. His research interest has been in Land Resources and Environmental Management. He has published over 40 research papers in referred journals and books. He has also attended and presented papers at many International Conferences. Dr. Emmanuel Oriola is a member of the Association of Nigerian Geographers, International Biogeographical Society and African Association of Remote Sensing of the Environment He has supervised Ph. D., M. Sc. Thesis in Geography and Master Degree Dissertations in Geographic Information System.



**Cynthia Chibuiké** is a Research Assistant in the Department of Geography and Environmental Management, University of Ilorin, Nigeria. She received her B. Sc. Degree (Environmental Management) from the Department of Soil and Environmental Management, Ebonyin State University, Abakaliki, Nigeria and has completed her M. Sc. Degree (Geography) at Department of Geography and Environmental Management, University of Ilorin, since May 2015. Her research interest is in Environmental Management.

# INSTRUCTIONS FOR AUTHORS CONTRIBUTING TO “GEOGRAPHY, ENVIRONMENT, SUSTAINABILITY”

## AIMS AND SCOPE OF THE JOURNAL

The scientific English language journal “GEOGRAPHY, ENVIRONMENT, SUSTAINABILITY” aims at informing and covering the results of research and global achievements in the sphere of geography, environmental conservation and sustainable development in the changing world. Publications of the journal are aimed at foreign and Russian scientists – geographers, ecologists, specialists in environmental conservation, natural resource use, education for sustainable development, GIS technology, cartography, social and political geography etc. Publications that are interdisciplinary, theoretical and methodological are particularly welcome, as well as those dealing with field studies in the sphere of environmental science.

Among the main thematic sections of the journal there are basics of geography and environmental science; fundamentals of sustainable development; environmental management; environment and natural resources; human (economic and social) geography; global and regional environmental and climate change; environmental regional planning; sustainable regional development; applied geographical and environmental studies; geo-informatics and environmental mapping; oil and gas exploration and environmental problems; nature conservation and biodiversity; environment and health; education for sustainable development.

## GENERAL GUIDELINES

1. Authors are encouraged to submit high-quality, original work: scientific papers according to the scope of the Journal, reviews (only solicited) and brief articles. Earlier published materials are accepted under the decision of the Editorial Board.
2. Papers are accepted in English. Either British or American English spelling and punctuation may be used. Papers in French are accepted under the decision of the Editorial Board.
3. All authors of an article are asked to indicate their **names** (with one forename in full for each author, other forenames being given as initials followed by the surname) and the name and full postal address (including postal code) of the **establishment(s)** where the work was done. If there is more than one institution involved in the work, authors' names should be linked to the appropriate institutions by the use of 1, 2, 3 etc superscript. **Telephone and fax numbers and e-mail addresses** of the authors could be published as well. One author should be identified as a **Corresponding Author**. The e-mail address of the corresponding author will be published, unless requested otherwise.
4. The GES Journal style is to include information about the author(s) of an article. Therefore we encourage the authors to submit their photos and short CVs.

5. The optimum size of a manuscript is about 3 000–5 000 words. Under the decision (or request) of the Editorial Board methodological and problem articles or reviews up to 8 000–10 000 words long can be accepted.
6. To facilitate the editorial assessment and reviewing process authors should submit “full” electronic version of their manuscript with embedded figures of “screen” quality as a **.pdf file**.
7. We encourage authors to list three potential expert reviewers in their field. The Editorial Board will view these names as suggestions only. All papers are reviewed by at least two reviewers selected from names suggested by authors, a list of reviewers maintained by GES, and other experts identified by the associate editors. Names of the selected reviewers are not disclosed to authors. The reviewers’ comments are sent to authors for consideration.

## MANUSCRIPT PREPARATION

Before preparing papers, authors should consult a current issue of the journal at <http://www.geogr.msu.ru/GESJournal/index.php> to make themselves familiar with the general format, layout of tables, citation of references etc.

1. Manuscript should be compiled in the following **order**: authors names; authors affiliations and contacts; title; abstract; key words; main text; acknowledgments; appendices (as appropriate); references; authors (brief CV and photo)
2. The **title** should be concise but informative to the general reader. The **abstract** should briefly summarize, in one paragraph (up to 1,500 characters), the general problem and objectives, the results obtained, and the implications. Up to six **keywords**, of which at least three do not appear in the title, should be provided.
3. The **main body** of the paper should be divided into: (a) **introduction**; (b) **materials and methods**; (c) **results**; (d) **discussion**; (e) **conclusion**; (f) **acknowledgements**; (g) **numbered references**. It is often an advantage to combine (c) and (d) with gains of conciseness and clarity. The next-level subdivisions are possible for (c) and (d) sections or their combination.
4. All **figures** (including photos of the authors) are required to be submitted as separate files in original formats (CorelDraw, Adobe Photoshop, Adobe Illustrator). Resolution of raster images should be not less than 300 dpi. Please number all figures (graphs, charts, photographs, and illustrations) in the order of their citation in the text. **Composite figures** should be labeled A, B, C, etc. Figure captions should be submitted as a separate file.
5. Tables should be numbered consecutively and include a brief title followed by up to several lines of explanation (if necessary). Parameters being measured, with units if appropriate, should be clearly indicated in the column headings. Each table should be submitted as a separate file in original format (MS Word, Excel, etc.).
6. Whenever possible, total number of **references** should not exceed 25–30. Each entry must have at least one corresponding reference in the text. In the text the surname of the author and the year of publication of the reference should be given in square brackets, i.e. [Author1, Author2, 2008]. Two or more references by the same author(s) published in the same year should be differentiated by letters a, b, c etc. For references with more than two authors, text citations should be shortened to the first name followed by et al.

7. References must be listed in alphabetical order at the end of the paper and numbered with Arabic numbers. References to the same author(s) should be in chronological order. Original languages other than English should be indicated in the end of the reference, e.g. (in French), (in Russian) etc.

**Journal references** should include: author(s) surname(s) and initials; year of publication (in brackets); article title; journal title; volume number and page numbers.

**References to books** should include: author(s) surname(s) and initials; year of publication (in brackets); book title; name of the publisher and place of publication.

**References to multi-author works** should include after the year of publication: chapter title; "In:" followed by book title; initials and name(s) of editor(s) in brackets; volume number and pages; name of the publisher and place of publication.

All references in Cyrillic should be transliterated (please use <http://www.translit.ru>); English translation of the name of publication is given in square brackets after its transliteration.

8. Authors must adhere to SI units. Units are not italicised.

9. When using a word which is or is asserted to be a proprietary term or trade mark, authors must use the symbol ® or TM.

10. As Instructions for Authors are subjected to changes, please see the latest "Example of manuscript style" at <http://www.geogr.msu.ru/GESJournal/author.php>

## MANUSCRIPT SUBMISSION

Authors are encouraged to submit their manuscripts electronically. Electronic submissions should be sent as e-mail attachments to [GESJournal@yandex.ru](mailto:GESJournal@yandex.ru)

ISSN 2071-9388

# SOCIALLY SCIENTIFIC MAGAZINE "GEOGRAPHY, ENVIRONMENT, SUSTAINABILITY"

No. 03(v. 09) 2016

**FOUNDERS OF THE MAGAZINE:** Faculty of Geography, Lomonosov Moscow State University and Institute of Geography of the Russian Academy of Sciences

The magazine is published with financial support of the Russian Geographical Society.

The magazine is registered in Federal service on supervision of observance of the legislation in sphere of mass communications and protection of a cultural heritage. The certificate of registration: ПИ МФС77-29285, 2007, August 30.

## EDITORIAL OFFICE

Lomonosov Moscow State University  
Moscow 119991 Russia  
Leninskie Gory,  
Faculty of Geography, 2108a  
Phone 7-495-9392923  
Fax 7-495-9328836  
E-mail: GESJournal@yandex.ru

## DESIGN & PRINTING

Advertising and Publishing Agency "Advanced Solutions"  
Moscow, 119071 Russia,  
Leninskiy prospekt, 19, 1  
Phone 7-495-7703659  
Fax 7-495-7703660  
E-mail: om@aov.ru

## DISTRIBUTION

East View Information Services  
10601 Wayzata Blvd, Minneapolis, MN 55305-1526 USA  
Phone +1.952.252.1201 Fax +1.952.252.1202  
E-mail: periodicals@eastview.com  
www.eastview.com

Sent into print 28.09.2016  
Order N gi316

Format 70 × 100 cm/16  
9,4 p. sh.  
Digital print  
Circulation 900 ex.